

Symmetric topological phases and tensor network states:

Author: Shenghan Jiang

Persistent link: <http://hdl.handle.net/2345/bc-ir:107410>

This work is posted on [eScholarship@BC](#),
Boston College University Libraries.

Boston College Electronic Thesis or Dissertation, 2017

Copyright is held by the author, with all rights reserved, unless otherwise noted.

Symmetric topological phases and tensor network states

Shenghan Jiang

A dissertation

submitted to the Faculty of

Department of Physics

in partial fulfillment

of the requirements for the degree of

Doctor of Philosophy in Physics

Boston College
Morrissey College of Arts and Sciences
Graduate School
May 2017

Symmetric topological phases and tensor network states

by

Shenghan Jiang

Submitted to the Department of Physics
on May 8, 2017, in partial fulfillment of the
requirements for the degree of
Doctor of Philosophy in Physics

Abstract

Classification and simulation of quantum phases are one of main themes in condensed matter physics. Quantum phases can be distinguished by their symmetrical and topological properties. The interplay between symmetry and topology in condensed matter physics often leads to exotic quantum phases and rich phase diagrams. Famous examples include quantum Hall phases, spin liquids and topological insulators.

In this thesis, I present our works toward a more systematically understanding of symmetric topological quantum phases in bosonic systems. In the absence of global symmetries, gapped quantum phases are characterized by topological orders. Topological orders in 2+1D are well studied, while a systematically understanding of topological orders in 3+1D is still lacking. By studying a family of exact solvable models, we find at least some topological orders in 3+1D can be distinguished by braiding phases of loop excitations.

In the presence of both global symmetries and topological orders, the interplay between them leads to new phases termed as symmetry enriched topological (SET) phases. We develop a framework to classify a large class of SET phases using tensor networks. For each tensor class, we can write down generic variational wavefunctions. We apply our method to study gapped spin liquids on the kagome lattice, which can be viewed as SET phases of on-site symmetries as well as lattice symmetries.

In the absence of topological order, symmetry could protect different topological phases, which are often referred to as symmetry protected topological (SPT) phases. We present systematic constructions of tensor network wavefunctions for bosonic symmetry protected topological (SPT) phases respecting both onsite and spatial symmetries.

Thesis Supervisor: Ying Ran

Title: Associate Professor

To My Parents.

Acknowledgments

I would like to thank my teachers, colleagues, friends and family for all their help and support during my years of graduate study.

First of all, I would like to express my sincere gratitude to my advisor Prof. Ying Ran for the continuous support of my PhD study and related research, for his patience, motivation, and immense knowledge. His guidance helped me in all the time of research and writing of this thesis. I could not have imagined having a better advisor and mentor for my PhD study. Words cannot express my thankfulness.

I would also like to thank the rest of my thesis committee: Prof. Kevin Bedell, Prof. Opeil Cyril, and Prof. Ziqiang Wang, for their insightful comments and encouragement.

I am also deeply thankful to Prof. Jung-Hong Han. I learnt a lot from him during his visit in Boston. My sincere thanks also goes to Prof. Dung-Hai Lee, who provided me an opportunity to visit his group in Berkeley, and for his help during my PostDoc application. I am also indebted to Prof. Frank Verstraete, who supports me during my visit in Ghent and teaches me a lot about tensor network techniques.

I thank my colleagues and collaborators for the stimulating discussions, and for all the fun we have had in the last five years. In particular, I am grateful to Dr. Andrej Mesaros for enlightening me the first glance of research. My thanks go to all my colleagues and friends: Bing Ye, Kun Jiang, Yi Zhang, Tianyi Sun, Yun Peng, Fan Ye, Xueyuan Wu, Hua Li, Jiantao Kong, Mengliang Yao, Chaobin Yang, Ran He, Wei Zhang, He Zhao, Wenping Cui, Shang Gao, Xu Yang, Tong Yang, Hung-Yu Yang, Zheng Ren . . . and many others. I have learned a lot from each of you. Another big thanks goes to all the staff members in the Physics department of Boston College.

Also, I would like to thank my parents. Without their persistent support, I could not have completed all my studies here.

Last but not the least, my deepest gratitude to my wife Leqi Yu, for her continued support and encouragement. She has always been my best friend and great companion. Her love is the greatest gift in my life.

Contents

1	Introduction and overview	1
1.1	Overview of quantum phases	1
1.2	Symmetry, topology and quantum phases	2
1.3	Entanglement and tensor networks	6
2	General modular transformation in 3+1D topologically ordered phases	9
2.1	Introduction	9
2.2	Cohomological gauge theory in 3+1D	12
2.2.1	Exactly solvable models	14
2.2.2	Geometrical reduction of 4-cocycles	16
2.3	Ground state on three-torus and membrane operators	18
2.3.1	Exact models on three-torus	18
2.3.2	MES as ground state basis	19
2.3.3	Membrane operator	22
2.4	Topological observables and their physical interpretation	25
2.4.1	\mathcal{S} and \mathcal{T} matrices from modular transformations	25
2.4.2	Braiding statistics and \mathcal{S} matrix	27
2.5	Examples	33
2.6	Discussion and conclusions	36
2.7	Supplementary material for the cohomology group	38
3	Symmetry enriched topological phases and tensor network states	41
3.1	Introduction	41

3.2	Symmetry, Gauge and PEPS	42
3.2.1	Introduction to PEPS	43
3.2.2	Gauge transformation on PEPS	45
3.2.3	Symmetric PEPS	46
3.2.4	Invariant gauge group and gauge structure	50
3.2.5	An example	60
3.3	Algorithm for Symmetric PEPS	61
3.3.1	General framework for classification	63
3.3.2	Classification of kagome PEPS	68
3.4	Physical Interpretation of Classes	80
3.4.1	Interpretation of Θ_R and χ_R	80
3.4.2	η_R and symmetry fractionalization	83
3.5	Discussion and Conclusions	91
3.6	Symmetry group of the kagome lattice	95
4	Symmetry protected topological phases and tensor network states	97
4.1	Introduction	97
4.2	The connection between SET phases and SPT phases via anyon con- densation	100
4.2.1	A criterion to generate general cohomological SPT phases via anyon condensation	101
4.2.2	Examples: anyon condensation induced SPT phases in the Chern- Simons K -matrix formalism	108
4.2.3	Possible realizations — SPT Valence Bond Solids	117
4.3	Symmetric tensor-network constructions in 2+1D	120
4.3.1	A simple example: Z_2 SPT	120
4.3.2	General Framework	126
4.3.3	A by-product: the general anyon condensation mechanism for realizing SPT phases	133
4.3.4	Algorithms to measure anyon quantum numbers	138

4.3.5 Examples 142

4.4 SPT phases in 3+1D 147

4.5 Discussion 149

4.6 SPT phases in 1+1D 150

4.7 The three cohomology classification from tensor equations in 2+1D . 152

List of Tables

4.1	Five examples of SPT phases studied in this section.	111
4.2	$SG = Z_2^{onsite} = \{I, \sigma\}$ or $SG = Z_2^{TP} = \{I, \mathcal{T} \cdot \mathcal{P}\}$. Denoting $Z_2^{onsite}/Z^{TP} = \{I, u\}$, two inequivalent 3-cocycles ω_0 (trivial) and ω_1 form a Z_2 group.	112
4.3	$SG = Z_2^{onsite} \times Z_2^T$, or $SG = Z_2^{onsite} \times Z_2^P$, or $SG = Z_2^{TP} \times Z_2^T$. Denoting $Z_2^{onsite}/Z^{TP} = \{I, u\}$ and $Z_2^T/Z_2^P = \{I, \eta\}$, the four inequivalent 3-cocycles $\omega_{[0,0]}$ (trivial), $\omega_{[1,0]}$, $\omega_{[0,1]}$, $\omega_{[1,1]}$ form a Z_2^2 group. Note that u is a unitary transformation and η is an anti-unitary transformation. .	112
4.4	The symmetry properties of the nontrivial SPT phase protected by $SG = Z_2^{onsite} = \{I, g\}$, and the SET phase before the anyon condensation.	114
4.5	The symmetry properties of the three nontrivial SPT phases protected by $SG = Z_2^{onsite} \times Z_2^T = \{I, g\} \times \{I, \mathcal{T}\}$, together with those of the corresponding SET phases before anyon condensations.	116
4.6	The symmetry properties of the three nontrivial SPT phases protected by $SG = Z_2^{onsite} \times Z_2^P = \{I, g\} \times \{I, \mathcal{P}\}$, together with those of the corresponding SET phases before anyon condensations.	117
4.7	The symmetry properties of the three nontrivial SPT phases protected by $SG = Z_2^{TP} \times Z_2^T \simeq Z_2^P \times Z_2^T = \{I, \mathcal{P}\} \times \{I, \mathcal{T}\}$, together with those of the corresponding SET phases before anyon condensations.	118
4.8	The symmetry properties of the nontrivial SPT phase protected by $SG = Z_2^{TP}$, and the SET phase before the anyon condensation.	118

List of Figures

2-1	S (left) and T (right) transformations on the (a) Two-torus and (b) Three-torus, which are defined by periodic boundary conditions. . . .	10
2-2	The 4-cocycle ω assigns a $U(1)$ complex number $\omega^\varepsilon(g_{54}, g_{43}, g_{32}, g_{21})$ to a 4-simplex, where ε is the chirality of the 4-simplex, defined as $\varepsilon = \text{sgn}[\det(\vec{12}, \vec{23}, \vec{34}, \vec{45})]$. The dashed lines represent that the vertex 5 has a different coordinate in the fourth dimension (time) with respect to the other vertices.	13
2-3	Geometric meaning of 3-cocycle $\beta_s(c, b, a)$ corresponds to evolution (along fourth dimension) of tetrahedron $[1234]$ to $[1'2'3'4']$	17
2-4	Evolution from a triangle to a 4D manifold. Phase associated with this colored manifold is $\gamma_{a,b}^\varepsilon(c, d)$, where $\varepsilon = \text{sgn}[\det(\vec{d}, \vec{c}, \vec{b}, \vec{a})]$. This phase can also be written as $\gamma_{b,a}^{\varepsilon'}(c, d)$, where $\varepsilon' = \text{sgn}[\det(\vec{d}, \vec{c}, \vec{a}, \vec{b})] = -\varepsilon$. So, we conclude that $\gamma_{a,b}(c, d) = \gamma_{b,a}^{-1}(c, d)$	17
2-5	The simplest triangulation of three-torus has a single vertex and three independent edges. Periodic boundary conditions are imposed on the cube.	18
2-6	Evolution from single vertex to two vertices.	21
2-7	The action of membrane operators.	22
2-8	A positive triple point (left) and a negative triple point (right), where we denote the orientations of sheets by their normals.	27
2-9	Movie for process $H^{-1}G^{-1}F^{-1}GFH$. The worldsheets in this process share the same topological properties as the three-flux-loop braiding process in Fig. 2-11.	29

2-10 Projection of the membrane process movie to three-dimensional space at $t = -\infty$. Lines show the pairwise intersections of projected worldsheets. Black lines: for F and H worldsheets; Blue: for F and G ; Red: for G and H . Although there are eight triple points here, the triple linking is still the same as for the three-flux-loop braiding process, Fig. 2-12. The directions $t_{1,2,3}$ show the time ordering of contributions to projection from worldsheets H, F, G , so clarify to which Tlk_{ijk} some triple point contributes (see after Eq. (2.33)). For example, at point a , direction of t_1, t_2, t_3 shows that worldsheet projection at this point comes from: H^{-1} rather than H , F rather than F^{-1} , G rather than G^{-1} , respectively. Therefore point a contributes to Tlk_{132} 29

2-11 Movies for three-flux-loop braiding. This process has nontrivial triple linking number of three worldsheets. Firstly, loop 1 (black) is created and grows (the black anti-loop is irrelevant and omitted here). Then loop 2 (blue) emerges, encircling loop 1 halfway. Then loop 3 (red) completely encircles loop 2. After this, loop 2 finishes the route around loop 1. Finally, loop 1 shrinks. 31

2-12 (color online) Movie in Fig. 2-11 projected to three-dimensional space at $t = -\infty$. Triple points are marked a, b, c, d . Lines show the pairwise intersections of the projected worldsheet components. Black lines: intersection of projected 1 and 2 worldsheet components; Blue lines: for 2 and 3; Red lines: 1 and 3. The projected component 1 in this figure takes the form of the sphere; 2 and 3 take the form of tori (not shown). The directions $t_{1,2}$ show the time ordering of contributions to projection from worldsheets 1, 2, so clarify to which Tlk_{ijk} some triple point contributes (see after Eq. (2.33)). For example, at point b , t_1, t_2 show that projection of 2 at this point comes from earlier time than 1 (3 is always between them), contributing to Tlk_{132} . This process has same triple linking number as the one in Fig. 2-10. 32

3-1 (a): The leg a is associated with the Hilbert space \mathbb{V}^a . (b): The site tensor (left) and the bond tensor (right) label quantum states on Hilbert spaces of tensor products of corresponding legs. (c): A new tensor can be obtained by contraction of the leg b on T^s and the leg a' on B_b , which can be expressed as $(T^s)_{abcd}^k (B_b)_{a'b'} \delta_{ba'}$. Note that we require leg b and leg a' to be dual spaces. (d): The whole PEPS wavefunction is obtained by contracting all virtual legs of site tensors and bond tensors. 44

3-2 Two PEPS describe the same quantum state, iff they are differ by gauge transformation together with U(1) phase factor. The origin of the gauge transformation is that we can multiply identity matrix $I = W \cdot W^{-1}$ between connected legs, which changes site tensors and bond tensors, but leave the whole wavefunction invariant. We can also view TN on the left as PEPS transformed by symmetry operation. Thus, this figure also express the condition for PEPS wavefunction to be symmetric. 46

3-3 (a): Site tensor and bond tensor are both invariant under Z_2 action on all virtual legs of tensors. (b): Tensors obtained by contracting Z_2 invariant tensors are also Z_2 invariant. (c): Acting g on one virtual leg of single bond tensor creates two fluxons (m) in plaquettes sharing the bond. (d): Z_2 odd tensor indicates there sitting a chargon. (e): By applying g (or creating fluxon loop) on the boundary of a region, we are able to determine chargon number is even or odd inside this region. 54

3-4 (a): kagome lattice and the elements of its symmetry group. $\vec{a}_{1,2}$ are the translation unit vectors, C_6 denotes $\pi/3$ rotation around honeycomb center and σ represents mirror reflection along the dashed red line. (b): Site tensor and bond tensor for kagome lattice in one unit cell. Virtual legs of site tensors are labeled as (x, y, s, i) , where (x, y) denotes the position of unit cell, $s = u, v, w$ is the sublattice index and $i = a, b, c, d$ specifies one of four legs. (c): One possible orientation of kagome lattice. Particularly, for NN RVB state, the orientation of bonds denotes the direction of spin singlets. 62

3-5 (a): Tensor $\hat{T}_{\mathcal{A}}$ and its “generalized inverse” $\hat{T}_{\mathcal{A}}^{-1}$ associated with patch \mathcal{A} . $\hat{T}_{\mathcal{A}}$ is obtained by contracting all bond tensors and site tensors inside patch \mathcal{A} . As a linear map from boundary legs to bulk legs, $\hat{T}_{\mathcal{A}}$ is either Z_2 even or Z_2 odd. (b): The local R -symmetry operator on patch \mathcal{A} . $\{\hat{T}_{\mathcal{A}}^{(i)}\}$ is an orthonormal basis, where every state in the basis is either Z_2 even or Z_2 odd. (c): The local symmetry operator for a series symmetry operations $R_1 \dots R_n$, where $R_1 \dots R_n = I$. If η_R is nontrivial, action of this operator on Z_2 even or Z_2 odd tensor gives different phase factor. This indicates symmetry fractionalization of chargons. 90

4-1 The Z_2 symmetric wavefunction on the honeycomb lattice. Each site contains three qubits. The six qubits around each plaquette are all in the same spin state. The Z_2 symmetry flips spins, which acts as σ_x . . . 121

4-2 The tensor state representing the nontrivial Z_2 SPT wavefunction defined in Eq.(4.20). An internal leg support two dimensional Hilbert space. Physical states are labeled by numbers in the circle, while virtual states are labeled by numbers at the end of internal legs. 122

4-3	Symmetry conditions for the Z_2 symmetric state. Here, X is short for σ_x , and $W_g (W_g^{-1})$ denotes the associated gauge transformation. For the wavefunction defined in Eq.(4.20), $W_g = 11\rangle\langle 00 + i 10\rangle\langle 01 + i 01\rangle\langle 10 + 00\rangle\langle 11 $	123
4-4	(a) Gauge transformations which leave local tensors invariant. Here, Z is short for σ_z . (b) The condensation of visons carrying Z_2 symmetry charge.	124
4-5	Tensors representing the double semion fixed point wavefunction . . .	126
4-6	IGG for double semion topological order	127
4-7	(a) An example of the plaquette IGG element λ_p . (b) The plaquette IGG element formed by complex number χ and χ^{-1} . This kind of plaquette IGG exists for any PEPS state. (c) A site tensor lives on the subspace which is invariant under action of IGGs. Here, p_1, p_2, p_3, p_4 are four neighbouring plaquettes around the tensor and $\alpha, \beta, \gamma, \delta$ denote legs of the tensor. The last equation indicates that a global IGG element is obtained from multiplication of plaquette IGG elements. . .	129
4-8	Measurement of the quantum number $\chi_{m_0}(g)$ carried by an m -particle for a local unitary symmetry g . According to Eq.(4.40,4.52), J commute with W_g , so we conclude that the quantum number is obtained by $\chi_{m_0}(g) \cdot J_p = W_g J_p$	138
4-9	(a) The procedure to create $ \Psi_{ex}\rangle$ which is $\mathcal{T} \cdot \mathcal{P}$ invariant. One first creates a pair of m_0 and m_0^\dagger from ground state, and then move away from each other. The global phase of $ \Psi_{ex}\rangle$ by requiring the wavefunction overlap between adjacent states to be real and positive. (b) $ \Psi'_{ex}\rangle$ is obtained by gluing between the original left-half of the tensor-network with the $\mathcal{T} \cdot \mathcal{P}$ transformed left-half tensor-network. The $\mathcal{T} \cdot \mathcal{P}$ transformed left-half tensor-network is obtained by transforming the physical legs of the left-half via $\mathcal{T} \cdot \mathcal{P}$, together with applying $W_{\mathcal{T}} \mathcal{T} \cdot W_{\mathcal{P}} \cdot \mathcal{T}^{-1}$ on all the virtual legs cut by the mirror line. $\chi_{m_0}(\mathcal{T} \cdot \mathcal{P})$ is defined as phase difference between $ \Psi_{ex}\rangle$ and $ \Psi'_{ex}\rangle$	140

4-10	(a) The honeycomb lattice and generators the lattice symmetry group. u, v labels sites while a, b, c labels bonds in one unit cell. (b) The IGG element formed by phases. We require $\chi_a \cdot \chi_b \cdot \chi_c = 1$	146
4-11	Symmetries and IGG in matrix product states.	151

Chapter 1

Introduction and overview

1.1 Overview of quantum phases

Condensed matter physics studies phases of matter and phase transitions. The most familiar phases are solids and liquids, which can be well understood by classical physics. More exotic phases includes superfluids, superconductors and magnetism. In this thesis, we are interested in quantum phases, i.e. phases in zero temperature.

Quantum phases are classified into two categories: gapped phases and gapless phases. Examples for gapless phases include superfluids, with phonons as gapless excitations and Fermi liquids, with massless fermionic quasiparticles as low-energy excitations. In this thesis, we will focus on another category: gapped quantum phases.

Traditionally, it was believed that phases of matter are classified by their symmetry properties. Landau's symmetry-breaking theory provide a deep insight into quantum phases and phase transitions. Different phases are characterized by different symmetries. Landau's symmetry-breaking theory can describe lots of phases, such as crystal phases, ferromagnetic and anti-ferromagnetic phases, superfluid phases, etc., and also phase transitions between them.

In the last few decades, it was realized that there are phases beyond the framework of Landau-Ginzburg symmetry breaking. The most famous examples are quantum Hall fluids[133]. Different quantum Hall states all share the same symmetry – charge conservation $U(1)$ symmetry. However, different Hall states support different

kinds of (fractional) excitations, which indicates that they are distinguished by new kinds of orders beyond symmetry-breaking. A relatively new examples are topological insulators[59, 110]. Topological insulators have the same symmetry as trivial band insulators, but they host gapless edge states when put on an open boundary system. These nontrivial edge states are also protected by a new kind of order.

So, how do we get systematic understanding of these new phases? What is the measurement signature for these exotic phases? Is there any way to simulate these phases numerically?

In this thesis, we will stress these questions and explore exotic phases by using exact solvable models and tensor networks. While the first method provides us clear physical understanding for the phases, tensor networks not only provide analytical understanding for these phases, but also give generic variational wavefunctions, which are very useful in numerics.

1.2 Symmetry, topology and quantum phases

In the following, we will mainly focus on gapped quantum phases. And we consider the case where ground states shares the same symmetry as local Hamiltonian, i.e. there is no spontaneously symmetry breaking.

It turns out that, symmetry, topology and the interplay between them lead to many exotic phenomena beyond transitional condensed matter physics. In the following, I will briefly introduce some exotic quantum phases due to nontrivial topology and symmetry.

Let us first consider the simplest case, where a local Hamiltonian has no global symmetry. In this case, different gapped quantum phases are only distinguished by their topological properties. In other words, they have different topological orders[154, 150]. One famous example is Kitaev's toric code model[81]. In that case, the low energy dynamics is described by Z_2 gauge theory. There are four types of elementary excitations: topologically trivial excitations, Z_2 charges e , Z_2 fluxes m and dyons ε which are bound states of e and m . These excitations are called anyons, due to their

nontrivial statistics. In the toric code example, e and m are mutual semions and ε is self-fermion.

Topological orders in 2+1D are well studied. They are classified by tensor categories[82]. Ground states of a topological ordered state are degenerate if one put the system on a closed manifold. Low-energy excitations are anyons, whose properties, including fusion rules and braiding statistics, are determined by the topological order. However, theory of topological orders in 3+1D was lacking in the past. It is natural to ask, what are measurement signatures for topological orders in 3+1D? Is there any mathematical tools to classify topological order in 3+1D? We try to give a partial answer of these question in Chapter 2. We find that, for topological orders in 3+1D, nontrivial excitations include particles as well as loops. In order to characterize topological orders, it is necessary to include braiding statistics involving three loops[145, 75, 148, 72, 144]. As a single loop travelling in spacetime forms a world-sheet, the three loop braiding process forms a nontrivial “linked” 2D manifold built up by three world sheets in spacetime. Nontrivial links are characterized by quantities named as triple linking numbers. One can extract Berry phases associated with the three loop braiding process by modular transformations of ground state manifolds. We provide exact solvable models in 3+1D, and show explicitly that different topological orders can be distinguished by three loop braiding Berry phase.

Now, let us add global symmetry, and consider the interplay between symmetry and topology. As an example, let us consider the famous Laughlin’s $\nu = 1/3$ fractional quantum Hall liquid (FQHL)[85], which is topological ordered with three-fold ground state degeneracy on torus and anyonic quasiparticle excitations in the bulk. In the physical realization of the Laughlin FQHL in 2DEG, there is also a global symmetry: the U(1) charge conservation for electrons. One can imagine what would happen if the U(1) charge conservation was absent, for instance, if a small electronic pairing was introduced via proximity effect. Because the topological order is robust towards arbitrary perturbation, the threefold ground state degeneracy and the anyonic statistics of quasiparticles would still be present.

Is the U(1) global symmetry unimportant for the FQHL physics then? Obviously,

this is not the case. In fact, this $U(1)$ symmetry allows one to find two striking experimental signatures of Laughlin’s state: the quantized Hall conductance $\sigma_{xy} = e^2/3h$, and the $e^* = e/3$ fractional charge carried by quasiparticles. The second signature is very interesting: the quasiparticles of a topologically ordered phase can carry a fraction of the quantum number of the fundamental degrees of freedom (electrons here) in the quantum system. Such phenomena are often referred to as “symmetry fractionalization”. This phenomena only occur when the system has topological order. The $e^* = e/3$ charge of quasiparticles is a remarkable demonstration of how the global symmetry can “act” on the topological order in a non-trivial fashion.

Another collection of fascinating quantum phases is the quantum spin liquid (QSL). Quantum spin liquids are often defined to be featureless Mott insulator phases, namely phases that respect full lattice symmetry as well as the spin rotational symmetry, with a half-integer spin per unit cell. Based on the Hastings’ generalization[60] of Lieb-Schultz-Mattis theorem[89] in higher dimensions, we know that gapped quantum spin liquids in two and higher spatial dimensions must host non-trivial ground state degeneracies on torus. But because there is no symmetry-breaking-induced ground state degeneracy, this indicates that the gapped QSLs are topologically ordered. Recently, there are signature of QSL both by numerics[162, 73] and experimental[58, 46] on kagome lattice.

How can one classify/understand QSL phases? Is the topological order enough to determine the nature of this QSL phase? The answer is negative. For example, it turns out that there are more than one QSL phase on the kagome lattice even for a given Z_2 topological order[147, 93]. Their distinctions are protected by the global symmetries. Roughly speaking, the way that the global symmetries act on the topological order are different for different phases. These phenomena have been called “symmetry enriched topological phases” or “symmetry enriched topological order”. When the global symmetries are absent, all these phases are no longer distinguishable and are adiabatically connected to one another. But when the global symmetries are present, one necessarily encounters phase transitions while going from one phase to another.

Now, let us consider gapped quantum phases with only global symmetry, and

assume there is no topological order. Namely, the bulk excitations are all trivial. It turns out that different symmetric quantum phases are classified by a new kind of orders named as symmetry protected topological (SPT) orders. The most famous examples are topological insulators. Consider a electronic system in 3+1D, with global charge conservation symmetry $U(1)$ and time reversal symmetry Z_2^T , there are two different gapped phases: trivial insulators and topological insulators. It is hard to distinguish them from their bulk properties. However, if one puts these two phases on manifold with open boundaries, topological insulators have nontrivial boundary states with a single Dirac cone, while trivial insulators will always support trivial boundary states. Notice, the single Dirac cone state is nontrivial in the sense that it can never exist in a purely 2D system with symmetry $U(1) \times Z_2^T$.

There are also SPT phases in bosonic (spin) systems. Unlike fermionic SPT phases, which usually have free fermion realization, bosonic SPT always require strong interaction, due to the fact that free bosons will always condense. As an example, we consider spin-1 Haldane phase, which is a one dimensional bosonic SPT phase protected by spin rotation symmetry $SO(3)$. If one puts Haldane phase on an open chain, although the phase is gapped in the bulk, there are gapless spin-1/2 modes on boundaries.

Bosonic SPT phases are generalized to higher dimensions in Ref. [21, 20]. They find these SPT phases are (partially) classified by group cohomology $H^{d+1}(SG, U(1))$, where d is the spatial dimension SG is the on-site global symmetry.

In condensed matter system, lattice symmetries, such translation and rotation, are usually very important. One may ask, are there any SPT phases protected by lattice symmetries? In fact, it is shown in Ref. [23, 118, 108], in 1+1D, there are nontrivial SPT phases protected by reflection symmetries. However, are there higher dimensional generalizations of lattice symmetry SPT phases? Can one develop a systematic way to classify SPT phases protected by both on-site symmetries and lattice symmetries? Further, in order to perform numerical simulations, is there any way to write down generic variational wavefunctions for a given SPT phases? We will try to answer the above questions in Chapter 4

1.3 Entanglement and tensor networks

Entanglement is one of the most exotic feature in the quantum world. Entanglement is a special kind of correlation between quantum objects. The most famous entangled state is called Einstein-Podolsky-Rosen (EPR) pair[41]. The state can be viewed simply as a spin singlet state formed by two spin-1/2's

$$|\psi\rangle = \frac{1}{\sqrt{2}}(|\uparrow\downarrow\rangle - |\downarrow\uparrow\rangle) \quad (1.1)$$

if we measure the spins of the two particles separately, we will find that the first one can point in any direction in space and the second one will always take the opposite direction. This provides the simplest example of entangled states in quantum systems.

There are a lot of ways to measure “how much” entanglement is contained in a particular state. The most used one is the entanglement entropy defined for pure states. In a bipartite system with two components A and B , the entanglement entropy between these two subsystems are

$$S_A = -\text{Tr}(\rho_A \ln \rho_A), \quad \text{where } \rho_A = \text{Tr}_B |\psi\rangle\langle\psi| \quad (1.2)$$

where Tr_B is the partial trace over states only in subsystem B . We can exchange A with B in the above formula and the resulting entanglement entropy would be the same. Entanglement entropy provides a simple description of entanglement in bipartite pure states. Another useful quantity to characterize entanglement is called entanglement spectrum. We define entanglement Hamiltonian as following:

$$\rho_A = e^{-H_A} \quad (1.3)$$

And the spectrum of H_A is called entanglement spectrum. Entanglement spectrum provides more sophisticated information about entanglement.

So, why does entanglement useful for quantum phases? How do we characterize quantum entanglement in many-body system?

For the first question, it turns out many quantum phases can be characterized by their entanglement properties. In fact, in modern condensed matter physics, entanglement patterns serve as defining features for many exotic quantum phases. For gapped quantum phases, the most important entanglement feature is called area law[160, 42]. If one bipartite the system into two parts A and B , the entanglement entropy between A and B is proportional to the length of the boundary L_A :

$$S_A = \alpha L_A + \dots \tag{1.4}$$

For example, in one dimension, boundaries are two points. So, entanglement entropy for 1D quantum phases is a constant independent of the size of subsystem A .

For topological ordered state in 2D, there is a negative constant correction for the entanglement entropy

$$S_A = \alpha L_A - \gamma \tag{1.5}$$

γ , named as topological entanglement entropy, only depends on types of topological orders. γ can be measured by numerics, which is a sharp measurement quantity for topological ordered states.

Entanglement entropy is not able to distinguish different SPT phases. However, it turns out that many SPT phases can be diagnosed by entanglement spectrum[47]. Sometimes, entanglement spectrum are more useful than nontrivial boundary states. For instance, there are one nontrivial SPT phases protected by reflection symmetry in 1D spin system. This phase has no nontrivial edge state, since edges always break reflection symmetry. The nontrivial measurement quantity is in fact the entanglement spectrum. Consider an infinite system, For nontrivial reflection SPT phase, the entanglement spectrum are two-fold degeneracy, while for trivial phase, there is no such degeneracy in entanglement spectrum.

From the previous discussion, we see that entanglement are very useful to characterize quantum phases. Is there an efficient representation of quantum states with nontrivial many-body entanglement? It turns out that tensor networks[45, 137, 138,

105, 140, 139] are a perfect tool to write down many-body entangled state. In one dimensional, it is proven that the gapped bosonic quantum phases can be classified by Matrix Product States (MPS). In 2D, Projected Entangled Pairs States(PEPS) have a built-in area law for the entanglement entropy, so become a perfect tool to describe gapped ground states. We will give a detailed review of the tensor network formalism in Chapter 3.

We should mention here, that tensor networks are not only useful tools to study strongly correlated systems, but also serve as powerful numerical methods. For example, DMRG[156], which achieve great success in simulating 1D system, can be expressed elegantly using MPS language. In two dimension, various PEPS algorithm serves as efficient variational methods for strongly coupled spin systems as well as interaction fermionic systems.

Chapter 2

General modular transformation in 3+1D topologically ordered phases

2.1 Introduction

Topologically ordered quantum phases of matter in 2+1D have been intriguing since their discovery decades ago (see [152] and references therein), due to exotic properties such as fractionalized quasiparticles with anyonic quantum braiding statistics.[150, 154] Early on it was realized that in such phases the topological degeneracy of the ground state on the torus corresponds to the number of types of particle excitations (superselection sectors).[155] Furthermore, it was shown that the matrix of Berry's phases experienced by the ground states under the modular transformations of the torus, the S and T transformations (Fig. 2-1a), are directly related to the quantum statistics of the quasiparticles.[150] In fact, to date the most fundamental conjecture remains that the matrices of S, T contain complete information about a topological order.[150] Therefore one can view the modular S, T matrices as the “non-local order parameters” in a topologically ordered phase.[4]

However, in three spatial dimensions some fundamental questions are yet completely unresolved: Is there a physical way to characterize different topological orders in 3+1D? Can braiding of excitations help us in the characterization? Clearly the problem is much more complex, since in 3d there are generically both point-like and

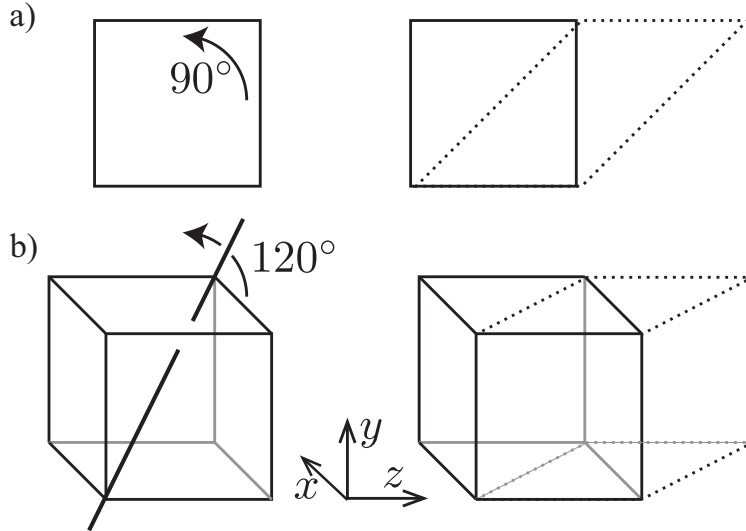


Figure 2-1: S (left) and T (right) transformations on the (a) Two-torus and (b) Three-torus, which are defined by periodic boundary conditions.

loop-like excitations, and their geometric interplay is rich. If some type of braiding can help us characterize the topological order in 3+1D, what is the topological property of that braiding process that is relevant?

Motivated by the fundamental role of modular transformations of the torus in 2+1D systems, our approach to these questions is based on considering the analogous transformations on the three-torus (e.g., a cube with periodic boundary conditions). The modular transformations S, T on the torus generate the group $SL(2, \mathbb{Z})$, which represents the different classes of continuous transformations on the torus.¹ In 3+1D quantum states, the analogue is the three-torus, which also has just two associated transformations S, T , generators of $SL(3, \mathbb{Z})$ group,[132, 101] namely a 120° rotation through a diagonal of the periodic cube and a shear, respectively (Fig. 2-1b). Very recently it has been conjectured that exactly these kinds of transformations can be used to characterize topological order in any dimension.[101]

One way to study topologically ordered states is using the exactly solvable models of discrete gauge theories introduced by Dijkgraaf and Witten (DW).[39, 3] Although these theories in 2+1D do not provide an exhaustive classification of all possible topo-

¹More precisely, $SL(2, \mathbb{Z})$ is the mapping class group of the two-torus, i.e., the group of isotopy-classes of automorphisms of the torus. The mapping class group is formed by Dehn twists of the torus.

logical orders,² they describe a physically interesting set of states. Most importantly for this work, such cohomological gauge theories with gauge group G are naturally defined in any spatial dimension, allowing us to study 3+1D topological orders. They also host both point-like and loop-like excitations, namely gauge charges and flux-loops, respectively. For simplicity, we restrict to the case of Abelian groups G , and then additionally to cases where loops have only Abelian braiding.

In this chapter, we will calculate the matrix elements of the three-torus S, T transformations in cohomological gauge theory, and relate them to the braiding of excitations. Most strikingly, we will argue that the S matrix elements relate to certain braiding processes involving *three* loops simultaneously. This is surprising since there is a simple, seemingly fundamental, braiding process of two loops, where one loop traces out a torus enclosing the other loop, which is relevant in other physical contexts.[2, 102] We then show that this specific three-loop braiding process is characterized by a non-trivial topological invariant, the *triple linking number*, [16] of the worldsheets of three loops in the 3+1D spacetime. This therefore is the appropriate generalization of situation in 2+1D spacetime, where braiding of particles occurs when particle worldlines, forming closed loops, are non-trivially linked.[154] The triple linking number (TLN) can be seen as a generalization of topological linking number of loops in three dimensions to topological linking of closed surfaces in four dimensions.

Recently, the connection between modular transformations on the ground state manifold in 2+1D and the statistics of quasiparticles was further exposed by the introduction of minimum entropy states (MES), a special choice of basis in ground state manifold.[170] The MES can be seen as eigenstates of topological operators describing tunneling of particles across some direction in the periodic system, and their overlaps simply give the matrix elements of modular transformations.[170] This is related to the fact that anyon braiding in 2+1D is mathematically expressed through the non-trivial algebra of the particle tunneling operators.[154] We will show that in 3+1D topological order, the non-trivial matrix elements of the S, T transformations

²Discrete gauge theories can only describe non-chiral states having quasiparticles with integer quantum dimension. Also, some distinct phases can differ by a physically irrelevant relabeling of quasiparticles.

in the MES basis are due to a non-trivial algebra of topological operators which involve membranes; a membrane represents the tunneling of a loop across two periodic directions in the three-torus, and truly involves the three dimensional nature of the system.

This chapter is organized as follows. In Section 2.2, we define the exactly solvable models in 3+1D, which are classified by cohomology group and can be viewed as extension of Dijkgraaf-Witten theory to 3+1D. In the following section, we put these models on three-torus, and get the ground state manifolds. Particularly, we find a MES basis, which is useful for interpretation. Further, we construct membrane operators defined as operators mapping between MES. We work out modular transformations on MES basis in Section. We find modular transformations to be directly related to braiding statistics of flux-loops and particles. We show this by both geometric and algebraic methods. In the last Section we solve these models for some illuminating examples.

2.2 Cohomological gauge theory in 3+1D

In this section, we define the cohomological gauge theory for a general manifold in 3+1D, based on the Dijkgraaf-Witten (DW) topological invariant. The theory is topological and defined by a discrete gauge group G . However, there are distinct topologically ordered states for a fixed G , and in 3+1D they are classified by the fourth cohomology group of G with coefficients in $U(1)$, namely $H^4(G, U(1))$. In Section 2.7 we give a brief review of cohomology concepts relevant for the rest of the paper, while referring the reader to, e.g., Refs.[21, 97], for more details.

In this paper we will work in 3+1D, and therefore the theory will be defined using the 4-cocycle (sometimes we call it simply cocycle) ω , for which the cocycle condition becomes:

$$\begin{aligned} & \omega(g_2, g_3, g_4, g_5) \cdot \omega(g_1, g_2 \cdot g_3, g_4, g_5) \cdot \omega(g_1, g_2, g_3, g_4 \cdot g_5) \\ & = \omega(g_1 \cdot g_2, g_3, g_4, g_5) \cdot \omega(g_1, g_2, g_3 \cdot g_4, g_5) \cdot \omega(g_1, g_2, g_3, g_4), \end{aligned} \tag{2.1}$$

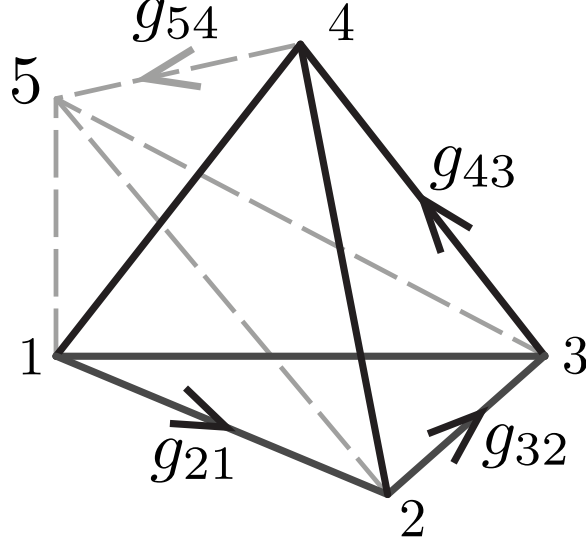


Figure 2-2: The 4-cocycle ω assigns a $U(1)$ complex number $\omega^\varepsilon(g_{54}, g_{43}, g_{32}, g_{21})$ to a 4-simplex, where ε is the chirality of the 4-simplex, defined as $\varepsilon = \text{sgn}[\det(\vec{12}, \vec{23}, \vec{34}, \vec{45})]$. The dashed lines represent that the vertex 5 has a different coordinate in the fourth dimension (time) with respect to the other vertices.

where $\omega \in H^4(G, U(1))$, and $g_i \in G$. In this paper, we will use the “canonical” 4-cocycle, meaning that $\omega(g_1, g_2, g_3, g_4) = 1$ if any of g_1, g_2, g_3, g_4 is equal to $\mathbf{1}$ (the identity element of group G).

The gauge theory is now defined by using ω to construct topological invariants of a 4D manifold. For a given 4D manifold M without boundary, one can triangulate it using a finite number of 4-simplices. The vertices of this triangulation are then ordered arbitrarily, and the ordering is represented by assigning arrows going from the lower to the higher ordered vertex on each edge, Fig. 2-2. Let us denote a 4-simplex of the triangulation, together with the ordering of its vertices, by σ_I , where $I = 1, 2, \dots, S$ labels 4-simplices and S is the total number of 4-simplices in M . Next, one defines a coloring φ of all the edges in the triangulation, by assigning group element to them. Let us denote the group element assigned to the bond connecting vertices j and i as g_{ij} , following the ordering from j to i : $j \rightarrow i$; we then automatically assign $g_{ji} = g_{ij}^{-1}$. In addition, the three assigned group elements for any given face must satisfy the constraint $g_{ij} \cdot g_{jk} \cdot g_{ki} = \mathbf{1}$, and i, j, k are the three vertices of the face. This constraint is the “zero-flux rule”.

With these definitions, one can assign a $U(1)$ phase to every 4-simplex by computing $\omega^\varepsilon(g_{54}, g_{43}, g_{32}, g_{21})$, where $\varepsilon = \text{sgn}[\det(\vec{12}, \vec{23}, \vec{34}, \vec{45})]$ determines the chirality of the simplex, as shown in Fig. 2-2.³ For a given coloring φ and simplex σ_I , we label this $U(1)$ phase as $W(\sigma_I, \varphi)^{\varepsilon(\sigma_I)}$. Finally, one can compute the product of all W for the simplices: $\prod_{I=1}^S W(\sigma_I, \varphi)^{\varepsilon(\sigma_I)}$. For a given coloring φ , we will have one such product. The key result[39] is that the complex number

$$Z_M = \frac{1}{|G|^V} \sum_{\substack{\varphi \in \text{all} \\ \text{possible} \\ \text{colorings}}} \prod_{I=1}^S W(\sigma_I, \varphi)^{\varepsilon(\sigma_I)}, \quad (2.2)$$

where $|G|$ is the number of elements in group G , and V is the number of vertices in the triangulation, is a topological invariant of the manifold M . More precisely, Z_M does not depend on the triangulation and the ordering of vertices (while different colorings are already summed over), owing to the cocycle condition in Eq. (2.1). One can further show that equivalent cocycles (i.e., cocycles differing by a coboundary) give the same value of Z_M . [39]

The topological invariant Z_M is exactly the partition function of the cohomological gauge theory, which is a topological quantum field theory for discrete gauge group G in 3+1D. It is the higher dimensional version of the DW theory[39, ?], and it only depends on inequivalent elements in $H^4(G, U(1))$.

2.2.1 Exactly solvable models

We define our exactly solvable models in 3+1D as Hamiltonian versions of the cohomological gauge theory. We consider space triangulated using a tetrahedron lattice with oriented edges (bonds), where these orientations are compatible with some ordering of lattice sites, and assign an element $g_{ij} \in G$ to each oriented edge $j \rightarrow i$, according to the above discussion.

An arbitrary quantum state in the Hilbert space \mathcal{H} of our model is then labeled

³The 4D coordinate system (x, y, z, w) itself has a chirality, analogously to the handedness of a 3d coordinate system, and if it changes, the ε also changes sign.

by $|a\rangle = |\{g_{ij}\}\rangle$. The building block for the Hamiltonian is the operator \hat{B}_p^s labeled by a group element $s \in G$, and a ‘‘plaquette’’ p containing all 4-simplices (tetrahedra) that share the vertex i . The plaquette operator acts on group elements on the edges that share i . To define its action, we introduce an additional edge rising into the fourth dimension, connecting i to an auxiliary vertex i' . To edge $i \rightarrow i'$ we assign the element $s \in G$. The group elements are changed as

$$\begin{aligned} g_{ij} &\rightarrow s \cdot g_{ij} \\ g_{ki} &\rightarrow g_{ki} \cdot s^{-1}, \end{aligned} \tag{2.3}$$

and these new values are represented on auxiliary edges $i' \rightarrow j$ and $k \rightarrow i'$. Further, the non-zero matrix elements of \hat{B}_p^s , namely $B_p^s = \langle f(s) | \hat{B}_p^s | i \rangle$, are assigned the following quantum amplitude

$$B_p^s \equiv \prod_{I=1}^6 W(\sigma_I, \varphi)^{\varepsilon(\sigma_I)}, \tag{2.4}$$

where the 4-simplices σ_I are built by triangulating the 4D volume formed by the tetrahedra in the plaquette p and the auxiliary edges.

It is important to note that the zero-flux rule is by construction satisfied on all faces (triangles) of 4-simplices, if it is satisfied in the tetrahedra of p , and this must be imposed for the B_p^s to be well-defined. We can then define the plaquette operators \hat{B}_p as having matrix elements

$$B_p = \frac{1}{|G|} \sum_{s \in G} B_p^s. \tag{2.5}$$

The \hat{B}_p are projectors, which can be easily checked using the cocycle property to show $\langle f | \hat{B}_p^s \hat{B}_p^{s'} | i \rangle = B_p^{s \cdot s'}$, which then implies $\langle f | \hat{B}_p \hat{B}_p | i \rangle = B_p$. Similarly, it can be shown that the plaquette operators commute, $[B_p, B_{p'}] = 0$, $\forall p, p'$.

Let us also introduce the operator Q_t , which projects flux in a triangle t to zero,

i.e., it enforces the zero-flux rule. Then the Hamiltonian takes the form

$$H = - \sum_t Q_t - \sum_p \hat{B}_p \prod_{t \in p} Q_t, \quad (2.6)$$

where the label $t \in p$ enumerates all the triangles making up the plaquette p . As mentioned above, the factor $\prod_{t \in p} Q_t$ is actually crucial to ensure that H is well-defined. Further, it is easy to see that plaquette operator term $\hat{B}_p \prod_{t \in p} Q_t$ actually commutes with the projectors $Q_{t'}$. Since all the terms in H commute with each other, the model is exactly solvable.

Let us briefly mention the connection of the Hamiltonian formulation to the gauge theory, which is exhibited in the ground state manifold. Since all the terms in H are projectors, the ground state manifold is the image of the projector $P = \prod_p \hat{B}_p \prod_{t \in p} Q_t$. On the other hand, P is exactly the projector defining the cohomological gauge theory on the 4D manifold having two copies of our spatial manifold M as boundaries (see Ref.[97] for details). The ground state sector of H , to which P projects with eigenvalue 1, is also the ground state sector of the cohomological gauge theory[39] defined on M .

2.2.2 Geometrical reduction of 4-cocycles

In this section we present some cohomology equations for reducing the 4-cocycle to lower order cocycles, and explain their geometric meaning. These equations crucially simplify all following calculations. From now on, we will focus on Abelian groups G for convenience.

First, let us consider a triangulated 4D manifold in Fig.2-3, with the shown coloring. (Note that some edges needed for full 4D triangulation are omitted, but coloring and ordering are fully defined.) The $U(1)$ phase calculated from all the 4-simplices spanning this 4D volume, with the 4-cocycle ω given, equals $\beta_s^\varepsilon(c, b, a)$, with:

$$\beta_s(c, b, a) = \frac{\omega(s, c, b, a) \cdot \omega(c, b, s, a)}{\omega(c, s, b, a) \cdot \omega(c, b, a, s)}, \quad (2.7)$$

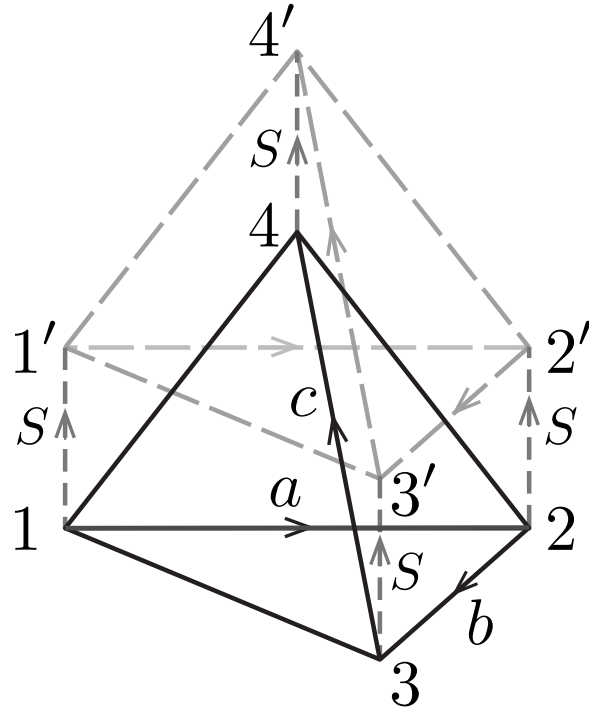


Figure 2-3: Geometric meaning of 3-cocycle $\beta_s(c, b, a)$ corresponds to evolution (along fourth dimension) of tetrahedron $[1234]$ to $[1'2'3'4']$.

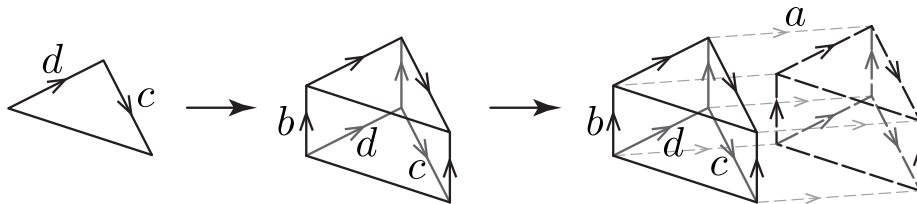


Figure 2-4: Evolution from a triangle to a 4D manifold. Phase associated with this colored manifold is $\gamma_{a,b}^\varepsilon(c, d)$, where $\varepsilon = \text{sgn}[\det(\vec{d}, \vec{c}, \vec{b}, \vec{a})]$. This phase can also be written as $\gamma_{b,a}^{\varepsilon'}(c, d)$, where $\varepsilon' = \text{sgn}[\det(\vec{d}, \vec{c}, \vec{a}, \vec{b})] = -\varepsilon$. So, we conclude that $\gamma_{a,b}(c, d) = \gamma_{b,a}^{-1}(c, d)$.

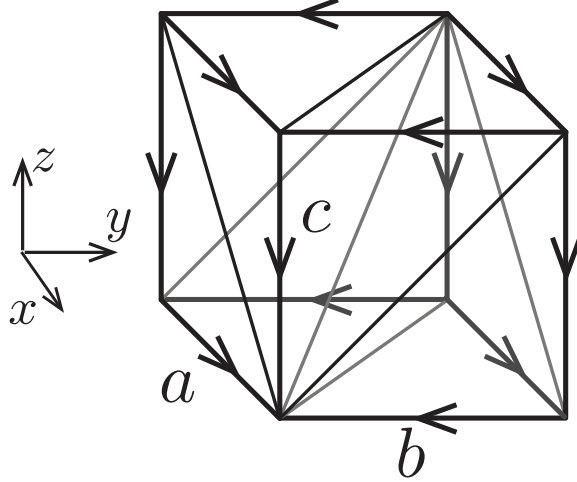


Figure 2-5: The simplest triangulation of three-torus has a single vertex and three independent edges. Periodic boundary conditions are imposed on the cube.

and $\varepsilon = \text{sgn}[\det(\vec{a}, \vec{b}, \vec{c}, \vec{s})]$. Using the 4-cocycle condition for ω , it is straightforward to show that β_s is a 3-cocycle. This shows that lifting all vertices of a tetrahedron produces a quantum phase which is only a 3-cocycle, for any given ω .

Another quantity that appears naturally from a cubic geometry is $\gamma_{a,b}$, whose geometric meaning is shown in Fig. 2-4. It is defined from the 3-cocycle β_a as:

$$\gamma_{a,b}(c, d) = \frac{\beta_a(b, c, d)\beta_a(c, d, b)}{\beta_a(c, b, d)}. \quad (2.8)$$

It is straightforward to show that $\delta\gamma_{a,b}(c, d, e) = 1$, namely, $\gamma_{a,b}$ is a 2-cocycle (see Section 2.7). Further, from Eq.(2.7) and Eq.(2.8), one can show that $\gamma_{a,b}(c, d) = \gamma_{b,a}^{-1}(c, d)$. This equality follows also from the geometry in Fig. 2-4.

2.3 Ground state on three-torus and membrane operators

2.3.1 Exact models on three-torus

We now put our model, Eq. (2.6), on the three-torus in 3+1D. It is important to note that the exactly solvable model has correlation length zero. Therefore, we can

consider the simplest triangulation of a three-torus shown in Fig.2-5. All eight cube vertices are identical due to periodic boundary conditions. It is triangulated by six tetrahedrons. There are three independent edges, which are assigned group elements $a, b, c \in G$, with G a finite group. Edges with the same direction share the same group element value. The corresponding quantum state is labeled by $|a, b, c\rangle$. We also require G to be Abelian for simplicity.

Since there is only one vertex, we denote the plaquette operator \hat{B}_p simply as \hat{B} , which equals $\frac{1}{|G|} \sum_{s \in G} B^s$. The action of B^s on state $|a, b, c\rangle$ is

$$\begin{aligned} B^s |a, b, c\rangle &= \frac{\gamma_{a,s}(b, c)}{\gamma_{a,s}(c, b)} |a, b, c\rangle. \\ &= \frac{\gamma_{a,b}(c, s)}{\gamma_{a,b}(s, c)} |a, b, c\rangle. \end{aligned} \tag{2.9}$$

We can directly write down the above result due to the observation that the 4D graph we obtain by acting with B^s is in fact made out of two copies of Fig. 2-4. Notice that the $U(1)$ phase obtained by action of B^s is a fully antisymmetric function of a, b, c, s , as can be seen both geometrically and algebraically.

2.3.2 MES as ground state basis

Let us first briefly review topological order in 2+1D. It is partially characterized by ground state degeneracy on torus.[154] One can understand this degeneracy by applying Wilson loop operators of distinct topological excitations winding around one of non-contractible loops on the torus. From this point of view, one can see that GSD equals the number of distinct topological superselection sectors.

Non-chiral topological order is fully determined by braiding statistics and topological spin of its topological excitations.[155] Remarkably, one can read the information about excitations from ground state by using modular transformations[150, 170], namely, by considering the \mathcal{S}, \mathcal{T} matrices of the S, T transformation in the ground state manifold. Dimension of \mathcal{S}, \mathcal{T} equals the number of topological sectors. In a proper ground state basis, we can obtain the ‘‘canonical form’’ of \mathcal{S}, \mathcal{T} matrices, for

which the entries of \mathcal{S} matrix are the braiding statistics and the diagonal elements of \mathcal{T} are the topological spins of quasiparticles. Ground state basis for canonical \mathcal{S}, \mathcal{T} matrices is formed by minimal entropy state (MES).[170]

We can extend these concepts to 3+1D. However, there is a major difference in this case: Topological excitations can be flux loops in 3+1D. Without loss of generality, we only consider the MES in z direction.

Inspired by the case of 2+1D cohomological gauge theories discussed in Ref.[66], we have found the MES in z direction as

$$|a, b, \lambda\rangle = \frac{1}{\sqrt{|G|}} \sum_{c \in G} \tilde{\chi}_\lambda^{a,b}(c) |a, b, c\rangle, \quad (2.10)$$

where $\tilde{\chi}_\lambda^{a,b}$ is a one-dimensional projective representation. Here, λ labels different projective representations of the group G , and the 2-cocycle γ from Eq. (2.8) plays the role of factor-system of these projective representations:

$$\tilde{\chi}_\lambda^{a,b}(c_1) \tilde{\chi}_\lambda^{a,b}(c_2) = \gamma_{a,b}(c_1, c_2) \tilde{\chi}_\lambda^{a,b}(c_1 c_2). \quad (2.11)$$

We will only consider the case of Abelian (one-dimensional) projective representations $\chi^{a,b}$ in this paper. This assumption implies that the 2-cocycle $\gamma_{a,b}$ is a 2-coboundary. We believe this is related to the physical assumption of Abelian statistics of loops.

Firstly, we verify that this state is indeed in the ground state manifold. Acting with projection operator \hat{B} on the state, we get

$$\begin{aligned} \hat{B}|a, b, \lambda\rangle &= \frac{1}{\sqrt{|G|^3}} \sum_{c \in G} \tilde{\chi}_\lambda^{a,b}(c) \sum_{s \in G} B^s |a, b, c\rangle \\ &= \frac{1}{\sqrt{|G|^3}} \sum_c \tilde{\chi}_\lambda^{a,b}(c) \cdot \frac{\gamma_{a,b}(c, s)}{\gamma_{a,b}(s, c)} |a, b, c\rangle \\ &= \frac{1}{\sqrt{|G|}} \sum_c \tilde{\chi}_\lambda^{a,b}(c) |a, b, c\rangle \\ &= |a, b, \lambda\rangle, \end{aligned} \quad (2.12)$$

where the second row uses Eq.(2.9), and in the third row we used $\gamma_{a,b}(c, s) = \gamma_{a,b}(s, c)$

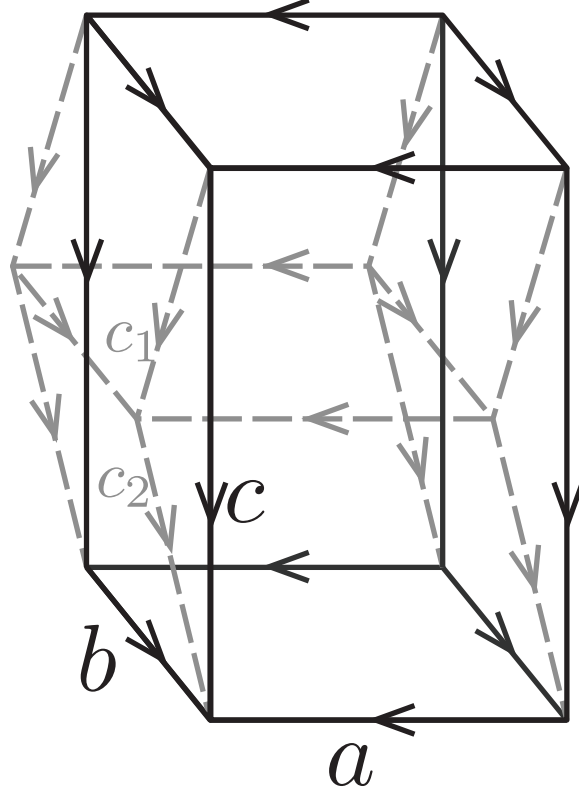


Figure 2-6: Evolution from single vertex to two vertices.

which follows from the above mentioned assumptions.

Next, we prove that this state is indeed an MES in z direction. Let us retriangulate the three-torus, so that it has two unit-cells in z direction. The ground state defined on this two unit-cell system can be evolved from that in one unit-cell, as shown in Fig. 2-6:

$$\begin{aligned}
 |a, b, \lambda\rangle &= \frac{1}{\sqrt{|G|}} \sum_{c \in G} \tilde{\chi}_\lambda^{a,b}(c) |a, b, c\rangle \\
 &= \frac{1}{\sqrt{|G|}} \sum_{c_1, c_2 \in G} \tilde{\chi}_\lambda^{a,b}(c_2 \cdot c_1) \gamma_{a,b}(c_2, c_1) |a, b, c_1, c_2\rangle \\
 &= \frac{1}{\sqrt{|G|}} \sum_{c_1} \tilde{\chi}_\lambda^{a,b}(c_1) \sum_{c_2} \tilde{\chi}_\lambda^{a,b}(c_2) |a, b, c_1, c_2\rangle.
 \end{aligned} \tag{2.13}$$

As seen from the above, $|a, b, \lambda\rangle$ defined on two unit-cells can be written as a direct product state. So, entanglement entropy of this state in z direction is zero, which must be minimum. We therefore conclude that this state is indeed an MES in z

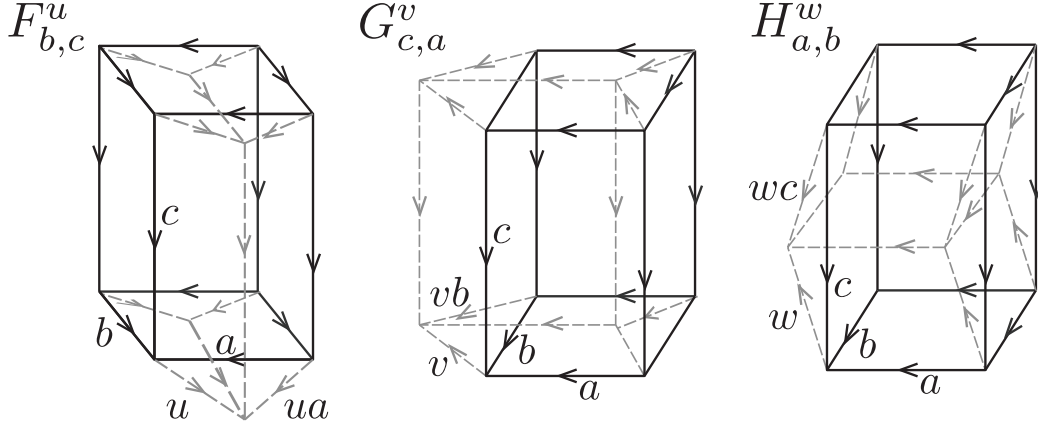


Figure 2-7: The action of membrane operators.

direction.

Similarly, it is easy to write down the MES in x and y directions:

$$|\mu, b, c\rangle = \frac{1}{\sqrt{|G|}} \sum_{a \in G} \tilde{\chi}_\mu^{b,c}(a) |a, b, c\rangle, \quad (2.14)$$

$$|a, \nu, c\rangle = \frac{1}{\sqrt{|G|}} \sum_{b \in G} \tilde{\chi}_\nu^{c,a}(b) |a, b, c\rangle, \quad (2.15)$$

whose properties can be derived in the same way as above.

2.3.3 Membrane operator

Although we constructed the MES in 3+1D, the physical picture is still unclear. Recall that in 2+1D all MES can be obtained from inserting ribbon operators (Wilson loop operators) into “trivial” MES, which corresponds to topological trivial sector. In the following we will show that membrane operators are the relevant operators for such a procedure in 3+1D.

Let us start with the MES in z direction, $|a, b, \lambda\rangle$. Characteristically in discrete gauge theory, we can interpret a group element as a label of flux-loop (or label of a membrane, which is the analogue of Dirac string in 3+1D), while a group representation labels a particle.[3] Then $|a, b, \lambda\rangle$ can be viewed as state with membrane a in yz plane and membrane b in zx plane, as well as string λ (world-line of particle) in z

direction. So, it is natural to define trivial MES as

$$|e, e, \mathbb{1}\rangle = \frac{1}{\sqrt{|G|}} \sum_{c \in G} |e, e, c\rangle, \quad (2.16)$$

where $e \in G$ is identity element. Here $\mathbb{1}$ means the trivial linear representation.

The central question becomes: What are the operators that send one MES to another? It is natural to assume that these operators correspond to membrane insertion in yz and zx plane, as well as string insertion in z direction. Besides, we expect that a string in $x(y)$ direction can measure a membrane in $yz(xz)$ plane while membrane in xy plane will measure strings in z direction.

Following this intuition, we define membrane insertion operators in yz , zx , xy planes, respectively, as shown in Fig. 2-7:

$$\begin{aligned} F_{b',c'}^u |a, b, c\rangle &= \delta_{bb'} \delta_{cc'} \cdot \gamma_{b,c}^{-1}(u, a) |ua, b, c\rangle, \\ G_{c',a'}^v |a, b, c\rangle &= \delta_{cc'} \delta_{aa'} \cdot \gamma_{c,a}^{-1}(v, b) |a, vb, c\rangle, \\ H_{a',b'}^w |a, b, c\rangle &= \delta_{aa'} \delta_{bb'} \cdot \gamma_{a,b}^{-1}(w, c) |a, b, wc\rangle, \end{aligned} \quad (2.17)$$

where u, v, w label the spatial planes of the membranes. Further, we can define

$$\begin{aligned} F_{u,\lambda}^{(z)} &= \sum_{b,c \in G} \tilde{\chi}_\lambda^{u,b}(c) F_{b,c}^u, \\ G_{v,\lambda}^{(z)} &= \sum_{c,a \in G} \tilde{\chi}_\lambda^{a,v}(c) G_{c,a}^v, \end{aligned} \quad (2.18)$$

where we interpret $F_{u,\lambda}^{(z)}$ as inserting membrane u (in yz plane) and string $\tilde{\chi}_\lambda^{u,b}$ in z direction, and interpret $G_{v,\lambda}^{(z)}$ as inserting membrane v (in zx plane) and string $\tilde{\chi}_\lambda^{a,v}$ in z direction. To confirm this, we act with these operators on state $|e, e, \mathbb{1}\rangle$, getting

$$\begin{aligned} F_{u,\lambda}^{(z)} |e, e, \mathbb{1}\rangle &= |u, e, \lambda\rangle \\ G_{v,\lambda}^{(z)} |e, e, \mathbb{1}\rangle &= |e, v, \lambda\rangle. \end{aligned} \quad (2.19)$$

It is not hard to obtain the ‘‘fusion rule’’ of membranes and strings, namely

$$\begin{aligned} F_{u_1, \lambda_1}^{(z)} F_{u_2, \lambda_2}^{(z)} &= F_{u_1 u_2, \lambda_3}^{(z)}, \\ G_{v_1, \lambda_1}^{(z)} G_{v_2, \lambda_2}^{(z)} &= G_{v_1 v_2, \lambda_3}^{(z)}, \end{aligned} \quad (2.20)$$

and

$$\begin{aligned} F_{u, \lambda_1}^{(z)} G_{v, \lambda_2}^{(z)} |a, b, \lambda\rangle &= |ua, vb, \lambda_3\rangle \\ G_{v, \lambda_1}^{(z)} F_{u, \lambda_2}^{(z)} |a, b, \lambda\rangle &= |ua, vb, \lambda_3\rangle, \end{aligned} \quad (2.21)$$

by using the properties of the 2-cocycle γ . Namely, assume $\tilde{\chi}_\mu^{a,b}$ is a projective representation with factor system $\gamma_{a,b}$,

$$\tilde{\chi}_\mu^{a,b}(c_1) \cdot \tilde{\chi}_\mu^{a,b}(c_2) = \gamma_{a,b}(c_1, c_2) \cdot \tilde{\chi}_\mu^{a,b}(c_1 \cdot c_2). \quad (2.22)$$

Then it follows that

$$\begin{aligned} \tilde{\chi}_{\mu_1}^{a,b_1}(c) \tilde{\chi}_{\mu_2}^{a,b_2} \gamma_{a,c}(b_1, b_2) &= \tilde{\chi}_{\mu_3}^{a,b_1 b_2}(c) \\ \tilde{\chi}_{\mu_1}^{a_1,b}(c) \tilde{\chi}_{\mu_2}^{a_2,b} \gamma_{c,b}(a_1, a_2) &= \tilde{\chi}_{\mu_3}^{a_1 a_2, b}(c) \end{aligned} \quad (2.23)$$

Similarly to the above derivations, we can define

$$\begin{aligned} H_{w,\mu}^{(x)} &= \sum_{a,b} \tilde{\chi}_\mu^{b,w}(a) H_{a,b}^w, \\ H_{w,\mu}^{(y)} &= \sum_{a,b} \tilde{\chi}_\nu^{w,a}(b) H_{a,b}^w, \end{aligned} \quad (2.24)$$

where $H^{(x)}(H^{(y)})$ creates membrane in xy plane and string in $x(y)$ direction. Acting

with these operators on MES in z direction, we get

$$\begin{aligned} H_{w,\mu}^{(x)}|a, b, \lambda\rangle &= \frac{\tilde{\chi}_\mu^{b,w}(a)}{\tilde{\chi}_\lambda^{a,b}(w)}|a, b, \lambda\rangle, \\ H_{w,\nu}^{(y)}|a, b, \lambda\rangle &= \frac{\tilde{\chi}_\nu^{w,a}(b)}{\tilde{\chi}_\lambda^{a,b}(w)}|a, b, \lambda\rangle. \end{aligned} \quad (2.25)$$

It is then natural to interpret $H^{(x)}(H^{(y)})$ as operator that measures strings in z direction and membrane in $yz(zx)$ plane.

We will also write down the remaining two operators that send MES to MES for later convenience:

$$\begin{aligned} F_{u,\nu}^{(y)} &= \sum_{b,c} \tilde{\chi}_\nu^{c,u}(b) F_{b,c}^u, \\ G_{v,\mu}^{(x)} &= \sum_{c,a} \tilde{\chi}_\mu^{v,c}(a) G_{c,a}^v. \end{aligned} \quad (2.26)$$

2.4 Topological observables and their physical interpretation

2.4.1 \mathcal{S} and \mathcal{T} matrices from modular transformations

In this section, we will calculate the Berry phase of ground states obtained during modular transformations. The derivation is largely a higher dimensional generalization of 2+1D case in Ref.[66].

In real space, we can write the modular transformations, Fig. 2-1b, as

$$\mathcal{S} = \begin{pmatrix} 0 & 0 & 1 \\ 1 & 0 & 0 \\ 0 & 1 & 0 \end{pmatrix}, \mathcal{T}^{31} = \begin{pmatrix} 1 & 0 & 0 \\ 0 & 1 & 0 \\ 1 & 0 & 1 \end{pmatrix}. \quad (2.27)$$

The question is what is the action of \mathcal{S} and \mathcal{T} on our exact models? We follow the strategy of Ref.[66], but generalize it to 3+1D. We consider a $T^3 \times [0, 1]$ manifold (T^3 is three-torus), and put the initial ground state at $T^3 \times 0$, final state at $T^3 \times 1$. Then we

carefully triangulate the 4D manifold $T^3 \times [0, 1]$ and compute the quantum amplitude from the initial to the final state. After lengthy but straightforward calculations, we find:

$$\begin{aligned} S|a, b, c\rangle &= |b, c, a\rangle \\ T^{31}|a, b, c\rangle &= \beta_b^{-1}(a, a^{-1}c, a)|a, b, a^{-1}c\rangle. \end{aligned} \quad (2.28)$$

Now we act by T^{31} on MES in z direction:

$$\begin{aligned} T^{31}|a, b, \lambda\rangle &= \frac{1}{\sqrt{|G|}} \sum_c \tilde{\chi}_\lambda^{a,b}(c) \beta_b^{-1}(a, a^{-1}, a) |a, b, a^{-1}c\rangle \\ &= \tilde{\chi}_\lambda^{a,b}(a) |a, b, \lambda\rangle. \end{aligned} \quad (2.29)$$

We can see that $|a, b, \lambda\rangle$ is indeed an eigenstate of \mathcal{T} matrix.

We can also get \mathcal{S} matrix element in z -direction MES basis:

$$\begin{aligned} \langle a', b', \lambda' | S | a, b, \lambda \rangle & \\ &= \frac{1}{|G|} \sum_{c, c'} \frac{\tilde{\chi}_\lambda^{a,b}(c)}{\tilde{\chi}_{\lambda'}^{a',b'}(c')} \langle a', b', c' | b, c, a \rangle \\ &= \frac{1}{|G|} \frac{\tilde{\chi}_\lambda^{a,b}(b')}{\tilde{\chi}_{\lambda'}^{a',b'}(a)} \cdot \delta_{a'b}. \end{aligned} \quad (2.30)$$

Taking into account our assumption that $\gamma_{a,b}$ is a 2-coboundary, the projective representation $\tilde{\chi}$ can be rewritten as $\tilde{\chi}_\mu^{ab}(g) = \varepsilon_{ab}(g) \cdot \chi_\mu(g)$, where $\chi_\mu(g)$ is an ordinary linear representation of G , and ε_{ab} is a 1-cocycle for which $\gamma_{a,b} = \delta\varepsilon_{ab}$ (see Section 2.7). Then we get a factorized form:

$$\langle a', b', \lambda' | S | a, b, \lambda \rangle = \frac{1}{|G|} \frac{\chi_\lambda^{a,b}(b')}{\chi_{\lambda'}^{a',b'}(a)} \cdot \frac{\varepsilon_{ab}(b')}{\varepsilon_{a'b'}(a)} \cdot \delta_{a'b}. \quad (2.31)$$

While the physical meaning of this element is not so clear for general case, it is instructive to see the simple case where $a' = b = e$. Then the 1-cocycle part of Eq.(2.31) is trivial and only $\chi_\lambda(b')/\chi_{\lambda'}(a)$ is left. We can interpret this phase

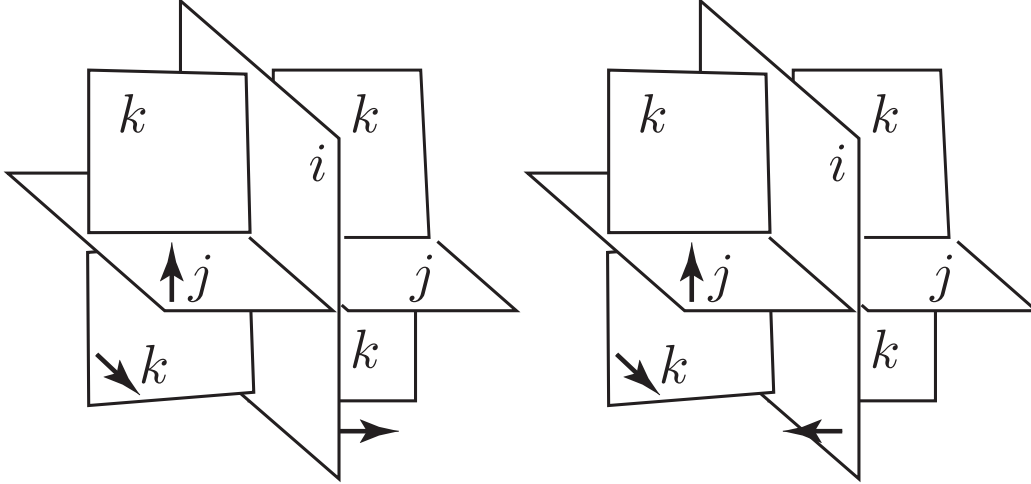


Figure 2-8: A positive triple point (left) and a negative triple point (right), where we denote the orientations of sheets by their normals.

as Aharonov-Bohm phase of particles going around a flux loop in three dimensions, namely, particle λ sees flux loop b' and particle λ' sees flux loop a . In the following, we will show how the most general form of \mathcal{S} matrix element, including the 1-cocycle contribution, can be interpreted as statistics of flux loops as well as particles.

2.4.2 Braiding statistics and \mathcal{S} matrix

In this section, we will show that the membrane operator algebra gives \mathcal{S} matrix elements. We will then interpret the membrane expression as a process involving a triple linking of worldsheets in 3+1D. Finally, we will identify such a process having certain triple linking as a particular braiding process of loops.

Before continuing, we briefly summarize the triple linking number (TLN) invariant.

Introduction to triple linking number

The triple linking number $Tlk_{ijk}(F)$ of oriented (two-dimensional) surface F smoothly embedded in four dimensions was defined in Ref.[16] as an analogue of the linking number of classical links. The indices i, j, k label three components of the surface F . In our case, they label the three flux-loop worldsheets in 3+1D.

$Tlk_{ijk}(F)$ is an integer topological invariant.[17] It can be non-zero only if the components i, j, k are distinct, and the Tlk obey the relations

$$\begin{aligned} Tlk_{123}(F) + Tlk_{231}(F) + Tlk_{312}(F) &= 0, \\ Tlk_{123}(F) + Tlk_{321}(F) &= 0, \end{aligned} \tag{2.32}$$

and are therefore fully determined by two integers. [17] Concretely, we choose:

$$\begin{aligned} a &\equiv Tlk_{123}(F) \\ b &\equiv Tlk_{132}(F), \end{aligned} \tag{2.33}$$

which implies $Tlk_{321}(F) = -a$, $Tlk_{231}(F) = -b$, $Tlk_{213}(F) = a - b$, $Tlk_{312}(F) = b - a$.

There are different ways to calculate the TLN.[17] We describe the one that is most convenient for the braiding problem: One projects the surface F from 3+1D onto a three-dimensional slice using an arbitrary projection direction, and looks for triple-points, namely, points in the projected manifold where all three projected components intersect. For each triple point s one checks the stacking order of surface components along the projection vector, and assigns the label of top component to i_s , the middle to j_s , and the bottom to k_s . Finally, the sign ϵ_s is calculated as the handedness of the three i_s, j_s, k_s surface normals at the point s , see Fig. 2-8. Having this information, $Tlk_{ijk}(F)$ equals the sum of ϵ_s over the points s for which $i_s = i, j_s = j, k_s = k$. If no triple point contributes to a certain choice ijk , then $Tlk_{ijk} = 0$, and this has to be consistent with other values of $i'j'k'$ according to relations Eq. (2.32).

The number of triple points and the stacking order of components both depend on the chosen projection vector in 3+1D, however the resulting TLN is topologically invariant.

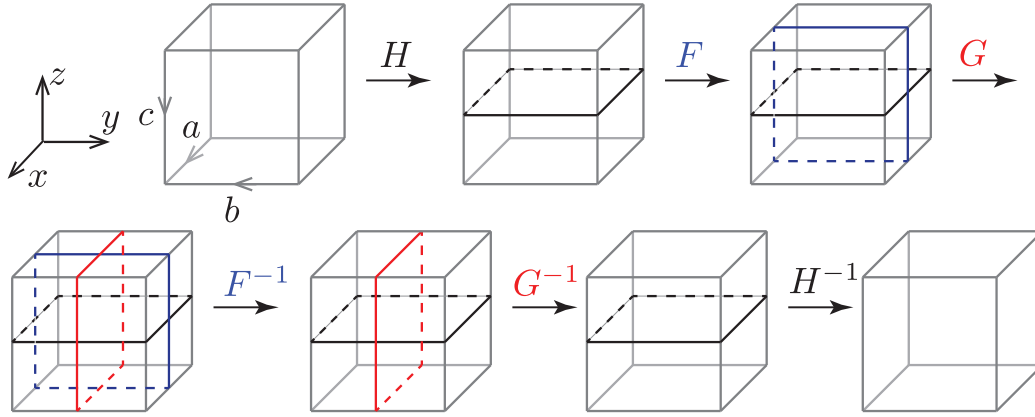


Figure 2-9: Movie for process $H^{-1}G^{-1}F^{-1}GFH$. The worldsheets in this process share the same topological properties as the three-flux-loop braiding process in Fig. 2-11.

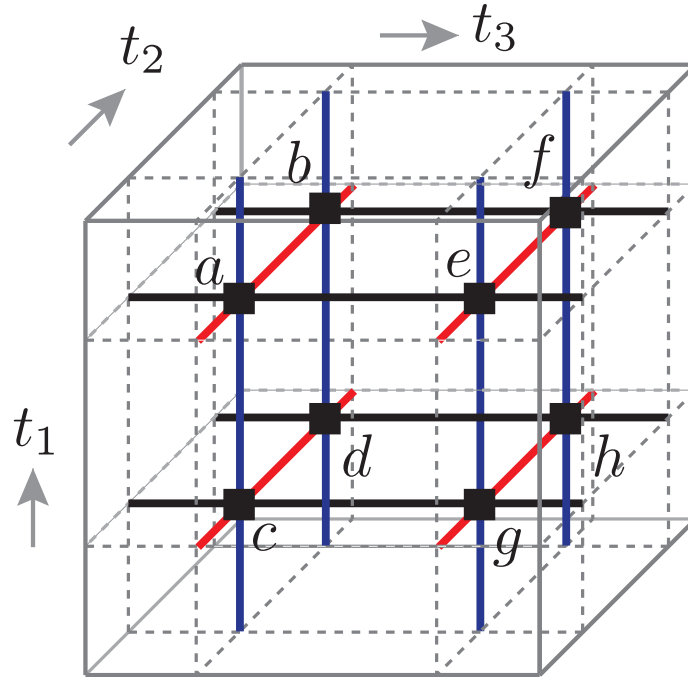


Figure 2-10: Projection of the membrane process movie to three-dimensional space at $t = -\infty$. Lines show the pairwise intersections of projected worldsheets. Black lines: for F and H worldsheets; Blue: for F and G ; Red: for G and H . Although there are eight triple points here, the triple linking is still the same as for the three-flux-loop braiding process, Fig. 2-12. The directions $t_{1,2,3}$ show the time ordering of contributions to projection from worldsheets H, F, G , so clarify to which Tlk_{ijk} some triple point contributes (see after Eq. (2.33)). For example, at point a , direction of t_1, t_2, t_3 shows that worldsheet projection at this point comes from: H^{-1} rather than H , F rather than F^{-1} , G rather than G^{-1} , respectively. Therefore point a contributes to Tlk_{132} .

Braiding statistics from membrane operator algebra

The algebra of membrane operators follows from their definition:

$$\begin{aligned} G_{v,\mu}^{(x)} F_{u,\nu}^{(y)} |a, b, c\rangle &= \frac{\tilde{\chi}_\nu^{c,u}(b) \tilde{\chi}_\mu^{v,c}(ua)}{\gamma_{b,c}(u, a) \gamma_{c,ua}(v, b)} |ua, vb, c\rangle, \\ F_{u,\nu}^{(y)} G_{v,\mu}^{(x)} |a, b, c\rangle &= \frac{\tilde{\chi}_\mu^{v,c}(a) \tilde{\chi}_\nu^{c,u}(vb)}{\gamma_{c,a}(v, b) \gamma_{vb,c}(u, a)} |ua, vb, c\rangle. \end{aligned} \quad (2.34)$$

One may ask is it possible to capture a braiding process through membrane operators, similarly to the 2+1D case of particle tunneling operators capturing their braiding.[154] The answer is yes. Actually, Fig. 2-9 depicts this process as a sequence of time events, using membrane operators defined above.

The quantum amplitude related to the “movie” in Fig. 2-9 can be expressed as $\langle H^{-1}G^{-1}F^{-1}GFH \rangle$, where the expectation value is obtained in state $|e, e, e\rangle$. Here we assign $H = H_{e,e}^w$, $G = G_{v,\mu}^{(x)}$ and $F = F_{u,\nu}^{(y)}$ for simplicity. Using Eq.(2.34), it is straightforward to get

$$\langle H^{-1}G^{-1}F^{-1}GFH \rangle = \frac{\tilde{\chi}_\mu^{v,w}(u)}{\tilde{\chi}_\nu^{w,u}(v)}. \quad (2.35)$$

We can see that the quantum amplitude equals \mathcal{S} matrix element $\langle w, u, \nu | S | v, w, \mu \rangle$ up to factor $|G|!$

A key question now becomes: What is a robust physical characterization of the process captured by the non-trivial membrane operator algebra? The answer is that in this process worldsheets of loops, which are represented by membrane operators, have a non-trivial TLN. First, we denote the worldsheet components H, F, G as 1, 2, 3, respectively. To calculate the value of TLN, we project the 4D “movie” onto the three-dimensional slice at time $t = -\infty$, and find eight triple intersection points of the projected worldsheets, Fig. 2-10. For simplicity of presentation, we offset the spatial position of inserted operator and its inverse, i.e., the membrane is moved slightly between the time of its appearance and disappearance. We checked that this does not influence the result. A straightforward calculation from each triple point gives: $b : Tlk_{123} = 1$, $a, e, f : Tlk_{132} = 1$, $d : Tlk_{231} = -1$, $c, g, h : Tlk_{321} = -1$. The

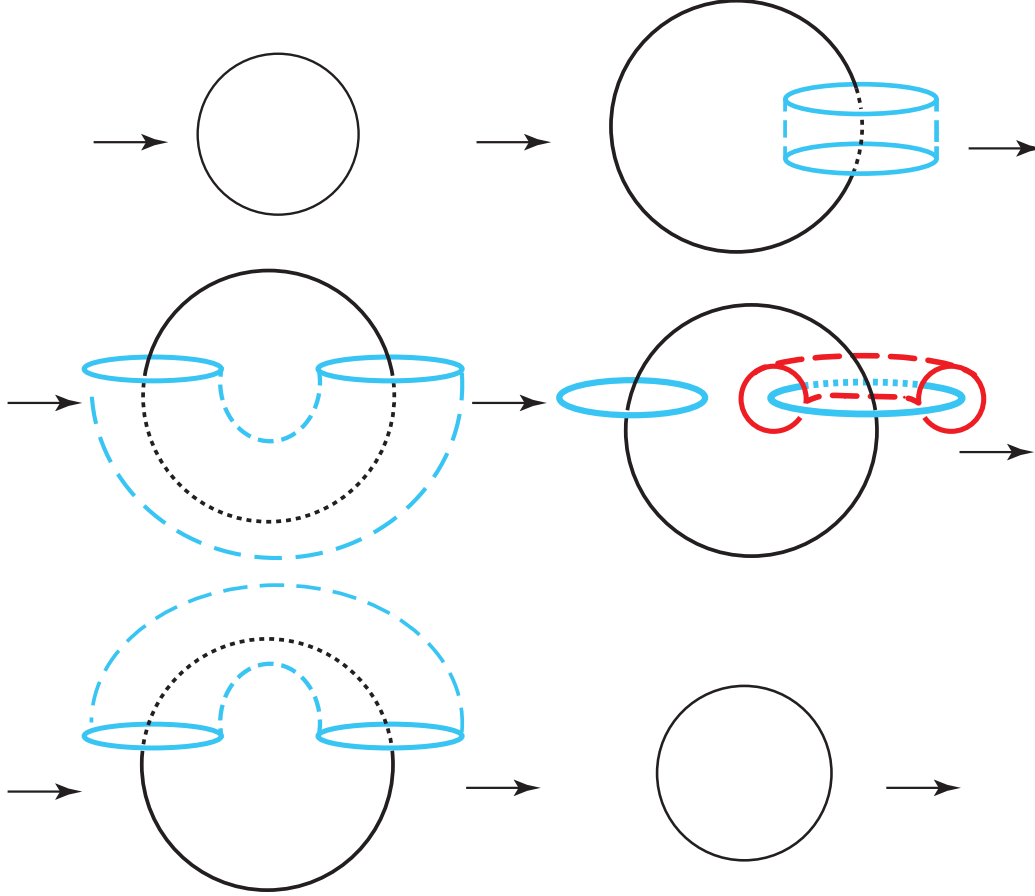


Figure 2-11: Movies for three-flux-loop braiding. This process has nontrivial triple linking number of three worldsheets. Firstly, loop 1 (black) is created and grows (the black anti-loop is irrelevant and omitted here). Then loop 2 (blue) emerges, encircling loop 1 halfway. Then loop 3 (red) completely encircles loop 2. After this, loop 2 finishes the route around loop 1. Finally, loop 1 shrinks.

obtained values of Tlk_{ijk} are consistent (Eq. (2.32)).

The membrane expression is therefore characterized by $a = 1, b = 1$, see Eq. (2.33).

Braiding process for flux loop

The membrane operators can in some sense be seen as representing an instantaneous event of creating a loop and expanding it until it shrinks in the periodic system. However, this kind of worldsheet evolution can be smoothly deformed to represent a more physically clear process. We therefore make a movie of three-flux-loop braiding process that gives exactly the same nontrivial triple linking number as the membrane process, as shown in Fig. 2-11. By projecting this braiding movie, we get Fig. 2-12,

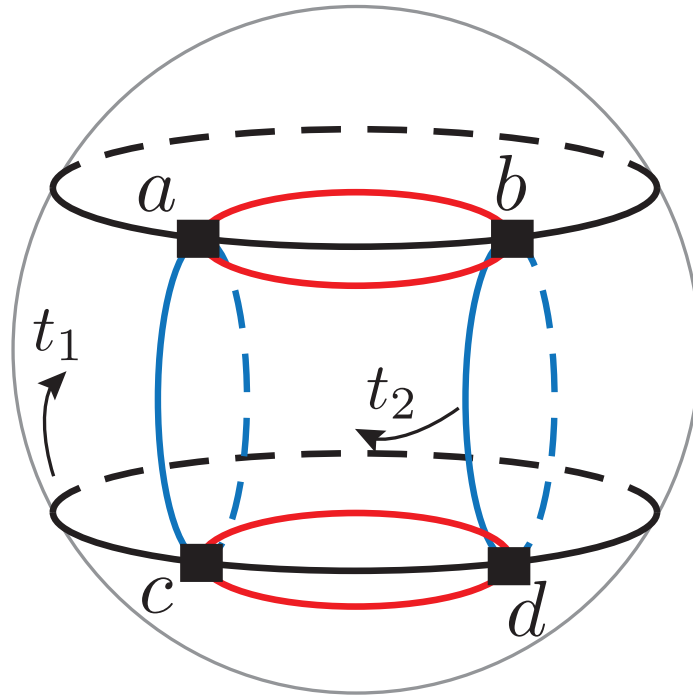


Figure 2-12: (color online) Movie in Fig. 2-11 projected to three-dimensional space at $t = -\infty$. Triple points are marked a, b, c, d . Lines show the pairwise intersections of the projected worldsheet components. Black lines: intersection of projected 1 and 2 worldsheet components; Blue lines: for 2 and 3; Red lines: 1 and 3. The projected component 1 in this figure takes the form of the sphere; 2 and 3 take the form of tori (not shown). The directions $t_{1,2}$ show the time ordering of contributions to projection from worldsheets 1, 2, so clarify to which Tlk_{ijk} some triple point contributes (see after Eq. (2.33)). For example, at point b , t_1, t_2 show that projection of 2 at this point comes from earlier time than 1 (3 is always between them), contributing to Tlk_{132} . This process has same triple linking number as the one in Fig. 2-10.

in which it is straightforward to measure the TLN: Triple point a gives $\text{Tlk}_{123} = 1$, triple point b gives $\text{Tlk}_{132} = 1$, triple point c gives $\text{Tlk}_{231} = -1$ and triple point d gives $\text{Tlk}_{321} = -1$. Again, the obtained values of Tlk_{ijk} are consistent (Eq. (2.32)).

It follows that the three-flux-loop braiding is characterized by $a = 1, b = 1$ (using Eq. (2.33)), which exactly matches the membrane calculation result.

2.5 Examples

Here we will present the example of $G = Z_2 \times Z_2$ cohomological gauge theories. Since $H^4(G, U(1)) = Z_2 \times Z_2$, they can represent different topological orders. This will show how the loop statistics can distinguish different topological orders.

It is convenient to label group G elements a as (a_1, a_2) , where $a_i \in \{0, 1\}$. Group multiplication rule $a \cdot b$ is defined as $(\langle a_1 + b_1 \rangle, \langle a_2 + b_2 \rangle)$, where we introduce notation $\langle x \rangle \equiv x \pmod{2}$.

Since the cohomology group is $H^4(Z_2 \times Z_2, U(1)) \cong Z_2 \times Z_2$, it can be parametrized by 4-cocycles

$$\{\omega_{ij} | i, j = 0, 1\}, \quad (2.36)$$

with multiplication rule

$$\omega_{ij}(a, b, c, d) \cdot \omega_{i'j'}(a, b, c, d) = \omega_{\langle i+i' \rangle \langle j+j' \rangle}(a, b, c, d). \quad (2.37)$$

The explicit form of these 4-cocycles is[26]

$$\begin{aligned} \omega_{00}(a, b, c, d) &= 1, \\ \omega_{01}(a, b, c, d) &= \exp\left[\frac{i\pi}{2} a_1 b_2 (c_2 + d_2 - \langle c_2 + d_2 \rangle)\right], \\ \omega_{10}(a, b, c, d) &= \exp\left[\frac{i\pi}{2} a_2 b_1 (c_1 + d_1 - \langle c_1 + d_1 \rangle)\right], \\ \omega_{11}(a, b, c, d) &= \omega_{01}(a, b, c, d) \cdot \omega_{10}(a, b, c, d). \end{aligned} \quad (2.38)$$

It is straightforward to check that these ω indeed satisfy the 4-cocycle condition.

One can now work out the induced 3-cocycle β_a and 2-cocycle $\gamma_{a,b}$ using their definitions in Eq.(2.7) and Eq.(2.8). For induced 3-cocycle, we get

$$\begin{aligned}\beta_{00,a}(b, c, d) &= 1, \\ \beta_{01,a}(b, c, d) &= \exp\left[\frac{i\pi}{2}(a_1b_2 - a_2b_1)(c_2 + d_2 - \langle c_2 + d_2 \rangle)\right], \\ \beta_{10,a}(b, c, d) &= \exp\left[\frac{i\pi}{2}(a_2b_1 - a_1b_2)(c_1 + d_1 - \langle c_1 + d_1 \rangle)\right], \\ \beta_{11,a}(b, c, d) &= \beta_{01,a}(b, c, d)\beta_{10,a}(b, c, d).\end{aligned}\tag{2.39}$$

It follows that the 3-cocycle β_a can be expressed as

$$\beta_a(b, c, d) = \exp\left[\frac{i\pi}{2}P_{ij}^a b_i(c_j + d_j - \langle c_j + d_j \rangle)\right],\tag{2.40}$$

where P_{ij}^a is some integer matrix. According to Ref.[37], then the induced 2-cocycle must be a coboundary $\gamma_{ab}(c, d) = \delta \varepsilon_{a,b}(c, d)$, where

$$\varepsilon_{ab}(c) = \exp\left(\frac{i\pi}{2}P_{ij}^a b_i c_j\right).\tag{2.41}$$

Altogether, for inequivalent 4-cocycles we get the induced 2-cocycle as

$$\begin{aligned}\varepsilon_{00,ab}(c) &= 1, \\ \varepsilon_{01,ab}(c) &= \exp\left[\frac{i\pi}{2}(a_1b_2c_2 - a_2b_1c_2)\right], \\ \varepsilon_{10,ab}(c) &= \exp\left[\frac{i\pi}{2}(a_2b_1c_1 - a_1b_2c_1)\right], \\ \varepsilon_{11,ab}(c) &= \varepsilon_{01,ab}(c) \cdot \varepsilon_{10,ab}(c).\end{aligned}\tag{2.42}$$

Now, we are ready to calculate statistics of loops and particles. We will focus on

$$\begin{aligned}|G| \cdot \langle w, u, \nu | S | v, w, \mu \rangle &= \frac{\tilde{\chi}_\mu^{vw}(u)}{\tilde{\chi}_\nu^{wu}(v)} \\ &= \frac{\chi_\mu(u)}{\chi_\nu(v)} \cdot \frac{\varepsilon_{vw}(u)}{\varepsilon_{wu}(v)}.\end{aligned}\tag{2.43}$$

In the second equality, we have defined

$$\begin{aligned}\tilde{\chi}_\mu^{vw}(u) &= \varepsilon_{vw}(u) \cdot \chi_\mu(u), \\ \tilde{\chi}_\nu^{wu}(v) &= \varepsilon_{wu}(v) \cdot \chi_\nu(v).\end{aligned}\tag{2.44}$$

where $\chi_\mu(\chi_\nu)$ is one-dimensional linear representation of $Z_2 \times Z_2$. One can easily check the above definition of $\tilde{\chi}_\mu$ and $\tilde{\chi}_\nu$ is consistent, due to $\gamma_{a,b}$ being a 2-coboundary. Labeling $\mu = (\mu_1, \mu_2)$ as $Z_2 \times Z_2$ group element,

$$\chi_\mu(u) = e^{i\pi(\mu_1 u_1 + \mu_2 u_2)} = e^{i\pi \vec{\mu} \cdot \vec{u}}.\tag{2.45}$$

First, let us consider the case $w = (0, 0)$. In this case, only the χ_λ factors are non-trivial in second line of Eq. (2.43), which is interpreted as contribution from Aharonov-Bohm phase of braiding particles around flux-loops. In this case, the phase factor equals $e^{i\pi(\vec{\mu} \cdot \vec{u} - \vec{\nu} \cdot \vec{v})}$, which is independent of choice of cocycle. Namely, statistics between particles and loops cannot distinguish different phases.

Then, we turn to the general case. We get an additional phase factor s_l beyond $e^{i\pi(\vec{\mu} \cdot \vec{u} - \vec{\nu} \cdot \vec{v})}$, and the s_l factor comes from ε in Eq. (2.43). In other words, it is present even when $\mu = \nu = 0$, i.e., χ representations are trivial, so there are no charged particles. Therefore, s_l represents statistics of flux-loops. We list s_l obtained from different 4-cocycles as follows

- ω_{00} : $s_l = 1$.
- ω_{01} : $s_l = e^{\frac{i\pi}{2}[u_1 v_2 + u_2 v_1]w_2 - 2u_2 v_2 w_1}$.
- ω_{10} : $s_l = e^{\frac{i\pi}{2}[(u_1 v_2 + u_2 v_1)w_1 - 2u_1 v_1 w_2]}$.
- ω_{11} : $s_l = e^{\frac{i\pi}{2}[(u_1 v_2 + u_2 v_1)(w_1 + w_2) - 2u_1 v_1 w_2 - 2u_2 v_2 w_1]}$.

We can see that flux-loop braiding can indeed distinguish different topological orders in 3+1D, recalling here that the membrane operator expression is identified with a particular type of three-flux-loop braiding. In particular, according to previous section

we can identify the flux-loops (blue, red, black) in Fig. 2-11 with fluxes (u, v, w) here, and there are no charges present.

Now, we turn to \mathcal{T} matrix element $\tilde{\chi}_\lambda^{u,v}(u) = \langle u, v, \lambda | T^{31} | u, v, \lambda \rangle$. In the same way as above, we get

- ω_{00} : $\tilde{\chi}_\lambda^{u,v}(u) = e^{i\pi\vec{\lambda}\cdot\vec{u}}$.
- ω_{01} : $\tilde{\chi}_\lambda^{u,v}(u) = e^{i\pi\vec{\lambda}\cdot\vec{u}} e^{\frac{i\pi}{2}(u_1 v_2 u_2 - u_2 v_1 u_2)}$.
- ω_{10} : $\tilde{\chi}_\lambda^{u,v}(u) = e^{i\pi\vec{\lambda}\cdot\vec{u}} e^{\frac{i\pi}{2}(u_2 v_1 u_1 - u_1 v_2 u_1)}$.
- ω_{11} : $\tilde{\chi}_\lambda^{u,v}(u) = e^{i\pi\vec{\lambda}\cdot\vec{u}} e^{\frac{i\pi}{2}(u_1 v_2 + u_2 v_1)(u_1 - u_2)}$.

While the $e^{i\pi\vec{\lambda}\cdot\vec{u}}$ can be interpreted as AB phase of particles going around loop, the remaining part also encodes information about loop statistics. While we do not have a proof at this time, we believe that this phase is related to the ribbon nature of flux loop, or in other words to a thickness of the membrane.

2.6 Discussion and conclusions

One of our main results is the construction of MES states on the three-torus for the 3+1D cohomological gauge theory, which can be trivially generalized to arbitrary number of unit-cells. The S, T transformation matrices take a simple form in this basis.

We discussed that the S -matrix elements are directly related to the braiding of loop excitations. The T -matrix elements, which are diagonal in the MES basis, correspond to the generalization of topological spin for loop excitations. Here physically the loop excitations are generally expected to be ribbon excitations with two different loop-edges. We expect that the geometrical interpretation of the T -matrix elements is related to the braiding involving different loop-edges.

Although we use exactly solvable models and 3+1D topological quantum field theories to compute their S, T matrices, these 3+1D S, T matrices are in principle

measurable quantities in practical model Hamiltonians. In particular, given a topologically ordered phase in 3+1D with its topologically degenerate ground sector on three-torus T^3 , one can firstly find a MES basis, similarly to the algorithms proposed in 2+1D.[170] For instance, for the S -matrix element between two MES $|\Xi_i\rangle$ and $|\Xi_j\rangle$: S_{ij} , one can perform the following thought numerical measurement. Because the topological properties do not depend of local geometry, we can assume that these ground states live on a cube with periodic boundary conditions. Then one can consider the state rotated by 120° along the (111) direction of the cube: $R_{120^\circ}|\Xi_i\rangle$. Because $R_{120^\circ}|\Xi_i\rangle$ and $|\Xi_j\rangle$ belong to the same topological phase, in the absence of symmetry there should exist a Hamiltonian path $H(\tau)$ ($\tau \in [0, 1]$) such that $|\Xi_j\rangle(|\Xi_i\rangle)$ are the ground state of $H(0)(H(1))$, and the ground state sectors of $H(\tau)$ are adiabatically connected. One can then define a projection operator \hat{P}_τ into the ground state sector of $H(\tau)$ for any given τ . The many-body quantum amplitude related to the adiabatic time-evolution process of the S -transformation can be computed as $\langle \Xi_j | \hat{P}_{N-1/N} \cdot \dots \cdot \hat{P}_{2/N} \cdot \hat{P}_{1/N} R_{120^\circ} | \Xi_i \rangle$ as $N \rightarrow \infty$. This computation is a realization of the topological quantum field theory time-evolution.

We expect that this quantum amplitude is related to the S -matrix elements s_{ij} at most by an overall ambiguity $U(1)$ phase $e^{i\theta}$, which is due to the non-universal local physics in the time-evolution, and a phase $e^{i\phi_i - i\phi_j}$ which is due to the gauge choice of $|\Xi_i\rangle, |\Xi_j\rangle$. Even with these ambiguities, such measurements can still be used to extract useful information about the S, T matrices which potentially could fully determine them.

Recently, there has been a lot of progress in relating topologically ordered phases to symmetry protected topological (SPT) and symmetry enriched topological (SET) phases, for example by partially or completely ungauging the gauge group G , i.e., by transformations between global and local symmetries.[86, 97, 19, 55, 166, 27, 68, 169, 161] We therefore expect that our work will be useful in characterization of SPT and SET phases too.

Finally, let us consider a trivial but ubiquitous example of $G = Z_2$. In this case, $H^4(G, U(1)) = Z_1$, so the cocycle can be set to identity map. The braiding phase

$\tilde{\chi}_\mu^{vw}(u)/\tilde{\chi}_\nu^{wu}(v)$ reduces to a linear representation $\chi_\mu(u)/\chi_\nu(v)$, where group elements $u, v = 0, 1$, and $\mu, \nu = 0, 1$ label the representations of Z_2 :

$$\chi_\mu(u) = e^{i\pi\mu u}. \quad (2.46)$$

The braiding phase therefore equals $e^{i\pi(\mu u - \nu v)}$. There is no contribution from flux-loop braiding, since the 1-cocycle factors in Eq. (2.31) are trivial. In summary, the modular S transformation for common Z_2 gauge theory in 3+1D tells us that particles see a flux-loop as a π -flux, and the flux-loops themselves have trivial braiding.

Using the MES basis and Eq. (2.29), (2.30), we directly obtain the \mathcal{S} and \mathcal{T} matrices of 3+1D Z_2 theory in their canonical form:

$$\mathcal{S} = \frac{1}{2} \begin{pmatrix} 1 & 1 & 0 & 0 & 1 & 1 & 0 & 0 \\ 1 & 1 & 0 & 0 & -1 & -1 & 0 & 0 \\ 1 & -1 & 0 & 0 & 1 & -1 & 0 & 0 \\ 1 & -1 & 0 & 0 & -1 & 1 & 0 & 0 \\ 0 & 0 & 1 & 1 & 0 & 0 & 1 & 1 \\ 0 & 0 & 1 & 1 & 0 & 0 & -1 & -1 \\ 0 & 0 & 1 & -1 & 0 & 0 & 1 & -1 \\ 0 & 0 & 1 & -1 & 0 & 0 & -1 & 1 \end{pmatrix}$$

$$\mathcal{T}^{31} = \text{Diag}(1, 1, 1, 1, 1, -1, 1, -1),$$

where the MES basis $|a, b, \lambda\rangle$, with $a, b, \lambda \in \{0, 1\}$, is here naturally ordered according to binary numbers with digits $ab\lambda$. These matrices are consistent with the \mathcal{S} and \mathcal{T} matrices derived for the same theory in Ref.[101].

2.7 Supplementary material for the cohomology group

We begin with a brief introduction to group cohomology. In this paper, we will not present the most general definition of group cohomology.

For a finite group G , and an abelian group M (M does not need to be finite or

discrete), one can consider an arbitrary function that maps n elements of G to an element in M ; $\omega : G^n \rightarrow M$ or equivalently $\omega(g_1, g_2, \dots, g_n) \in M, \forall g_1, g_2, \dots, g_n \in G$. Such a group function is called an n -cochain. The set of all n -cochains, which is denoted as $C^n(G, M)$, forms an abelian group in the usual sense: $(\omega_1 \cdot \omega_2)(g_1, g_2, \dots, g_n) = \omega_1(g_1, g_2, \dots, g_n) \cdot \omega_2(g_1, g_2, \dots, g_n)$, in which the identity n -cochain is a group function whose value is always the identity in M .

One can define a mapping δ from $C^n(G, M)$ to $C^{n+1}(G, M)$: $\forall \omega \in C^n(G, M)$, define $\delta\omega \in C^{n+1}(G, M)$ as

$$\begin{aligned} \delta\omega(g_1, \dots, g_{n+1}) &= \omega(g_2, \dots, g_{n+1}) \cdot \omega^{(-1)^{n+1}}(g_1, \dots, g_n) \\ &\times \prod_{i=1}^n \omega^{(-1)^i}(g_1, \dots, g_{i-1}, g_i \cdot g_{i+1}, g_{i+1}, \dots, g_{n+1}). \end{aligned} \quad (2.47)$$

It is easy to show that the mapping δ is nilpotent: $\delta^2\omega = 1$ (here 1 denotes the identity $(n+2)$ -cochain). In addition, for two n -cochains ω_1, ω_2 , obviously δ satisfies $\delta(\omega_1 \cdot \omega_2) = (\delta\omega_1) \cdot (\delta\omega_2)$.

An n -cochain $\omega(g_1, \dots, g_n)$ is called an n -cocycle if and only if it satisfies the condition: $\delta\omega = 1$, where 1 is the identity element in $C^{n+1}(G, M)$. When this condition is satisfied, we also say that $\omega(g_1, \dots, g_n)$ is an n -cocycle of group G with coefficients in M . The set of all n -cocycles, denoted by $Z^n(G, M)$, forms a subgroup of $C^n(G, M)$.

Not all different cocycles are inequivalent. Below we define an equivalence relation in $Z^n(G, M)$. Because δ is nilpotent, for any $(n-1)$ -cochain $c(g_1, \dots, g_{n-1})$, we can find the n -cocycle δc . And if an n -cocycle b can be represented as $b = \delta c$, for some $c \in C^{n-1}(G, M)$, b is called an n -coboundary. The set of all n -coboundaries, denoted by $B^n(G, M)$, forms a subgroup of $Z^n(G, M)$. Two n -cocycles ω_1, ω_2 are equivalent (denoted by $\omega_1 \sim \omega_2$) if and only if they differ by an n -coboundary: $\omega_1 = \omega_2 \cdot b$, where $b \in B^n(G, M)$.

The n -th cohomology group of group G with coefficients in M , $H^n(G, M)$, is formed by the equivalence classes in $Z^n(B, M)$. More precisely: $H^n(G, M) = Z^n(G, M)/B^n(G, M)$.

In this paper we will make a lot of use of 4-cocycles ω . We will always choose them to be in ‘‘canonical’’ form, which means that $\omega(g_1, g_2, g_3, g_4) = 1$ if any of g_1, g_2, g_3, g_4

is equal to $\mathbb{1}$ (the identity element of group G). For any of the inequivalent cocycles mentioned above, it is always possible to choose a gauge such that ω becomes canonical [21].

Chapter 3

Symmetry enriched topological phases and tensor network states

3.1 Introduction

In this chapter and next chapter, we develop a generic framework to write down general variational wavefunctions for a large class of symmetric topological phases using tensor network methods. In this chapter, we will mainly focus on symmetry enriched topological phases (SET phases). And in the next chapter, we will consider symmetry protected topological phases for both on-site symmetries as well as lattice symmetries.

In physical systems, one needs to consider both global symmetries and topological orders. In particular, it is very important to understand the interplay between global symmetries and the topological order. Here, we attempt to build a partial but systematic understanding of gapped quantum phases with both global symmetries and topological orders, which have been termed as SET phases. In particular, we will focus on cases with toric code type topological orders (conventional discrete gauge theory) in 2+1D. And we will consider symmetries include both on-site symmetries and lattice symmetries. We focus on a particular type of tensor networks: Projected Entangled Pairs states (PEPS). We find, in the presence of topological orders and global symmetries, PEPS states are grouped to different classes, which are related,

but not limited to different SET types. For each class, we can write down general variational wavefunctions, which are very useful for numerical simulations.

This chapter is organized as follows. In Sec.3.2, we introduce some basics of PEPS. In particular, We discuss gauge redundancy as well as the implementation of symmetries in PEPS. We introduce a special kind of gauge transformation named as invariant gauge group (*IGG*). In phases with no symmetry breaking, *IGG* leads to low-energy gauge dynamics. Further, for fractional filled systems, there are minimal required non-trivial *IGGs* for any symmetric PEPS under our basic assumption. This phenomenon is consistent with the Hastings-Oshikawa-Lieb-Schultz-Mattis theorem[61, 103, 90]. In Sec.3.3, we classify symmetric PEPS according to their distinct short-range physics, which is characterized by algebraic data Θ 's, χ 's and η 's. Relations of the data χ 's and η 's to second cohomology are discussed.

As a main example, we give the classification result for symmetric PEPS on the kagome lattice with a half-integer spin per site and $IGG = Z_2$, and obtain the constraints on the sub-Hilbert spaces for local tensors for each given class. The detailed calculation is presented in Ref.[76]. We give the physical interpretation of the algebraic data in Section 3.4. Particularly, we construct fractionalized symmetry operators to explicitly show that η 's are describing the symmetry fractionalization of spinons in the Z_2 QSL member phase. Detectable signatures of the data Θ 's, χ 's and η 's are discussed. In Sec.4.5 we consider generalizations and limitations of our study, comment on relations with previous works, and conclude.

3.2 Symmetry, Gauge and PEPS

In this section, we give a brief introduction to PEPS. As we will see later, even for the same many-body wavefunction, PEPS representations are not unique, and different representations are connected by gauge transformations. Further, we will study the implementation of symmetry on PEPS as well as the gauge dynamics in the PEPS language. Particularly, for certain systems, gauge structures will naturally emerge.

3.2.1 Introduction to PEPS

Projected Entangled Pair States (PEPS) is a type of tensor networks (TN). The basic ingredients of TN are “legs”, and every leg is associated with a Hilbert space, as seen in Fig.(3-1a). In the following, we will use “leg” to denote the associated Hilbert space. As shown in Fig(3-1b), tensors formed by several legs simply describe quantum states living in the tensor product of these legs,

$$T^{abc\dots} \in \mathbb{V}^a \otimes \mathbb{V}^b \otimes \mathbb{V}^c \otimes \dots \quad (3.1)$$

where \mathbb{V}^i labels Hilbert space associated with leg i . If two legs are the bra space and the ket space of the same set of quantum states, they are named as dual space to each other. New tensors can be obtained by contracting states in dual spaces, or by tracing out states in dual spaces, as shown in Fig.(3-1c).

A TN representation of many-body wavefunction can be viewed as a large tensor, which is obtained by contracting small building block tensors. Thus, a TN is formed by uncontracted legs (physical legs) and contracted legs (virtual legs). From another point of view, we can also treat a TN as a combination of a linear map from the virtual Hilbert space (the tensor product of all virtual legs) to the physical Hilbert space, together with an “input” virtual state.

Let us construct a PEPS on a two dimensional lattice. We first put tensors at both sites and bonds, named as site tensors (T^s) and bond tensors (B_b) respectively, see Fig.(3-1b). Every site tensor can be viewed as a linear map from several virtual legs to one physical leg, while a bond tensor, which is in fact a matrix, labels a quantum state (bond state) in the tensor product space of two virtual legs. Thus, as shown in Fig.(3-1d), by contracting virtual legs of site tensors with bond tensors, we get a PEPS as a combination of a linear map from the virtual Hilbert space to the physical Hilbert space together with an input virtual state, where the map is given by the tensor product of all site tensors and the input state is the tensor product of all bond

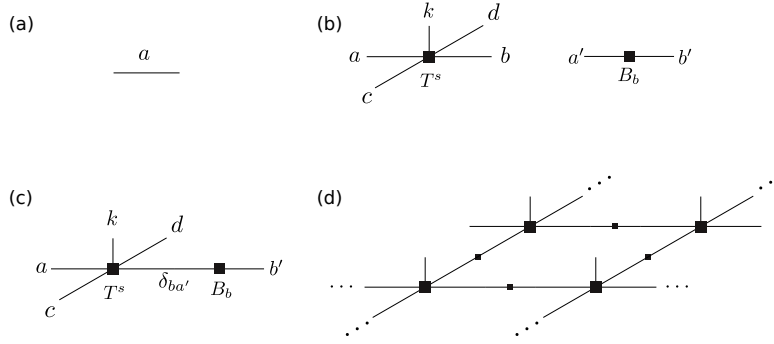


Figure 3-1: (a): The leg a is associated with the Hilbert space \mathbb{V}^a . (b): The site tensor (left) and the bond tensor (right) label quantum states on Hilbert spaces of tensor products of corresponding legs. (c): A new tensor can be obtained by contraction of the leg b on T^s and the leg a' on B_b , which can be expressed as $(T^s)_{abcd}^k (B_b)_{a'b'} \delta_{ba'}$. Note that we require leg b and leg a' to be dual spaces. (d): The whole PEPS wavefunction is obtained by contracting all virtual legs of site tensors and bond tensors.

states. We can express the PEPS representation of the wavefunction as

$$|\psi\rangle = \sum_{\{k_s\}} \text{tTr} \left((T^1)^{k_1} \dots (T^{N_s})^{k_{N_s}} B_1 \dots B_{N_b} \right) |k_1 \dots k_{N_s}\rangle, \quad (3.2)$$

where $1, 2, \dots, N_s(N_b)$ label sites (bonds), while k_s is the physical index. tTr means tensor trace, namely, contraction of all virtual legs.

We define that a bond tensor (matrix) is a maximal entangled state, iff singular values of this matrix all equal some nonzero constant. By multiplying some constant, we can simply set singular values of maximal entangled states to be 1. When performing numerical simulations, it is more convenient to use maximal entangled bond states, or even set bond tensors to be identity matrices. As we will see later, by using the gauge redundancy of PEPS, it is always possible to do so.

In the following, we will assume that all virtual legs label Hilbert spaces with the same dimension D , while a physical leg is associated with a d -dimensional Hilbert space.

3.2.2 Gauge transformation on PEPS

The representation of a many-body wavefunction on PEPS is far from unique. Particularly, as shown in Fig.(3-2), we are always allowed to multiply W and W^{-1} to two connected virtual legs respectively. This action will change the connected small tensors while leaving the contracted tensor invariant,

$$(T^s)_{abcd}^k \delta_{ba'} (B_b)_{a'b'} = [(T^s)_{abcd}^k W_{bl}] \delta_{ll'} [(W^{-1})_{l'a'}] (B_b)_{a'b'} \quad (3.3)$$

Every contracted pair of virtual legs will contribute a gauge redundancy $GL(D, \mathbb{C})$. All such gauge transformations form a group $[GL(D, \mathbb{C})]^{2N_b}$ which we call the gauge transformation group of the PEPS (N_b is the number of bond tensors in the TN). The meaning of the gauge transformation can be understood as a change of basis on virtual legs.

From another point of view, in general, for two PEPS whose tensors differ at most by gauge transformations defined above together with overall $U(1)$ phase factors, as shown in Fig.(3-2), the two PEPS must describe the same physical state (up a $U(1)$ phase). In principal, these overall $U(1)$ phase factors can occur in gauge transformations on both site tensors and bond tensors. But it is straightforward to redefine the gauge transformations such that the phase factors only appear on site tensors. Mathematically, two PEPS denoted by $\{\tilde{T}^s, \tilde{B}_b\}$ and $\{T^s, B_b\}$ respectively describe the same physical state if there exist gauge transformations $\{W(s, i)\}$ and $U(1)$ phase factors $\{e^{i\theta(s)}\}$ (s labels a site and i labels a virtual leg on the site.), such that

$$\begin{aligned} (T^s)_{\alpha\beta\dots}^k &= e^{i\theta(s)} \cdot [W(s, 1)]_{\alpha\alpha'} [W(s, 2)]_{\beta\beta'} \dots (\tilde{T}^s)_{\alpha'\beta'\dots}^k \\ (B_b)_{\alpha\beta} &= [W(b, 1)]_{\alpha\alpha'} [W(b, 2)]_{\beta\beta'} (\tilde{B}_b)_{\alpha'\beta'}. \end{aligned} \quad (3.4)$$

Here $W(b, j)$ represents a gauge transformation on the leg j of the bond tensor B_b , and if a site leg (s, i) and a bond leg (b, j) are connected, then $W(s, i) = [W(b, j)^{-1}]^t$.

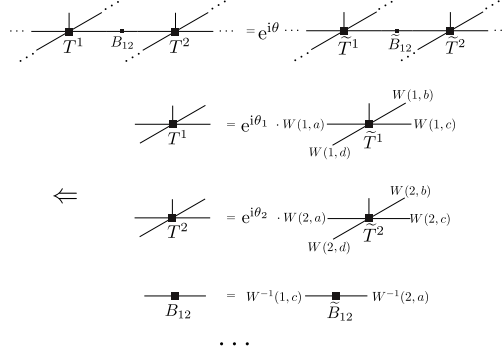


Figure 3-2: Two PEPS describe the same quantum state, iff they are differ by gauge transformation together with U(1) phase factor. The origin of the gauge transformation is that we can multiply identity matrix $I = W \cdot W^{-1}$ between connected legs, which changes site tensors and bond tensors, but leave the whole wavefunction invariant. We can also view TN on the left as PEPS transformed by symmetry operation. Thus, this figure also express the condition for PEPS wavefunction to be symmetric.

(The superscript- t stands for the matrix transpose.)

3.2.3 Symmetric PEPS

The purpose of this section is to introduce a generic way to implement both on-site symmetries[104, 171, 123, 124, 8, 149, 125] and lattice space group symmetries[104] on PEPS. We firstly discuss the finite size symmetric quantum state that can be represented by a single PEPS; i.e., such a state would form a one-dimensional representation of the symmetry group. Then we define the symmetric PEPS on an infinite lattice, which is the main object to be (partially) classified in the current study.

On-site unitary symmetries

The action of a global on-site unitary symmetry S on a finite size PEPS wavefunction is defined as

$$S|\psi\rangle = |\tilde{\psi}\rangle = \sum_{\{k_s\}} \text{tTr} \left((T^1)^{k_1} \dots (T^{N_s})^{k_{N_s}} B_1 \dots B_{N_b} \right) U_S \otimes U_S \dots |k_1 k_2 \dots k_{N_s}\rangle, \quad (3.5)$$

U_S is the representation of S on Hilbert space of physical leg. These local actions of an on-site symmetry give a new TN, with site tensors \tilde{T}^s and bond tensors \tilde{B}_b defined as,

$$\begin{aligned}\tilde{T}^s &= S \circ T^s = \sum_l (U_S)_{kl} (T^s)^l \\ \tilde{B}_b &= S \circ B_b = B_b\end{aligned}\tag{3.6}$$

We focus on those PEPS that are invariant under the global symmetry up to an overall U(1) phase factor. Following the discussion in the previous section, we consider the PEPS $|\psi\rangle$ that differs from the transformed PEPS $|\tilde{\psi}\rangle$ only by gauge transformations together with overall phase factors, as shown in Fig.(3-2):

$$\begin{aligned}T^s &= \Theta_S W_S S \circ T^s \\ B_b &= W_S S \circ B_b\end{aligned}\tag{3.7}$$

Here, gauge transformation W_S and phase factor Θ_S associated with symmetry S is defined as

$$\begin{aligned}\Theta_S \circ T^s &= e^{i\theta_S(s)} (T^s)_{\alpha\beta\gamma\delta}^k \\ W_S \circ T^s &= [W_S(s, 1)]_{\alpha\alpha'} [W_S(s, 2)]_{\beta\beta'} \dots (T^s)_{\alpha'\beta' \dots}^k \\ W_S \circ B_b &= [W_S(b, 1)]_{\alpha\alpha'} [W_S(b, 2)]_{\beta\beta'} (B_b)_{\alpha'\beta'}.\end{aligned}\tag{3.8}$$

According to the definition of a gauge transformation, if site virtual leg (s, i) and bond leg (b, j) are connected, then $W_S(s, i) = [W_S(b, j)^{-1}]^t$. Further, we always choose W_S such that only site tensors transform with extra U(1) phase factors. Note that so far we do not require matrices on the leg (s, i) $W_S(s, i)$ to form a representation of the on-site symmetry group when S is tuned. We will come back to this shortly.

Time reversal symmetry

The representation of the global time reversal symmetry \mathcal{T} on a many-body wavefunction is $U_{\mathcal{T}} \otimes U_{\mathcal{T}} \dots K$, where K denotes the complex conjugation and $U_{\mathcal{T}}$ is a unitary matrix acting on local physical Hilbert space. Its action on PEPS is defined as

$$\begin{aligned} \mathcal{T}|\psi\rangle &= \sum_{\{k_s\}} \text{tTr} \left((T^1)^{k_1} \dots (T^{N_s})^{k_{N_s}} B_1 \dots B_{N_b} \right)^* \\ &U_{\mathcal{T}} \otimes U_{\mathcal{T}} \dots |k_1 k_2 \dots k_{N_s}\rangle, \end{aligned} \quad (3.9)$$

Namely, the local actions on a single site or a bond tensor read

$$\begin{aligned} \tilde{T}^s &= \mathcal{T} \circ T^s = \sum_l (U_{\mathcal{T}})_{kl} (T^s)^{*l} \\ \tilde{B}_b &= \mathcal{T} \circ B_b = B_b^* \end{aligned} \quad (3.10)$$

We consider the PEPS that is symmetric under \mathcal{T} . Similar to the previous discussion, we consider a PEPS satisfying:

$$\begin{aligned} T^s &= \Theta_{\mathcal{T}} W_{\mathcal{T}} \mathcal{T} \circ T^s \\ B_b &= W_{\mathcal{T}} \mathcal{T} \circ B_b \end{aligned} \quad (3.11)$$

where $W_{\mathcal{T}}$ belongs to the gauge transformation group of the PEPS.

Lattice symmetry

The definition of a lattice space group symmetry R on PEPS is

$$\begin{aligned} \tilde{T}^s &= R \circ (T^s)^k \equiv \sum_{\alpha\beta\dots} (T^{R^{-1}(s)})_{R^{-1}(\alpha\beta\dots)}^k \\ \tilde{B}_b &= R \circ B_b \equiv \sum_{\alpha\beta} (B_{R^{-1}(b)})_{R^{-1}(\alpha\beta)} \end{aligned} \quad (3.12)$$

The action of R on site and bond tensor follows the natural definition of lattice symmetries. For instance, for a square lattice, after a translation along the right direction by one lattice spacing, the transformed site tensor at a given position equals the original site tensor on the left neighboring site. Note that the symmetry R not only acts on site and bond indices; it may also act nontrivially on virtual legs. For example, the 90° rotation of a site tensor on the square lattice permute the four virtual legs. Again, we consider those PEPS symmetric under R satisfying the following conditions:

$$\begin{aligned} T^s &= \Theta_R W_R R \circ T^s \\ B_b &= W_R R \circ B_b \end{aligned} \tag{3.13}$$

where W_R belongs to the gauge transformation group of the PEPS.

Symmetric PEPS on infinite lattices

Space groups of lattices are usually defined for infinite lattices. This is because for a finite size sample, the lattice symmetry group is a finite group whose group structure is non-generic. In this chapter, we will focus on PEPS on infinite lattices satisfying Eq.(3.7,3.11,3.13) under symmetry transformations. And *we define such PEPS as symmetric PEPS on infinite lattices, or simply as symmetric PEPS*. They form the main object to be (partially) classified in the current investigation.

A natural question that arises at this point is: are symmetric PEPS defined above general enough to capture ground states of quantum phases? Let us limit our discussion within those quantum phases whose entanglement entropies do not violate the boundary law so that in principle they may be represented as PEPS.

Basically, *we expect that the symmetric PEPS on infinite lattices defined above are capable to capture all non-symmetry-breaking liquid phases. After putting on finite lattices and performing a scaling with respect to both the bond dimension D and lattice sizes, we expect the symmetric PEPS are also capable to capture the neighbor-*

ing ordered phases of the liquid phases. Here by “neighboring” (or “in the vicinity below”), we mean that the symmetry breaking in these phases is only sharply defined in the thermodynamic limit (namely, in the long-range physics). Note that we do not have a proof supporting the statement above. Nevertheless we are not aware of any counterexamples, so at least it is a reasonable conjecture.¹.

Sometimes one is forced to use more than one PEPS to represent ground state quantum wavefunctions. For instance, in a quantum spin system with $SU(2)$ spin rotation symmetry, this happens for the ferromagnetic phase, whose ground states form a large spin representation. However, such ferromagnetic phases are *not* in the vicinity of any non-symmetry-breaking liquid phases.

3.2.4 Invariant gauge group and gauge structure

Among the gauge transformations, there is a special subgroup which we call the invariant gauge group (IGG). Note that generally a gauge transformation will leave the physical wavefunction invariant while transforming the site tensors and bond tensors nontrivially in a PEPS. However, by definition, the action of IGG elements on PEPS even leaves all site tensors invariant up to overall $U(1)$ phases and all bond tensors completely invariant². So IGG can be viewed as the “symmetry” of the building block tensors with actions only on virtual legs³. In the following, we will see that IGG is directly related to gauge dynamics[29, 127, 117, 127, 63]. We will also give examples where nontrivial IGG ’s emerge naturally in fractional filled systems under a basic assumption.

Note that the collection of all gauge transformations that leave all site tensors

¹On the other hand, this conjecture may be due to our current lack of understanding. For example, we are not aware how to construct a fully gapped (i.e., with correlators fall off exponentially) bosonic integer quantum hall liquid using a symmetric PEPS with a finite bond dimension D . But there is no known principle forbidding such a construction.

²One could consider a gauge transformation leaving both site tensors and bond tensors up to overall $U(1)$ phases. However one can always straightforwardly redefine the gauge transformation so that the bond tensors are completely invariant.

³ IGG is closely related to the concept of G -injectivity proposed in Ref.[104], which is used to characterize topological order of toric code type with gauge symmetry G in PEPS. Further, G -injectivity is generalized to twisted G -injectivity as well as MPO injectivity, which can characterize more exotic topological order[11, 14] or even topological order with chiral edge states[143, 164]. However, these phases are beyond the scope of the current IGG framework in our chapter

invariant up to overall U(1) phases and bond tensors completely invariant forms an infinite group, which we denote as \overline{IGG} . These gauge transformations satisfy Eq.(3.4) with $\widetilde{T}^s = T^s, \widetilde{B}_b = B_b$. Namely, a gauge transformation $\{W(s, i)\}$ is in the \overline{IGG} of a PEPS formed by $\{T^s, B_b\}$ iff it satisfies:

$$\begin{aligned} (T^s)_{\alpha\beta\dots}^k &= e^{i\theta(s)} \cdot [W(s, 1)]_{\alpha\alpha'} [W(s, 2)]_{\beta\beta'} \dots (T^s)_{\alpha'\beta'\dots}^k \\ (B_b)_{\alpha\beta} &= [W(b, 1)]_{\alpha\alpha'} [W(b, 2)]_{\beta\beta'} (B_b)_{\alpha'\beta'}, \end{aligned} \tag{3.14}$$

for certain U(1) phase factors $\{e^{i\theta(s)}\}$. Here $W(b, j)$ represents a gauge transformation on the leg j of the bond tensor B_b , and if a site leg (s, i) and a bond leg (b, j) are connected, then $W(s, i) = [W(b, j)^{-1}]^t$.

Clearly, if certain gauge transformation $\{W(s, i)\}$ belongs to \overline{IGG} , then one can straightforwardly multiply U(1) phases $\chi(s, i)$ to the $W(s, i)$ -matrices: $\{W(s, i)\} \rightarrow \{\widetilde{W}(s, i) = \chi(s, i)W(s, i)\}$ and obtain another element in \overline{IGG} , if $\chi(s, i) = \chi^*(s', i')$ when (s, i) and (s', i') are the two virtual legs connected by one bond tensor. If we view the U(1) phase factors $\{\chi(s, i)\}$ leaving the bond tensors completely invariant as a special kind of gauge transformations, they form an infinite abelian subgroup in the center of \overline{IGG} , which we denote as the χ -group, since they commute with any gauge transformations.

In general one should work with the infinite group \overline{IGG} . In this chapter, for simplicity, we define IGG as the quotient group:

$$IGG \equiv \frac{\overline{IGG}}{\chi\text{-group}}. \tag{3.15}$$

In addition, we will mainly focus on the cases in which IGG is a simple finite abelian group Z_n . In this situation, it is straightforward to show that $\overline{IGG} = IGG \times \chi\text{-group}$, indicating IGG is just a simpler way to express \overline{IGG} . This also means that we could equally view IGG as a Z_n subgroup of \overline{IGG} . In particular, there exist a generator $g \in \overline{IGG}$, but $g \notin \chi\text{-group}$ and g satisfies $g^n = I$ where I is the identity gauge

transformation — the do-nothing gauge transformation.

Note that if IGG is a more complicated group, since the center extension with respect to χ - group can be nontrivial, it is possible that $\overline{IGG} \neq IGG \times \chi$ - group. In this situation it is better to directly work with \overline{IGG} .

IGG and gauge dynamics

Here we will discuss the physical meaning of IGG . We use $IGG = Z_2$ as an example. The following discussion can be easily generalized to other IGG groups.

First, let us clarify the action of Z_2 IGG on PEPS. Every virtual leg accommodates a representation of $Z_2 = \{1, g\}$. Note that we do not require representations on different legs to be the same. However, we require two connected legs accommodate representations dual to each other, so that applying the g actions on connected legs is just a special gauge transformation. The nontrivial Z_2 IGG element is an action of g on all virtual legs. Following the definition of IGG , all site tensors are invariant up to ± 1 and all bond tensors are completely invariant under this action, as shown in Fig.(3-3a). Further, it is straightforward to derive that any patch cut from PEPS is invariant up to ± 1 under the g actions on boundary virtual legs, as shown in Fig.(3-3b).

The physical meaning of IGG is related to the gauge dynamics. To see this, let us first review the Z_2 gauge theory. There are two phases in the Z_2 gauge theory: the deconfined phase and the confined phase. In the deconfined phase, the Z_2 gauge theory describes Z_2 topological order (toric code). The low-energy excitations include four types of quasiparticles: the trivial particle 1, the chargon e , the fluxon m and the bound state of chargon and fluxon $f = em$. e, m and f can only be created in pairs. Each particle is its own anti-particle, $e^2 = m^2 = f^2 = 1$. e, m are bosons while f is a fermion. The braiding statistics of the three nontrivial particles are mutually fermionic. In the confined phase, topologically nontrivial quasiparticles are confined.

To see the connection between IGG and the gauge theory, let us create nontrivial excitations on PEPS with Z_2 IGG . We can define e particles living on sites while m particles living on plaquettes. As shown in Fig.(3-3c), to create two m particles

in neighboring plaquettes, we simply multiply the nontrivial Z_2 element g on one of two contracted virtual legs shared by the two plaquettes. The insertion of g only on one side of contracted legs is not a gauge transformation, and in general will change the wavefunction. One can also create a pair of m particles spatially separated from each other by applying the single-sided g -actions over a string of bonds. The fluxons are located at the end of the string. Note that although the positions of fluxons are physical, the position of the string connecting them are not physical since one can perform Z_2 gauge transformations on site tensors to move the string around while leaving the physical wavefunction invariant.

Now, let us turn to e particles. Let us first define Z_2 even/odd tensors. The action of g on boundary virtual legs of a tensor generally gives a phase factor ± 1 . If the phase factor is $+1/-1$, we call it Z_2 even/odd. The Z_2 parities of tensors depend on the representations of g on virtual legs. If we do not worry about the lattice symmetry for the moment, for a Z_2 even/odd tensor, we can simply redefine g on one virtual leg by -1 , thus this tensor becomes Z_2 odd/even. So we can assume all tensors are Z_2 even for the remaining discussion in this subsection. Creating an e particle on a single site corresponds to changing the site tensor from Z_2 even to Z_2 odd, as seen in Fig.(3-3d). To detect the number of chargons on a patch of PEPS, we simply apply g on all boundary virtual legs; namely, we create an m loop on the boundary. If there is an odd number of chargons on that patch, this patch tensor should be Z_2 odd and the g action on the boundary picks up a -1 , see Fig.(3-3e). This -1 can be understood as the Berry phase from braiding e and m . One can easily convince oneself that an odd number of chargons cannot be created on a closed manifold.

If $IGG = Z_2$ PEPS describe deconfined phases, then separating topological quasi-particles is expected to cost zero tension. Consequently one can insert m loops wrapping around torus holes to construct the four-fold degenerate ground states on a torus. However if $IGG = Z_2$ PEPS describe confined phases, which we expect to be possible after a scaling with both bond dimension D and system sizes, this is no longer true.

As a final remark, there turns out to be two distinct types of Z_2 gauge theories: the toric code theory and the double-semion theory[39, 81, 88]. They have

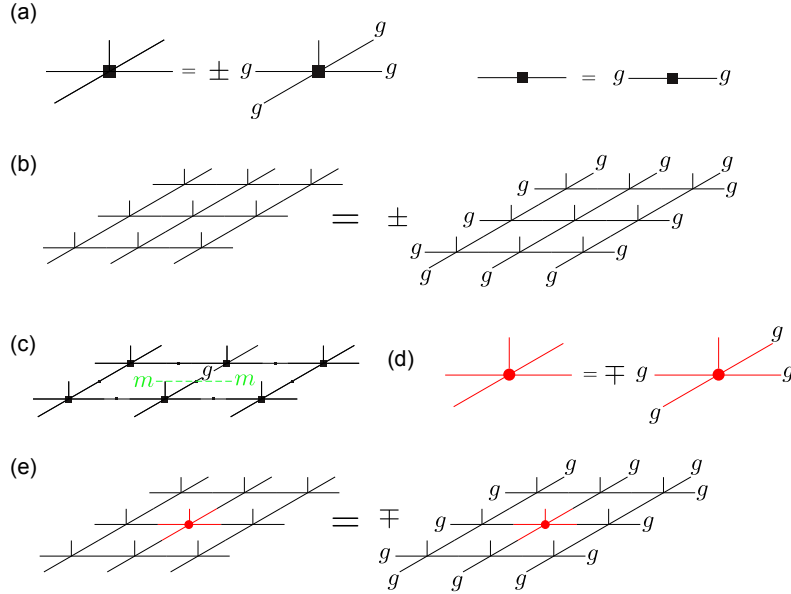


Figure 3-3: (a): Site tensor and bond tensor are both invariant under Z_2 action on all virtual legs of tensors. (b): Tensors obtained by contracting Z_2 invariant tensors are also Z_2 invariant. (c): Acting g on one virtual leg of single bond tensor creates two fluxons (m) in plaquettes sharing the bond. (d): Z_2 odd tensor indicates there sitting a chargeon. (e): By applying g (or creating fluxon loop) on the boundary of a region, we are able to determine chargeon number is even or odd inside this region.

distinct topological orders; e.g., the topological spins (the exchange statistics phases) of quasiparticles are $[1, 1, 1, -1]$ ($[1, 1, i, -i]$) for the $[1, e, m, em]$ particles in a toric code (double-semion) topological order. We emphasize that the $IGG = Z_2$ PEPS discussed here, when describing a deconfined phase, hosts the toric code topological order. The simplest way to see this is to realize the self braiding statistics phases of both the e and the m in the $IGG = Z_2$ PEPS are trivial, so they cannot be semions.

Indeed, when moving an e chargeon around a loop by a sequence of hopping, one realizes the Berry's phase is independent of whether there are other e chargeons inside the loop. Similarly, when moving an m fluxon around a loop (giving rise to an m loop), the topological Berry's phase is simply ± 1 depending on the Z_2 parity of the PEPS patch inside the loop, independent of whether there are other m fluxons inside the loop.

Natural emergence of nontrivial IGG

We will show that, under a basic assumption, the symmetric PEPS for certain quantum systems must have nontrivial IGG 's. *This basic assumption is that the W matrices on every virtual leg form (generally reducible) representations or projective representations for the on-site symmetries* (see Eq.3.7,3.11). Under this assumption, the nontrivial IGG in certain systems is a natural consequence of the global symmetry, even in the absence of specific Hamiltonians.

Consider a spin- $\frac{1}{2}$ system on a square lattice; i.e., the physical leg on every site tensor is a 2-dimensional spin- $\frac{1}{2}$ Hilbert space. For this system, we will show a symmetric PEPS under the basic assumption must feature an IGG containing a Z_2 subgroup. Since $SU(2)$ spin rotation group has no projective representations, the basic assumption ensures that every virtual leg must form a representation of $SU(2)$, which generally is a direct sum of a number of half-integer spin representations and a number of integer spin representations. Eq.(3.7) now has the following simple interpretation: the site tensors are spin singlets formed by the virtual spins and the physical spin- $\frac{1}{2}$, and the bond tensors are spin singlets formed the virtual spins only.

Now we can consider the particular 2π $SU(2)$ rotation, and denote the corresponding $W(s, i)$ matrix on a virtual leg (s, i) as $J(s, i)$, which is simply a direct sum of the minus identity transformation in the half-integer spin subspace and the identity transformation in the integer spin subspace. Next, consider the combination of transformations $\{J(s, i)\}$ *acting on the virtual legs only* — this is a particular gauge transformation. Since the physical spin- $\frac{1}{2}$ only picks up an overall -1 in the 2π $SU(2)$ rotation, and the bond tensors are spin singlets, we know that the gauge transformation $\{J(s, i)\}$ is an element in \overline{IGG} .

To see this system featuring a nontrivial IGG , we only need to show $\overline{IGG} \neq \chi - group$. We will demonstrate that the gauge transformation $\{J(s, i)\} \notin \chi - group$. To do this, we impose the C_4 rotational symmetry and the translation symmetry of the square lattice. Note that $\{J(s, i)\} \in \chi - group$ if and only if for every virtual leg, the dimension of either the half-integer spin subspace or the integer spin subspace

vanishes. However, this cannot be true. The site tensor is a spin singlet, which requires the virtual legs to combine into a spin- $\frac{1}{2}$ so that it can further combine with the physical spin- $\frac{1}{2}$ to form a singlet. Therefore, if $\{J(s, i)\} \in \chi - group$, on a single site tensor, we must have an odd number of virtual legs which contain purely half-integer spins while the remaining virtual legs contain purely integer spins. This explicitly breaks the C_4 rotational symmetry.

Consequently, there is at least one element $J \equiv \{J(s, i)\}$ in \overline{IGG} but not in $\chi - group$, and $J^2 = e$. This tells us that IGG at least contains a Z_2 subgroup $\{I, J\}$.

The above argument can be easily generalized to other symmetries, such as the time reversal symmetry. For the time reversal symmetry, consider a system with one Kramer doublet on every physical leg. To form a Kramer singlet PEPS, one must combine an odd number of Kramer doublets on virtual legs of every site tensor. However, for site tensors on a square lattice, there are even number (four) of virtual legs per site, and the C_4 symmetry dictates that the transformation \mathcal{T}^2 on *virtual legs only* gives a nontrivial element of the IGG which is at least Z_2 .

We point out that translational symmetry itself is enough for the above argument and one does not necessarily consider C_4 . This is because translational symmetry relates the left (down) virtual leg with the right (up) virtual leg connected to the same site tensor via the fact that the virtual legs connected by a bond need to form a spin singlet (or a Kramer singlet). What is really important for the above argument is the existence of a half-integer spin (or a Kramer doublet) per unit cell. One way to see this is to consider a honeycomb lattice with spin- $\frac{1}{2}$ per site, i.e., two spin- $\frac{1}{2}$'s per unit cell. In this case, every site has three virtual legs and it is possible to construct symmetric PEPS wavefunctions with purely half-integer spins on virtual legs, in which case the 2π spin rotation *on the virtual legs only* becomes an element in the $\chi - group$.

Next, let us consider a system with fractional filled hard core bosons and see how a nontrivial IGG naturally emerges. As an exercise, we can simply translate the previous discussions on spin- $\frac{1}{2}$ systems into $\frac{1}{2}$ -filled hard-core boson systems on the square lattice. The physical leg for the hard-core bosons is two dimensional Hilbert

space with basis labeled as $|0\rangle$ and $|1\rangle$. When mapped to a spin- $\frac{1}{2}$ system, $|0\rangle(|1\rangle)$ is identified as the down spin (up spin). The U(1) charge transformation for the hard-core boson system can be written as $\exp[i\theta(S_z^i + \frac{1}{2})]$ using the spin operator on the leg- i . Note that spin-0 is identified as charge- $\frac{1}{2}$, a projective representation of the charge U(1). Since a bond tensor is a spin singlet formed by two virtual spins in the spin language, the representation of U(1) group in the hard-core boson language on a bond tensor is

$$[e^{i\theta(S_z^a + \frac{1}{2})} \cdot e^{i\theta(S_z^b + \frac{1}{2})}]^* = e^{-i\theta} \quad (3.16)$$

where the complex conjugation comes from the fact that bond virtual legs transform as conjugate representation of site virtual legs, and we have used $S_z^a + S_z^b = 0$ for the two virtual legs a and b . So, every bond tensor carries charge -1 .

Further, since the site tensor is also a spin singlet, we require $\sum_{i=0}^5 S_z^i = 0$, where $i = 0$ labels the physical leg and other $i \neq 0$ label virtual legs. Therefore the representation of U(1) symmetry on a site tensor reads

$$\prod_{i=0}^4 e^{i\theta(S_z^i + \frac{1}{2})} = e^{i\frac{5}{2}\theta} \quad (3.17)$$

Namely, every site tensor carries charge- $\frac{5}{2}$. Consequently each unit cell carries charge- $\frac{1}{2}$.

Note that in this exercise, the bond tensor transform nontrivially under U(1), so the virtual leg transformation $W = e^{i\theta(S_z + \frac{1}{2})}$ does not satisfy Eq.(3.7) in our definition of symmetric PEPS. But one could easily redefine the virtual leg transformation W 's so that the charge carried by the bond is absorbed to a neighboring site, and Eq.(3.7) is satisfied using the redefined W 's.

The essential results from previous discussions on the spin- $\frac{1}{2}$ systems can now be translated as following statement: the virtual leg hosts both integer charges and half integer charges of U(1), so 2π rotation of U(1) symmetry on all virtual legs gives the nontrivial Z_2 IGG.

In the following, on the square lattice, we provide a general argument that a nontrivial minimal required IGG emerges for a symmetric PEPS with fractional-filled bosons under our basic assumption. Further, this minimal required IGG is given by the 2π rotation of the $U(1)$ symmetry on the virtual legs only.

Firstly, we have the physical legs carrying integer charges. And if the tensor network is symmetric under the $U(1)$ symmetry, for site tensors and bond tensors, we can rewrite Eq.(3.7) as

$$\begin{aligned} W_S S \circ T^s &= \Theta_S T^s \\ W_S S \circ B_b &= \Theta_S B_b \end{aligned} \tag{3.18}$$

where symmetry operation S can be any $U(1)$ group element. Note that we put Θ_S operation on bond tensors as well to pick up the possible phase factors. As mentioned before, this phase factor on the bond can always be tuned away by redefining W_S . But for the moment, let us keep it since we want to include the previous exercise.

We can view the left side as the $U(1)$ action on a site/bond tensor. Under the basic assumption, the above equation indicates every site/bond tensor carries a fixed $U(1)$ charge, which can be a fractional charge. In the presence of the lattice symmetry, we expect all virtual legs of site tensors share the same $U(1)$ reducible projective representation. (Virtual legs of bond tensors have the conjugate representation). Our plan is to assume the 2π rotation of $U(1)$ symmetry is trivial (only a phase factor) on the virtual leg, and then demonstrate a contradiction. This assumption dictates that the irreducible charges carried by a virtual leg can only differ by integer numbers. Namely, the basis for virtual legs of site tensors can be written as

$$\{|x\rangle, |x + n_1\rangle, |x + n_2\rangle, \dots\} \tag{3.19}$$

where x can be any fractional number and n_i are integers. Under symmetry operation

U_θ , state $|x + i\rangle$ transform as

$$U_\theta|x + n_i\rangle = e^{i\theta(x+n_i)}|x + n_i\rangle \quad (3.20)$$

So, 2π rotation on any state of the above Hilbert space will give the same phase factor $e^{ix\theta}$. Similarly, the basis for bond legs are

$$\{|-x\rangle, |-x - n_1\rangle, |-x - n_2\rangle, \dots\} \quad (3.21)$$

Recall that a single tensor should carry a fixed charge. Consequently a bond tensor should carry charge $-2x - n_b$, where n_b is some integer. And a site tensor should carry charge $4x + n_s$. Since the physical leg only carries integer charges, n_s should also be an integer. We then conclude that, for a single unit cell, the charge should be $n_s - n_b$, which must be an integer. This contradicts with the fact that the system is at a fractional filling. Therefore to construct a symmetric PEPS at a fractional filling under our basic assumption, the 2π rotation of $U(1)$ symmetry must be nontrivial on all virtual legs, and the nontrivial IGG naturally emerges.

We discussed the naturally emerged IGG in certain quantum systems. It is possible for the ground state symmetric PEPS to have a larger IGG which contains the naturally emerged IGG as a subgroup. We call the naturally emerged IGG as the *minimal required IGG* . A larger IGG than the minimal required IGG has important implications in both conceptual understandings and numerical simulations. We will come back to this point in Sec.(3.3) and Sec.(4.5).

The minimal required IGG 's in systems at fractional fillings are consistent with the Hastings-Oshikawa-Lieb-Schultz-Mattis (HOLSM) theorem. Consider a 2+1D system with an odd number of spin- $\frac{1}{2}$ per unit cell, the HOLSM theorem states that it is impossible to have a featureless trivial insulator. In other words, the ground state must either be gapless, break the spin rotation or the lattice translation symmetry, or be topological ordered with a ground state degeneracy.

In our formalism, a half-integer spin per site on the square lattice (and similarly on the kagome lattice) enforces a minimal Z_2 IGG , consistent with the HOLSM theorem.

For instance, if $IGG = Z_2$, the system could be in either a deconfined phase with a toric code topological order, or a confined phase. But the confined phase corresponds to either e or m condensation, which leads to spin rotation or lattice translation symmetry breaking.

For a honeycomb lattice spin- $\frac{1}{2}$ system, there are two spin- $\frac{1}{2}$ per unit cell and the HOLS theorem does not apply. As mentioned above, symmetric PEPS on the honeycomb with a trivial IGG can be constructed, which is consistent with the possible trivial symmetric insulator phase in this system as pointed out in [80, 79].

3.2.5 An example

Here, we will give a simple PEPS with $IGG = Z_2$ defined on the kagome lattice. In particular, we will write the PEPS description for a nearest neighboring (NN) resonating valence bond (RVB) state that preserves all lattice symmetry. The lattice symmetry generators for kagome lattice are shown in Fig.(3-4).

As shown in Ref.[163], there are four different kinds of symmetric NN RVB states defined on kagome lattice with spin- $\frac{1}{2}$ per site. Also, by solving projective symmetry group (PSG) equations for the Schwinger-boson mean field ansatz on the kagome lattice, one finds eight distinct PSG classes. And four of them can be realized by NN pairing terms[147]. One can check that the four NN RVB states are exactly representative states for these four PSG classes. Here, we will focus on one particular PSG class, named as $Q_1 = Q_2$ state in Ref.[115, 147]. This particular PSG class is a promising candidate phase[93, 129, 92] for the Z_2 spin liquid reported in recent DMRG simulations[162, 38, 73]. Here, we will explicitly write down this NN RVB state in the PEPS language.

In fact, this state has already been studied extensively in PEPS[119, 107]. Here, we will slightly modify the construction. Every physical leg is a spin- $\frac{1}{2}$ and virtual leg accommodates spin representation $0 \oplus \frac{1}{2}$, with basis $\{|0\rangle, |\uparrow\rangle, |\downarrow\rangle\}$. Bond tensors

are spin singlets, which can be written as a matrix in this basis,

$$B_b = \begin{pmatrix} 1 & 0 & 0 \\ 0 & 0 & -i \\ 0 & i & 0 \end{pmatrix} \quad (3.22)$$

where the direction of bond tensor is shown in Fig.(3-4c). A bond tensor with the inverse direction is transpose of the above matrix. Tensors for different sites are equal to each other, and can be written as,

$$T^s = |\uparrow\rangle \otimes (|\downarrow 000\rangle + |0\downarrow 00\rangle - i|00\downarrow 0\rangle - i|000\downarrow\rangle) - \\ |\downarrow\rangle \otimes (|\uparrow 000\rangle + |0\uparrow 00\rangle - i|00\uparrow 0\rangle - i|000\uparrow\rangle) \quad (3.23)$$

where the order of site virtual legs is given in Fig.(3-4b). We can view site tensors as superposition of singlets formed by one physical leg and one of the four virtual legs, while the coefficient of singlets need to be carefully chosen to make PEPS symmetric under lattice symmetries. One can verify the state defined above is consistent with the PEPS representation of NN RVB given in Ref.[107] up to a gauge transformation.

As discussed before, the Z_2 IGG here is generated by the 2π spin rotation of all virtual legs. Since all tensors are spin-singlet, they are invariant under this operation up to -1 factors on the site tensors. This NN RVB PEPS belongs to one of the crude classes proposed in this chapter. Roughly speaking, according to global symmetry, we can find the generic sub-Hilbert space that the building block tensors must live within for each given crude class, which vastly generalize the one-dimensional sub-Hilbert space defined as in Eq.(3.23).

3.3 Algorithm for Symmetric PEPS

For a given quantum model with certain given symmetry groups, we propose a general simulation scheme to study its phase diagram as follows:

1. One classifies symmetric PEPS according to their short-range physics. More

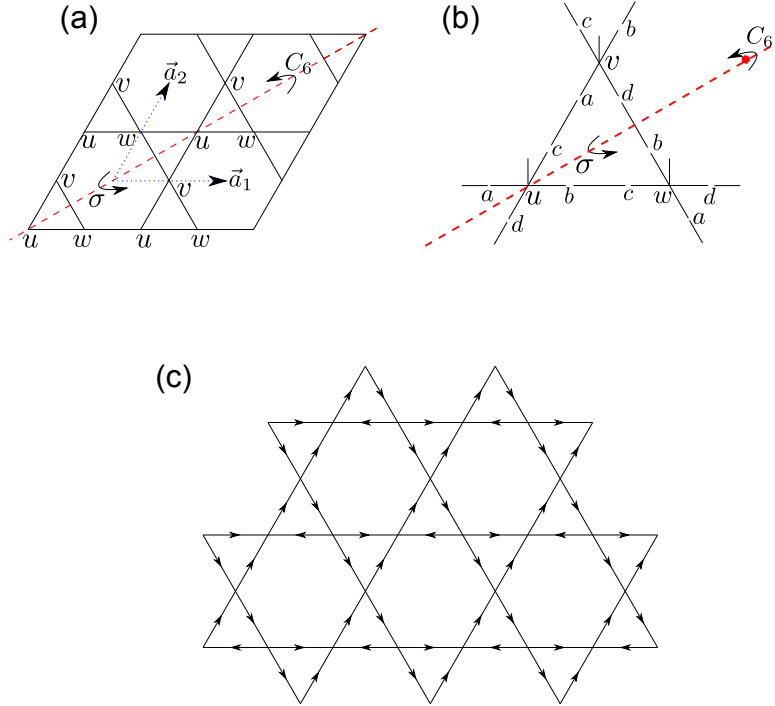


Figure 3-4: (a): kagome lattice and the elements of its symmetry group. $\vec{a}_{1,2}$ are the translation unit vectors, C_6 denotes $\pi/3$ rotation around honeycomb center and σ represents mirror reflection along the dashed red line. (b): Site tensor and bond tensor for kagome lattice in one unit cell. Virtual legs of site tensors are labeled as (x, y, s, i) , where (x, y) denotes the position of unit cell, $s = u, v, w$ is the sublattice index and $i = a, b, c, d$ specifies one of four legs. (c): One possible orientation of kagome lattice. Particularly, for NN RVB state, the orientation of bonds denotes the direction of spin singlets.

precisely, crude classes are distinguished by ways of implementing symmetries on virtual legs.

2. For each class, by enforcing symmetry transformation rules, one finds constraint Hilbert spaces for the building block tensors in the PEPS representation.
3. One performs the energy density minimization for every class in the constrained Hilbert space, and determines the class which gives the lowest energy density. The quantum phase of the model will be a member phase of this crude class. This finishes the short-range part of the simulation task.
4. At last, one could try to completely determine the quantum phase diagram by studying the long-range physics, e.g., by measuring correlation functions for the symmetric PEPS with the minimal energy density. With a careful scaling analysis, together with the sharp information on the long-range physics obtained from the short-range physics, possible long range symmetry breaking orders may be identified.

As the main example, we will demonstrate this simulation scheme for a half-integer spin system on the kagome lattice. We will start with classifying and constructing generic symmetric PEPS with $IGG = Z_2$ that preserve the full lattice symmetry as well as the spin rotation and the time reversal symmetries. As we will show shortly, the condition $IGG = Z_2$ actually dictates that the virtual legs form (projective) representations of on-site symmetries. Therefore when we consider $IGG = Z_2$ symmetric PEPS, we already made our basic assumption in an implicit way. In addition, although we focus on the minimal required IGG under our basic assumption, the discussions can also be easily generalized to symmetric PEPS with a larger IGG .

3.3.1 General framework for classification

From now on we assume $\overline{IGG} = IGG \times \chi - group$, which is always true if IGG is a simple finite abelian group Z_n .

Consider the gauge transformation associated with a symmetry R : W_R , and the corresponding phase on site tensors: Θ_R . We have $T^s = \Theta_R W_R R \circ T^s$ and $B_b = W_R \circ B_b$, as shown in Sec.3.2.3. However, since both site tensors and bond tensors are invariant under the IGG action (up to phases for site tensors), we conclude that tensors are also invariant under a new symmetry operation defined as $W'_R \equiv \eta_R W_R$ and $\Theta'_R \equiv \mu_R \Theta_R$,

$$\begin{aligned} T^s &= \Theta'_R W'_R R \circ T^s \\ B_b &= W'_R R \circ B_b, \end{aligned} \tag{3.24}$$

where $\eta_R \in IGG$ and $\mu_R \equiv \{\mu_R(s)\}$ is a set of phase factors on site tensors associated with η_R , such that $\mu_R \eta_R \circ T^s = T^s$. For instance, for a half-integer spin system described by PEPS with $IGG = \{I, J\}$, if $\eta_R = J$ corresponds to the 2π $SU(2)$ rotation on the virtual legs, then $\mu_R(s) = -1$ for all sites.

Similarly one could modify W_R and Θ_R with any element in the χ -group, i.e., bond dependent phase factors $\{\varepsilon_R(s, i)\}$ as:

$$\begin{aligned} W_R(s/b, i) &\rightarrow \varepsilon_R(s/b, i) W_R(s/b, i) \\ \Theta_R(s) &\rightarrow \prod_i \varepsilon_R^*(s, i) \Theta_R(s), \end{aligned} \tag{3.25}$$

where we have $\varepsilon_R(s, i) = \varepsilon_R(b, j)^*$ if (s, i) and (b, j) are connected. Further, $\varepsilon_R(b, 1) = \varepsilon_R(b, 2)^*$ for the two legs of the same bond tensor, as required in the definition of the χ -group.

Basically, the symmetry transformation on the virtual legs W_R is ambiguous since it can be combined with any element in \overline{IGG} . Mathematically, the representation of R on the Hilbert space of PEPS (including both the virtual and physical Hilbert spaces) form a new group, which is the original symmetry group SG extended by the \overline{IGG} . This extension is related to the 2-cohomology $H^2(SG, IGG)$ and $H^2(SG, U(1))$. Particularly, we can view those \overline{IGG} elements as “representations” of the identity element in the symmetry group on virtual legs.

Keeping these discussions in mind, let us consider a discrete symmetry group SG as an example. SG is always defined by a collection of group identities. For instance, elements $R_1, R_2, \dots, R_n \in SG$ satisfy the following relation:

$$R_1 R_2 \dots R_n = e \quad (3.26)$$

Then, acting $R_1 R_2 \dots R_n$ on a symmetric PEPS, one obtains a combined transformation sending every tensor back to the same tensor:

$$\begin{aligned} T^s &= \Theta_{R_1} W_{R_1} R_1 \Theta_{R_2} W_{R_2} R_2 \dots \Theta_{R_n} W_{R_n} R_n \circ T^s \\ B_b &= W_{R_1} R_1 W_{R_2} R_2 \dots W_{R_n} R_n \circ B_b \end{aligned} \quad (3.27)$$

By definition, the transformation leaving all tensors invariant (up to phases on site tensors) can only be an element in \overline{IGG} . Explicitly writing down Eq.(3.27) on virtual legs of site tensors, we conclude that

$$\begin{aligned} &W_{R_1}(s, i) W_{R_2}(R_1^{-1}(s, i)) \dots \\ &W_{R_n}(R_{n-1}^{-1} \dots R_1^{-1}(s, i)) = \eta(s, i) \chi(s, i) \end{aligned} \quad (3.28)$$

where $\eta(s, i)$ is the action of $\eta \in IGG$ on the virtual leg (s, i) . Further, $\{\chi(s, i)\}$ is an element in the χ -group. We point out that since $W_R(s, i) = [W_R^{-1}(b, j)]^t$ if (s, i) and (b, j) are connected, W_R on virtual legs of bond tensor gives us no extra equation. However, phase factors on site tensors will give an extra condition, which reads

$$\begin{aligned} &\Theta_{R_1}(s) \Theta_{R_2}(R_1^{-1}(s)) \dots \Theta_{R_n}(R_{n-1}^{-1} \dots R_1^{-1}(s)) \\ &= \mu(s) \prod_i \chi^*(s, i) \end{aligned} \quad (3.29)$$

Here $\mu^*(s)$ is the phase factor obtained after applying η on the s-site tensor.

Our goal is to solve Eq.(3.28) and Eq.(3.29) for all group identities and obtain the representations of symmetry operation on virtual legs (W_R) as well as phase factors on site tensors (Θ_R). Recall that the same physical wavefunction can be represented

by many PEPS which differ from each other by gauge transformations (note that these are general gauge transformations which may not be in \overline{IGG}). One should really solve Eq.(3.28) and Eq.(3.29) up to gauge equivalence.

Under a gauge transformation $V \equiv \{V(s, i)\}$ on virtual legs, $(T^s)' \equiv V \circ T^s$ and $B'_b \equiv V \circ B_b$ satisfy the following conditions:

$$\begin{aligned}
(T^s)' &= V\Theta_R W_R R \circ T^s \\
&= (V\Theta_R V^{-1})(VW_R R V^{-1} R^{-1}) R V \circ T^s \\
&= \Theta_R W'_R R \circ (T^s)',
\end{aligned} \tag{3.30}$$

and

$$\begin{aligned}
B'_b &= V W_R R \circ B_b \\
&= (V W_R R V^{-1} R^{-1}) R V \circ B_b \\
&= W'_R R B'_b.
\end{aligned} \tag{3.31}$$

Here we use the fact that V commutes with Θ_R in the last step of Eq.(3.30). Here, $W'_R \equiv V W_R R V^{-1} R^{-1}$. Writing the above expression explicitly on virtual leg (s, i) , we get

$$W_R(s, i) \rightarrow V(s, i) \cdot W_R(s, i) V^{-1}(R^{-1}(s, i)) \tag{3.32}$$

while Θ_R is invariant. Particularly, $\eta \in IGG$ changes as

$$\eta(s, i) \rightarrow V(s, i) \cdot \eta(s, i) V^{-1}(s, i) \tag{3.33}$$

And phase factors μ and χ in Eq.(3.29) are invariant.

Apart from the above gauge transformation, one can change site tensors by phase factors, which do not affect physical observables. Note that one could also change bond tensors by phase factors, but such a modification is always equivalent to a gauge

transformation together with a changing of phase factors on site tensors. Unlike gauge transformations, a modification of phase factors on site tensors may change the physical wavefunction up to an overall phase. When site tensors change as $T^s \rightarrow \Phi \circ T^s = \Phi(s) \cdot T^s = e^{i\varphi(s)}T^s$, W_R associated with the symmetry R is invariant, but Θ_R goes to $\Phi\Theta_R R\Phi^{-1}R^{-1}$. Namely, the phase factor $\Theta_R \equiv \{e^{i\theta_R(s)}\}$ will change as

$$\Theta_R(s) \rightarrow \Theta_R(s)\Phi(s)\Phi^*(R^{-1}(s)) \quad (3.34)$$

Basically, we should solve for the W_R and Θ_R in Eq.(3.28) and Eq.(3.29) up to two kinds of equivalences. First, if two sets of W_R and Θ_R are related by Eq.(3.32) and Eq.(3.34), they are equivalent and we denote this situation as the *gauge equivalence*. The gauge equivalence contains the V -ambiguity in Eq.(3.32) and the Φ -ambiguity in Eq.(3.34).

Second, if two sets of W_R and Θ_R are different by an \overline{IGG} element, they are also equivalent and we denote this situation as the *group extension equivalence*. Summarizing our discussion in Eq.(3.24,3.25), it means that one could modify W_R and Θ_R as $W_R \rightarrow W'_R = \eta_R \varepsilon_R W_R$ and $\Theta_R \rightarrow \Theta'_R = \mu_R \varepsilon_R \Theta_R$, where $\eta_R \in \overline{IGG}$ and $\varepsilon_R \in \chi - \text{group}$ and

$$\begin{aligned} W'_R(s, i) &= \eta_R(s, i) \varepsilon_R(s, i) W_R(s, i) \\ \Theta'_R(s) &= \mu_R(s) \prod_i \varepsilon_R^*(s, i) \Theta(s). \end{aligned} \quad (3.35)$$

Note that to save notation, we define $\varepsilon_R \Theta_R$ as multiplying $\prod_i \varepsilon_R^*(s, i)$ on $\Theta(s)$. The group extension equivalence contains an η -ambiguity and an ε -ambiguity in Eq.(3.35). *Note that different from the gauge equivalence, we have an η -ambiguity and an ε -ambiguity for each symmetry element R .*

We will solve Eq.(3.28) and Eq.(3.29) for the whole symmetry group up to both the gauge equivalence and the group extension equivalence. Eventually we will obtain many classes of PEPS satisfying inequivalent W_R and Θ_R transformation rules. Among all combinations of W_R and Θ_R within the same equivalence class, we can

choose a particular representative, and construct explicit forms of W_R and Θ_R by fixing the η -ambiguity, the ε -ambiguity, the V -ambiguity and the Φ -ambiguity. These W_R and Θ_R specify the sub-Hilbert spaces for the building block tensors in each class. We sometimes call the whole procedure of fixing the four ambiguities as *gauge fixing*.

Practically, we often firstly use the group extension equivalence to simplify Eq.(3.28) and Eq.(3.29). For instance, one can use the ε -ambiguity to simplify $\{\chi(s, i)\}$ in Eq.(3.28) and Eq.(3.29): under a transformation $W_{R_i} \rightarrow \varepsilon_{R_i} W_{R_i}$, according to Eq.(3.28), we find

$$\chi(s, i) \rightarrow \varepsilon_{R_1}(s, i) \dots \varepsilon_{R_n}(R_{n-1}^{-1} \dots R_1^{-1}(s, i)) \chi(s, i). \quad (3.36)$$

Moreover, one can use the η -ambiguity to simplify the $\{\eta(s, i)\}$ and $\{\mu(s)\}$ in Eq.(3.28) and Eq.(3.29). For example, if some symmetry operation R appears only once in the group identity $R_1 R_2 \dots R_n = e$, one could use the η -ambiguity for R to make sure $\{\eta(s, i) = 1\}$ and $\{\mu(s) = 1\}$ for this group condition.

After the group extension equivalence is used, we will use the gauge equivalence (the V -ambiguity and the Φ -ambiguity) to solve for explicit forms of W_R and Θ_R . Note that the group extension equivalence and the gauge equivalence are not completely independent. For example, after fixing the V -ambiguity and the Φ -ambiguity, it is possible some part of the ε -ambiguity and the η -ambiguity are also fixed. In the following we demonstrate this procedure in an example: the half-integer spin systems on the kagome lattice.

3.3.2 Classification of kagome PEPS

Here, we will classify symmetric kagome PEPS wavefunction with a half-integer spin- S per site, which preserves all lattice symmetries, the time reversal symmetry as well as the spin rotation symmetry. We will only assume $IGG = Z_2 = \{I, J\}$ without specifying the physical meaning of J . Later we will prove that J can always be chosen to be the 2π spin rotation on the virtual legs. Let us begin with setting up some useful facts.

First, we can use the V -ambiguity to diagonalize $J(x, y, s, i)$ for every virtual leg (x, y, s, i) , where (x, y, s) labels a site on the lattice by the coordinates of the unit cell x, y and the sublattice index $s = u, v, w$, and $i = a, b, c, d$ labels one of the four virtual legs coming out of the site tensor. (see Fig.3-4 for illustrations) In this gauge, $\forall(x, y, s, i)$, the matrix $J(x, y, s, i)$ is a direct sum of an identity matrix and a minus identity matrix. Let us denote $J(x_0, y_0, s_0, i_0) = I_{D_1} \oplus (-I_{D_2})$ for some given virtual leg (x_0, y_0, s_0, i_0) , where $D_1 + D_2 = D$. We will consider the generic case in which $D_1 \neq D_2$.

Using the lattice symmetry, it is straightforward to prove that one can always redefine $\{J(x, y, s, i)\}$ by multiplying with an element ε in the χ -group: $\varepsilon(x, y, s, i) = \pm 1$ so that $J(x, y, s, i) = I_{D_1} \oplus (-I_{D_2})$, $\forall(x, y, s, i)$. (Such a modification is allowed in our definition of IGG .) For example, consider a particular lattice symmetry operation R , which could be the 60° degree rotation C_6 or the lattice translation T_1 or T_2 of the kagome lattice (see Section 3.6 for precise definitions), we always have a group relation $R^{-1} \cdot e \cdot R = e$. Using Eq.(3.28) for this group relation and choosing J to replace the e on the LHS:

$$\begin{aligned} & W_R^{-1}(R(x, y, s, i))J(R(x, y, s, i))W_R(R(x, y, s, i)) \\ & = \eta(x, y, s, i)\chi(x, y, s, i). \end{aligned} \tag{3.37}$$

The η on the RHS must be J , otherwise we would find J to be an element in the χ -group, violating $IGG = Z_2$. Therefore we know that $J(R(x, y, s, i))$ and $J(x, y, s, i)$, which are generally on two different virtual legs, are related by a similarity transformation $W_R(R(x, y, s, i))$ and an overall phase factor $\chi(x, y, s, i)$. But we are already in a gauge such that $J(x, y, s, i)$ are all diagonal. We then conclude that $J(R(x, y, s, i)) = \pm J(x, y, s, i)$. Since all virtual legs are related by lattice symmetries, we know $J(x, y, s, i) = \varepsilon(x, y, s, i)J(x_0, y_0, s_0, i_0)$, where $\varepsilon(x, y, s, i) = \pm 1 \forall(x, y, s, i)$.

Next, we show $\{\varepsilon(x, y, s, i)\} \in \chi$ -group. Namely, if (x, y, s, i) and (x', y', s', i') are connected by a bond tensor B_b , then $\varepsilon(x, y, s, i) = \varepsilon(x', y', s', i')$. This is because if $\varepsilon(x, y, s, i) = -\varepsilon(x', y', s', i')$, then the matrix $(B_b)_{\alpha\beta}$ satisfying Eq.(3.14) for $W = J$

would not have a full rank, since $D_1 \neq D_2$. This means that some singular value of (B_b) vanishes, dictating an IGG larger than Z_2 . For instance, one can multiply an arbitrary $U(1)$ phase on the zero singular value eigenstate on one of the two virtual legs, leaving the bond tensor B_b invariant.

Therefore $\{\varepsilon(x, y, s, i)\} \in \chi - group$ and we can always redefine J such that $J(x, y, s, i) = I_{D_1} \oplus (-I_{D_2}), \forall(x, y, s, i)$. From now on we will work within this gauge and denote the matrix $I_{D_1} \oplus (-I_{D_2})$ simply as J .

This allows us to denote the $\eta(x, y, s, i)$ transformation in Eq.(3.28) simply as η since it is site and virtual leg independent. In addition, according to Eq.(3.33), the remaining V -ambiguity: $V(x, y, s, i)$ must commute with J . In other words, $V(x, y, s, i)$ are block diagonal with two blocks, and the sizes of blocks are D_1 and D_2 respectively.

Now we can consider an arbitrary symmetry transformation R , which could be either a lattice symmetry or an on-site symmetry. Eq.(3.37) still holds for R and the η on the RHS must be J . Consequently we have:

$$\begin{aligned} & W_R^{-1}(R(x, y, s, i)) \cdot J \cdot W_R(R(x, y, s, i)) \\ & = \chi(x, y, s, i)J. \end{aligned} \tag{3.38}$$

Squaring this equation leads to $\chi(x, y, s, i) = \pm 1$. However only the $+$ sign is possible since otherwise the matrix $W_R(R(x, y, s, i))$ will not have a full rank, again due to $D_1 \neq D_2$. Thus we have proved that $W_R(x, y, s, i)$ commutes with $J, \forall(x, y, s, i)$ and $\forall R$. Mathematically, this means that when we extend the symmetry group by $\overline{IGG} = IGG \times \chi - group$, \overline{IGG} is in the center of the extended group.

Let us consider the phase factors $\mu_J(x, y, s)$ on site tensors obtained when applying the nontrivial element J on the virtual legs. This determines whether the site tensor is Z_2 even or Z_2 odd. Now we are ready to show that $\mu_J(x, y, s)$ is site independent in the current gauge. Namely if one site tensor is Z_2 even (odd), the same is true for all site tensors. Consider a lattice symmetry R which send a site (x, y, s) to the site (x', y', s') , Eq.(3.13) states that the two site tensors are related by a possible

permutation of virtual indices (e.g. induced by a lattice rotation) together with multiplications of W_R matrices on the virtual legs as well as a overall phase factor $\Theta_R(x, y, s)$. Because W_R matrices all commute with J , it is straightforward to see that the $\mu_J(x, y, s) = \mu_J(x', y', s')$. Because all sites are related to each other by lattice symmetries, $\mu_J(x, y, s)$ are identical for all sites. Thus in the discussion below we will simply denote the $\eta \in IGG$ associated phase factors $\mu(x, y, s)$ in Eq.(3.29) as μ , since it does not depend on the site.

By applying the condition $IGG = Z_2$ to the kagome lattice with the symmetry group described in Section 3.6, we are able to solve the equations for symmetry operations, i.e. Eq.(3.28,3.29), by gauge fixing. For the purpose of presentation, here we only demonstrate the calculation for the translation symmetry, and list the full results of the classification. The calculation for other symmetries is in paper [76].

Let us consider the translation symmetry group. This group is isomorphic to $Z \times Z$: the group is defined by its generators T_1, T_2 as well as the relation between generators,

$$T_2^{-1}T_1^{-1}T_2T_1 = e \quad (3.39)$$

As shown in Eq.(3.13), for PEPS symmetric under T_i ($i = 1, 2$), we have

$$\begin{aligned} T^{(x,y,s)} &= \Theta_{T_i} W_{T_i} T_i \circ T^{(x,y,s)} \\ B_{(xysi|x'y's'i')} &= W_{T_i} T_i \circ B_{(xysi|x'y's'i')} \end{aligned} \quad (3.40)$$

From the group relation $T_2^{-1}T_1^{-1}T_2T_1 = e$, we have

$$\begin{aligned} W_{T_2}^{-1}(T_2(x, y, s, i)) W_{T_1}^{-1}(T_1 T_2(x, y, s, i)) W_{T_2}(T_1 T_2(x, y, s, i)) \\ W_{T_1}(T_1(x, y, s, i)) = \eta_{12} \chi_{12}(x, y, s, i) \end{aligned} \quad (3.41)$$

as well as

$$\begin{aligned} & \Theta_{T_2}^*(T_2(x, y, s))\Theta_{T_1}^*(T_1T_2(x, y, s))\Theta_{T_2}(T_1T_2(x, y, s)) \\ & \Theta_{T_1}(T_1(x, y, s)) = \mu_{12} \prod_i \chi_{12}^*(x, y, s, i) \end{aligned} \quad (3.42)$$

where $\eta_{12} \in \{I, J\}$, and $\{\chi_{12}(x, y, s, i)\} \in \chi - group$.

Under transformations $W_{T_i} \rightarrow \varepsilon_{T_i} W_{T_i}$ and $\Theta_{T_i} \rightarrow \varepsilon_{T_i} \Theta_{T_i}$, we have

$$\begin{aligned} \chi_{12} & \rightarrow \varepsilon_{T_2}^*(x, y + 1, s, i)\varepsilon_{T_1}^*(x + 1, y + 1, s, i) \cdot \\ \varepsilon_{T_2}(x + 1, y + 1, s, i)\varepsilon_{T_1}(x + 1, y, s, i)\chi_{12}(x, y, s, i) & \end{aligned} \quad (3.43)$$

Thus, we are able to set all $\chi_{12}(x, y, s, i) = 1$ via the ε_{T_i} -ambiguity.

According to Eq.(3.32) and Eq.(3.34), by doing a gauge transformation $V(x, y, s, i)$ and multiply phase factors $\Phi(x, y, s)$:

$$\begin{aligned} W_{T_2}(x, y, s, i) & \rightarrow V(x, y, s, i)W_{T_2}(x, y, s, i)V^{-1}(x, y - 1, s, i) \\ \Theta_{T_2}(x, y, s) & \rightarrow \Theta_{T_2}(x, y, s)\Phi(x, y, s)\Phi^*(x, y - 1, s) \end{aligned} \quad (3.44)$$

We are able to set $W_{T_2}(x, y, s, i) = I$ as well as $\Theta_{T_2}(x, y, s, i) = 1$. Thus we obtain $T^{(x, y, s)} = T^{(0, y, s)}$. The remaining V -ambiguity preserving the form of W_{T_2} should satisfy $V(x, y, s, i) = V(x, 0, s, i)$, and the remaining Φ -ambiguity preserving the form of Θ_{T_2} should satisfy $\Phi(x, y, s) = \Phi(x, 0, s)$. In addition, any nontrivial ε_{T_2} transformation will change the form of $W_{T_2} = I$, so ε_{T_2} is fixed to be 1. Together with the condition $\chi_{12}(x, y, s, i) = 1$, the remaining ε_{T_1} -ambiguity satisfies $\varepsilon_{T_1}(x, y, s, i) = \varepsilon_{T_1}(x, 0, s, i)$.

Similarly, for T_1 transformation, using the remaining V -ambiguity and Φ -ambiguity, we have

$$\begin{aligned} W_{T_1}(x, y, s, i) & \rightarrow V(x, 0, s, i)W_{T_1}(x, y, s, i)V^{-1}(x - 1, 0, s, i) \\ \Theta_{T_1}(x, y, s) & \rightarrow \Theta_{T_1}(x, y, s)\Phi(x, 0, s)\Phi^*(x - 1, 0, s) \end{aligned} \quad (3.45)$$

Thus we can set $W_{T_1}(x, 0, s, i) = \mathbf{I}$ and $\Theta_{T_1}(x, 0, s) = 1$. To maintain this form of W_{T_1} , we find that there is no remaining ε_{T_1} -ambiguity: ε_{T_1} is fixed to be 1. The remaining V -ambiguity and Φ -ambiguity satisfy $V(x, y, s, i) = V(s, i)$ and $\Phi(x, y, s) = \Phi(s)$; namely they are only dependent on the sublattice index and the virtual leg index from a site, but are independent of the unit cell coordinates. Further, in this gauge, site tensors are translational invariant (but could be sublattice dependent),

$$T^{(x,y,s)} = T^{(x,0,s)} = T^s \doteq T^{(0,0,s)}, \quad s = u, v, w \quad (3.46)$$

Thus, in the gauge that we choose so far, we can solve Eq.(3.41), and get the implementation of translation symmetry on PEPS as

$$\begin{aligned} W_{T_1}(x, y, s, i) &= \eta_{12}^y \\ W_{T_2}(x, y, s, i) &= \mathbf{I} \\ \Theta_{T_1}(x, y, s) &= \mu_{12}^y \\ \Theta_{T_2}(x, y, s) &= 1 \end{aligned} \quad (3.47)$$

So for systems with translational symmetries and $IGG = Z_2$, there are at least two distinct classes of wavefunction. In the context of quantum spin liquids, these two classes are known as *zero flux state* and *π flux state*, corresponding to $\eta_{12} = \mathbf{I}$ and $\eta_{12} = \mathbf{J}$ respectively. Condensations of spinons in these two spin liquids lead to different types of magnetic orders[147]. In the above gauge, although all site tensors related by the translation symmetry share the same form, bond states related by the translation symmetry are in general *different* if η_{12} is nontrivial.

The calculation for other symmetries is similar as the above procedure. The basic idea is to keep fixing gauge by the four ambiguities. And when we find certain algebraic data, such as the η_{12} introduced above, that cannot be removed by the ambiguities, they describe different symmetric PEPS classes. We only list the result here.

This classification scheme will always lead to three finite sets of algebraic indices

η 's, χ 's and Θ 's and we will discuss their physical meanings in Sec.3.4. Although in general systems every set of indices is nonempty, for a half-integer spin system on the kagome lattice described by PEPS with $IGG = Z_2$, we have:

- η_{12} , η_{C_6} and η_σ , where $\eta \in \{I, J\}$. The corresponding $\mu_{12}, \mu_{C_6}, \mu_\sigma$ are determined by η 's.
- χ_σ and $\chi_\mathcal{T}$, where $\chi = \pm 1$.
- There turns out to be no tunable Θ indices in this example.

So the number of classes equals to $2^5 = 32$. By choosing a gauge, the symmetry operations on PEPS can be solved as

$$\begin{aligned}
W_{T_1}(x, y, s, i) &= \eta_{12}^y, \\
W_{T_2}(x, y, s, i) &= I, \\
W_{C_6}(x, y, u, i) &= \eta_{12}^{xy + \frac{1}{2}x(x+1) + x+y} w_{C_6}(u, i), \\
W_{C_6}(x, y, v, i) &= \eta_{12}^{xy + \frac{1}{2}x(x+1) + x+y}, \\
W_{C_6}(x, y, w, i) &= \eta_{12}^{xy + \frac{1}{2}x(x+1)}, \\
W_\sigma(x, y, s, i) &= \eta_{12}^{x+y+xy} w_\sigma(s, i), \\
W_\mathcal{T}(x, y, s, i) &= w_\mathcal{T}(s, i), \\
W_{\theta\vec{n}}(x, y, s, i) &= \bigoplus_i (I_{n_i} \otimes e^{i\theta\vec{n}\cdot\vec{S}_i}). \tag{3.48}
\end{aligned}$$

In this gauge all W_R matrices are unitary. The last equation is for the $SU(2)$ spin rotation along \vec{n} direction by an angle θ . In addition, in this gauge we choose $J = W_{2\pi}(x, y, s, i) = \bigoplus_i (I_{n_i} \otimes e^{i2\pi\vec{n}\cdot\vec{S}_i})$; namely J is the direct sum of I_{D_1} for the integer spin subspace and $-I_{D_2}$ for the half-integer spin subspace and $D_1 + D_2 = D$.

For the rotation transformation $w_{C_6}(u, i)$, we have

$$\begin{aligned}
w_{C_6}(u, a) &= w_{C_6}(u, c) = I, \\
w_{C_6}(u, b) &= w_{C_6}(u, d) = \eta_{12}\eta_{C_6}, \tag{3.49}
\end{aligned}$$

For the reflection transformation $w_\sigma(s, i)$, we have

$$\begin{aligned}
w_\sigma(u, a) &= \mathbf{I}, & w_\sigma(u, b) &= \chi_\sigma \eta_{12} \eta_{C_6}, \\
w_\sigma(u, c) &= \chi_\sigma \eta_{12} \eta_{C_6} \eta_\sigma, & w_\sigma(u, d) &= \eta_\sigma; \\
w_\sigma(v, a) &= \eta_{12}, & w_\sigma(v, b) &= \chi_\sigma \eta_{12}, \\
w_\sigma(v, c) &= \eta_{C_6} \eta_\sigma, & w_\sigma(v, d) &= \chi_\sigma \eta_{C_6} \eta_\sigma; \\
w_\sigma(w, a) &= \chi_\sigma \eta_{C_6}, & w_\sigma(w, b) &= \eta_{C_6}, \\
w_\sigma(w, c) &= \eta_{12} \eta_\sigma, & w_\sigma(w, d) &= \chi_\sigma \eta_{12} \eta_\sigma;
\end{aligned} \tag{3.50}$$

And for the time reversal transformation $w_\mathcal{T}$, we have

$$\begin{aligned}
w_\mathcal{T}(u, a) &= w_\mathcal{T}, & w_\mathcal{T}(u, b) &= \eta_{12} \eta_{C_6} w_\mathcal{T}, \\
w_\mathcal{T}(u, c) &= \eta_{12} \eta_{C_6} \eta_\sigma w_\mathcal{T}, & w_\mathcal{T}(u, d) &= \eta_\sigma w_\mathcal{T}; \\
w_\mathcal{T}(v, a) &= \eta_{12} \eta_{C_6} w_\mathcal{T}, & w_\mathcal{T}(v, b) &= w_\mathcal{T}, \\
w_\mathcal{T}(v, c) &= \eta_\sigma w_\mathcal{T}, & w_\mathcal{T}(v, d) &= \eta_{12} \eta_{C_6} \eta_\sigma w_\mathcal{T}; \\
w_\mathcal{T}(w, a) &= w_\mathcal{T}, & w_\mathcal{T}(w, b) &= \eta_{12} \eta_{C_6} w_\mathcal{T}, \\
w_\mathcal{T}(w, c) &= \eta_{12} \eta_{C_6} \eta_\sigma w_\mathcal{T}, & w_\mathcal{T}(w, d) &= \eta_\sigma w_\mathcal{T};
\end{aligned} \tag{3.51}$$

where

$$w_\mathcal{T} = \begin{cases} \bigoplus_i (\mathbf{I}_{n_i} \otimes e^{i\pi S_i^y}) & \text{if } \chi_\mathcal{T} = 1 \\ \bigoplus_i (\Omega_{n_i} \otimes e^{i\pi S_i^y}) & \text{if } \chi_\mathcal{T} = -1 \end{cases} \tag{3.52}$$

Here n_i is dimension of the extra degeneracy associated with spin- S_i . Namely, the total degeneracy for spin- S_i living on one virtual leg equals $n_i \times (2S_i + 1)$. We have the virtual bond dimension

$$D = \sum_i n_i (2S_i + 1) \tag{3.53}$$

And, $\Omega_{n_i} = i\sigma_y \otimes \mathbf{I}_{n_i/2}$ is a n_i dimensional antisymmetric matrix.

For Θ_R 's, we have

$$\begin{aligned}
\Theta_{T_1}(x, y, s) &= \mu_{12}^y, \\
\Theta_{T_2}(x, y, s) &= 1, \\
\Theta_{C_6}(x, y, u) &= \mu_{12}^{xy + \frac{1}{2}x(x+1) + x+y} \Theta_{C_6}(u), \\
\Theta_{C_6}(x, y, v) &= \mu_{12}^{xy + \frac{1}{2}x(x+1) + x+y}, \\
\Theta_{C_6}(x, y, w) &= \mu_{12}^{xy + \frac{1}{2}x(x+1)}, \\
\Theta_\sigma(x, y, s) &= \mu_{12}^{x+y+xy} \Theta_\sigma(s), \\
\Theta_\tau(x, y, u/w) &= 1, \\
\Theta_\tau(x, y, v) &= \mu_{12} \mu_{C_6}, \\
\Theta_{\theta\bar{n}} &= 1,
\end{aligned} \tag{3.54}$$

where

$$\begin{aligned}
\Theta_{C_6}(u) &= (\mu_{12} \mu_{C_6})^{\frac{1}{2}}; \\
\Theta_\sigma(u) &= (\mu_\sigma)^{\frac{1}{2}}; \\
\Theta_\sigma(v) &= \mu_{C_6} \Theta_{C_6}(u) \Theta_\sigma(u); \\
\Theta_\sigma(w) &= \mu_\sigma \mu_{C_6} (\Theta_{C_6}(u) \Theta_\sigma(u))^{-1}.
\end{aligned} \tag{3.55}$$

Note that in Eq.(3.55) $\Theta_{C_6}(u)$ and $\Theta_\sigma(u)$ contain square roots so there appear to be two possible values of each of them differing by a minus sign, giving rise to Θ -indices. However, these minus signs can be tuned away using the η -ambiguities in the definition of W_{C_6} and W_σ since every site tensor is Z_2 odd. So one could simply fix an arbitrary choice for the square roots here. This is the reason why there turns out to be no tunable Θ indices in this example.

Even after all these transformation rules are determined by gauge fixing, we still have some remaining V -ambiguity for each class. (Note that there is no remaining nontrivial η, ε and Φ ambiguities.) To preserve the lattice symmetry, the remaining V -ambiguity is independent of sites and legs. To preserve the form of $W_{\theta\bar{n}}$, the remaining

V -ambiguity must have the following form:

$$V = \bigoplus_i (\tilde{V}_{S_i} \otimes \mathbb{I}_{2S_i+1}), \quad (3.56)$$

where \tilde{V}_{S_i} is a n_i dimensional matrix. In addition, the time-reversal transformation $W_{\mathcal{T}}$ further constrains the form of component matrices \tilde{V}_{S_i} . When $\chi_{\mathcal{T}} = 1$, one can show that \tilde{V}_{S_i} must be a *real* matrix. For the purpose of presentation we only consider $\chi_{\mathcal{T}} = 1$ classes here. The $\chi_{\mathcal{T}} = -1$ cases involve quaternion matrices and we leave the general and detailed discussions in [76].

Next, we are at the stage to construct the constrained sub-Hilbert spaces for building block tensors for all classes, according to the W_R transformation rules. The basic idea is to determine the generic form of a single site/bond tensor using the W_R 's with R leaving the site/bond invariant, and then generate all other site/bond tensors using all W_R 's. The generic forms of site tensors are straightforwardly determined in this fashion, with a set of real continuous variational parameters whose number basically equals the dimension of the constrained site sub-Hilbert space. However, for bond tensors, we will use the remaining V -ambiguity to bring them into canonical forms which are maximal entangled bond states containing *no* continuous variational parameters.

To make sure a bond tensor B_b to be invariant under the $SU(2)$ spin rotation, it must have the following form:

$$B_b = \bigoplus_{i=1}^M \left(\tilde{B}_b^{S_i} \otimes K_{S_i} \right), \quad (3.57)$$

where $\tilde{B}_b^{S_i}$ is n_i dimensional matrix, and K_{S_i} is the fixed $(2S_i + 1)$ dimensional matrix representing the spin singlet formed by two spin- S_i on the two virtual legs shared by B_b . For example, we get $K_{S=0} = 1$, $K_{S=\frac{1}{2}} = i\sigma_y$.

As shown in [76], when $\chi_{\mathcal{T}} = 1$ and a given S_i , depending on the four possible values of η_{σ} and χ_{σ} , the component matrix $\tilde{B}_b^{S_i}$ must be a purely real/imaginary symmetric/antisymmetric matrix. Then we can use the remaining V -ambiguity in

Eq.(3.56) to simplify $\tilde{B}_b^{S_i}$, because under a \tilde{V}_{S_i} transformation, $\tilde{B}_b^{S_i}$ transforms as:

$$\tilde{B}_b^{S_i} \rightarrow \tilde{V}_{S_i} \cdot \tilde{B}_b^{S_i} \cdot \tilde{V}_{S_i}^t \quad (3.58)$$

Clearly we can use a real orthogonal \tilde{V}_{S_i} to diagonalize (block diagonalize) $\tilde{B}_b^{S_i}$ if $\tilde{B}_b^{S_i}$ is a symmetric (antisymmetric) matrix. After this, the eigenvalues of $\tilde{B}_b^{S_i}$ could have arbitrary norms. But then we can use another real diagonal \tilde{V}_{S_i} matrix to normalize the eigenvalues so that they are only ± 1 (if $\tilde{B}_b^{S_i}$ is purely real) or $\pm i$ (if $\tilde{B}_b^{S_i}$ is purely imaginary).

This procedure fixes B_b to be maximal entangled states with no continuous variational parameters. However, the relative number of $+1(+i)$ eigenvalues and $-1(-i)$ eigenvalues cannot be further tuned away by gauge fixing and will serve as discrete variational parameters on the bond tensors.

The previous discussions in the subsection are general for any half-integer spin- S . *Below we focus on the case with $S = \frac{1}{2}$.* For simplicity, we demonstrate the results for with $D = 3$. The basis of virtual legs of site tensors are $\{|0\rangle, |\uparrow\rangle, |\downarrow\rangle\}$. Namely, virtual legs are formed by one spin singlet and one spin doublet. Note that virtual legs of bond tensors are dual to those of site tensors, so the basis are $\langle 0|, \langle \uparrow|, \langle \downarrow|$. Symmetric PEPS with larger D are also conceptually straightforward but technically involved to obtain, and we leave the general construction in [76]

As discussed in [76], only classes satisfying $\eta_\sigma = J$, $\chi_\sigma = 1$ and $\chi_\tau = 1$ can be realized with $D = 3$. So the realizable classes reduce to $2^2 = 4$ with $D = 3$. At such a small D , it turns out that each class has only two continuous variational parameters. (Note that for $D = 6$, i.e. two spin singlet and two spin doublet on the virtual leg, we find that all the 32 classes can be realized. And each class has 47 continuous variational parameters.) Following the above procedure we can bring the bond tensor

on a given bond b_0 into the canonical form:

$$B_{b_0} = \begin{pmatrix} \pm 1 & 0 & 0 \\ 0 & 0 & -i \\ 0 & i & 0 \end{pmatrix} \quad (3.59)$$

All other bond tensors are generated by combination of translation and rotation symmetries as:

$$B_{R(b)} = R^{-1} W_R R \circ B_{b_0} \quad (3.60)$$

where $R = T_1^{n_1} T_2^{n_2} C_6^{n_{C_6}}$ with $n_1, n_2, n_{C_6} \in \mathbb{Z}$.

One can view a bond tensor as a quantum state living in the Hilbert space formed by the tensor product of two virtual legs. Namely, we have

$$\hat{B}_{b_0} = \pm \langle 0, 0 | - i \langle \uparrow, \downarrow | + i \langle \downarrow, \uparrow | \quad (3.61)$$

Here we use notation \hat{B}_{b_0} as the quantum state representation while B_{b_0} as the matrix (tensor) representation.

At a given site s_0 , the generic form of the site tensor for all classes can be summarized as:

$$\begin{aligned} \hat{T}^{s_0} = & \{ \hat{K}_0 + \hat{K}_{12}(p_1, p_2) \} + \Theta_{C_6}^{-1}(u) \{ a \leftrightarrow b, c \leftrightarrow d \} + \Theta_{\sigma}^{-1}(u) \cdot \\ & \{ a \leftrightarrow d, b \leftrightarrow c \} + \mu_{12} \mu_{C_6} (\Theta_{C_6}(u) \Theta_{\sigma}(u))^{-1} \{ a \leftrightarrow c, b \leftrightarrow d \} \end{aligned} \quad (3.62)$$

with real continuous parameters p_1, p_2 . Here a, b, c, d denote virtual leg of sites, as shown in Fig.(3-4). \hat{K}_0 and \hat{K}_{12} denote linear independent spin singlet states, which

can be expressed as

$$\begin{aligned}
\hat{K}_0 &= |\uparrow\rangle \otimes |\downarrow 000\rangle - |\downarrow\rangle \otimes |\uparrow 000\rangle \\
\hat{K}_{12} &= p_1 \cdot (|\uparrow\rangle \otimes |0 \downarrow \uparrow \downarrow\rangle + |\downarrow\rangle \otimes |0 \uparrow \downarrow \uparrow\rangle) + \\
&\quad p_2 \cdot (|\uparrow\rangle \otimes |0 \downarrow \downarrow \uparrow\rangle + |\downarrow\rangle \otimes |0 \uparrow \uparrow \downarrow\rangle) - \\
&\quad (p_1 + p_2) \cdot (|\uparrow\rangle \otimes |0 \uparrow \downarrow \downarrow\rangle + |\downarrow\rangle \otimes |0 \downarrow \uparrow \uparrow\rangle),
\end{aligned} \tag{3.63}$$

where the first spin lives on the physical leg, while the following four spins live on virtual legs a, b, c, d respectively. Note that we have chosen a particular gauge such that all site tensors share the same form.

By direct comparison, the NN RVB state ($Q_1 = Q_2$ state) given in Sec.(3.2.5) is represented as the PEPS defined in Eq.(3.59) and Eq.(3.62), with $p_1 = p_2 = 0$ and:

$$\begin{aligned}
\eta_{12} = \eta_{C_6} &= \mathbf{I}, \quad \eta_\sigma = \mathbf{J}; \\
\chi_\sigma = \chi_{\mathcal{T}} &= 1;
\end{aligned} \tag{3.64}$$

3.4 Physical Interpretation of Classes

We will discuss the physical meanings of different classes, which are labeled by Θ_R , χ_R as well as η_R . In this section, we will focus on the non-symmetry-breaking liquid member phase in each crude class.

3.4.1 Interpretation of Θ_R and χ_R

Although it happens to be true that the kagome half-integer spin example has no tunable Θ_R indices, Θ_R indices do appear in general quantum systems.

In fact, the Θ_R indices and the χ_R indices generally appear even when the IGG is trivial. For instance, we could consider a system on the kagome lattice with *no* on-site symmetry (i.e., remove the spin $SU(2)$ rotation and the time-reversal symmetry in our main example), and consequently the minimal required IGG is trivial. Assuming

IGG being trivial in this system, we will not have the η indices but still have the χ indices. The calculation procedure of transformation rules almost remains the same as before if we simply limit all the η 's to be identity. Eventually we will arrive at Eq.(3.55) replacing all the μ_R by $+1$. Note that there is no η -ambiguities to tune away the signs for the square roots as in the half-integer spin case. In this system, apart from the χ indices, we do have two tunable Θ indices in the PEPS classification: $\Theta_{C6}(u) = \pm 1$ and $\Theta_\sigma(u) = \pm 1$.

Different Θ_R indices can be viewed as different symmetry quantum numbers (for either on-site symmetries or space group symmetries) carried by each site tensor. These quantum numbers of the site tensors, generally speaking, directly contribute to the quantum numbers of a finite size sample. The physics of Θ_R indices is similar to the physics of the so-called “fragile Mott insulator” discussed by Yao and Kivelson[165]. And similar indices in one-dimensional matrix product states have been investigated recently[52]. For instance, in the fragile Mott insulator example[165], a Mott insulator wavefunction is constructed on the checkerboard lattice which carries nontrivial point group quantum numbers on the odd-by-odd unit cell lattices. This distinguishes the fragile Mott insulator from trivial insulators which carries trivial quantum numbers on the same lattices. And such nontrivial quantum numbers can be traced back to the quantum numbers carried by the wavefunction on every square cluster on the checkerboard lattice. If one tries to use a site tensor in PEPS to represent the square cluster wavefunction, it is clear that this site tensor forms a nontrivial representation of the point group symmetry.

The physical meaning of χ_R may be more well-known. These are generalizations of the symmetry fractionalizations in the 2d AKLT model[1]. Let's firstly briefly describe the PEPS construction of the $SO(3)$ symmetric spin-2 AKLT state on the square lattice. In this construction, each virtual leg forms a spin-1/2 projective representation of the $SO(3)$ symmetry group of the spin-2 system. Each site tensor is given by the only singlet state formed by the physical spin-2 and the four virtual spin-1/2's, and each bond tensor is formed by the only spin singlet formed by the two spin-1/2's on the two ends of the bond. Such an AKLT wavefunction can be shown

to be the unique gapped ground state of the AKLT Hamiltonian on the square lattice with periodic boundary conditions[53].

However, when the system has an open boundary, one needs to specify a symmetric boundary condition. But one encounters the following problem: each site tensor on the boundary has only three virtual spin-1/2's and it is impossible for form a spin-singlet with the physical spin-2. Basically each site on the boundary can be viewed as a half-integer spin — which is a projective representation of the original $SO(3)$ group. One sometimes calls this phenomena as the symmetry fractionalization in 2d *in the absence of topological orders*. When coupled together along a translational symmetric edge, the low energy dynamics of the edge states can be effectively described by a translational symmetric half-integer spin chain, which would give a gapless excitation spectrum assuming no spontaneous translational symmetry breaking. Clearly, in the PEPS construction, the origin of such symmetry fractionalization behavior is due to the fact that projective representations appear in the virtual legs.

For an on-site symmetry R , this is exactly the physics that χ_R captures. For instance, the $\chi_{\mathcal{T}}$ index appearing in the kagome example is really about the projective representations of the symmetry group $SU(2) \times \mathcal{T}$ on the virtual legs. As mentioned before, when $\chi_{\mathcal{T}} = 1$, the half-integer (integer) spins on the virtual legs form Kramer doublet (singlet) under the time-reversal transformation. This is the usual representation of $SU(2) \times \mathcal{T}$. However when $\chi_{\mathcal{T}} = -1$, the half-integer (integer) spins on the virtual legs form Kramer singlet (doublet) under the time-reversal transformation. This is a nontrivial projective representation of $SU(2) \times \mathcal{T}$. We expect that $\chi_{\mathcal{T}} = -1$ would give rise to nontrivial signatures in entanglement spectra and physical edge states.

For a spatial symmetry R , the physical meaning of χ_R is less obvious. But it's one-dimensional analog has been investigated in the context of matrix product states[23, 118, 109, 108]. In our example, the χ_{σ} is capturing similar physics in 2d kagome lattice, which basically describes how the tensor network forms possible projective representations of the spatial reflection. We speculate that nontrivial χ_{σ} would give rise to signatures in entanglement spectra when the partition of the system respects

the σ reflection.

In summary, Θ_R is capturing local contributions to symmetry group quantum numbers, and χ_R is capturing the symmetry fractionalizations *not* due to topological orders.

3.4.2 η_R and symmetry fractionalization

Here, we will show that η 's are directly related to the symmetry fractionalization of spinon excitations (chargons). To see this, let us firstly introduce the concept of symmetry fractionalization in the presence of topological orders. We will use the unitary on-site symmetry as an example. Related discussions can be found in Ref.[98] and Ref.[44].

Starting from a topologically ordered ground state with a global symmetry group SG , consider an excited state, having n -quasiparticles (which do not have to be of the same type) spatially located at position $\mathbf{r}_1, \mathbf{r}_2, \dots, \mathbf{r}_n$, far apart from one another. Let's denote this state by $|\psi(\mathbf{r}_1, \mathbf{r}_2, \dots, \mathbf{r}_n)\rangle$. For any symmetry transformation $U(g)$ by a group element $g \in SG$, $U(g)$ will generally transform this state to another state:

$$U(g) \circ |\psi(\mathbf{r}_1, \mathbf{r}_2, \dots, \mathbf{r}_n)\rangle \rightarrow |\tilde{\psi}(\mathbf{r}_1, \mathbf{r}_2, \dots, \mathbf{r}_n)\rangle \quad (3.65)$$

One way to describe the symmetry fractionalization on quasiparticles is the following condition: there exist local operators $U_1(g), U_2(g), \dots, U_n(g)$, such that $U_i(g)$ is a local operator acting only in a finite region around the spatial position \mathbf{r}_i , and does not touch the other quasiparticles; in addition, $U_1(g), U_2(g), \dots, U_n(g)$ satisfy:

$$\begin{aligned} & U_1(g) \cdot U_2(g) \cdots U_n(g) |\psi(\mathbf{r}_1, \mathbf{r}_2, \dots, \mathbf{r}_n)\rangle \\ &= U(g) |\psi(\mathbf{r}_1, \mathbf{r}_2, \dots, \mathbf{r}_n)\rangle = |\tilde{\psi}(\mathbf{r}_1, \mathbf{r}_2, \dots, \mathbf{r}_n)\rangle \end{aligned} \quad (3.66)$$

Note that technically Eq.(3.66) is *not* a general condition for symmetry fractionalization phenomena. For example, let us consider SG to be an on-site $U(1)$ symmetry, and assume that Eq.(3.66) holds for a wavefunction $|\psi(\mathbf{r}_1, \mathbf{r}_2, \dots, \mathbf{r}_n)\rangle$. We can then

just add one extra $U(1)$ charge outside the regions that $U_i(g)$ ($i = 1, \dots, n$) act and obtains a new wavefunction $|\bar{\psi}(\mathbf{r}_1, \mathbf{r}_2, \dots, \mathbf{r}_n)\rangle$. It is perfectly fine to imagine the extra charge as if it already exists in the ground state. Physically the local operators that transform quasiparticles: $U_i(g)$ for $|\bar{\psi}\rangle$ should be exactly the same as before, since $|\psi\rangle$ and $|\bar{\psi}\rangle$ are locally identical around $\mathbf{r}_1, \mathbf{r}_2, \dots, \mathbf{r}_n$. However, clearly Eq.(3.66) is no longer true for $|\bar{\psi}\rangle$, because the global symmetry $U(g)$ picks up an extra $U(1)$ phase from the added $U(1)$ charge.

In fact, Eq.(3.66) implicitly assumes that, under a global symmetry transformation, there is no phase “locally accumulated” in the ground state wavefunction. But, as demonstrated above, generally there could be such “locally accumulated” phases in the ground state, and Eq.(3.66) should be modified up to the “locally accumulated” phases.

How to sharply define such “locally accumulated” phases in general? The answer to this question is important to provide a general sharp definition of $U_i(g)$. But to answer this question, one needs a tool capable to diagnose wavefunctions locally, which is exactly the power of PEPS. For the moment, let us postpone answering this question in the framework of PEPS, and have some further discussion on symmetry fractionalizations.

First, fractionalized symmetry transformations are local operators and cannot change the quasiparticle species (or more precisely, the superselection sector of a quasiparticle). Thus, we can investigate the transformation rules of each anyon species individually. However, anyons do not need to form a representation of SG due to the nontrivial fusion rule. For example, in a Z_2 topological ordered phase, two chargons fuse to one trivial particle. We can multiply each chargon in the system by a fixed element in an $IGG' = Z_2 = \{1, -1\}$. Clearly, the total phase becomes unity, and physical wavefunction is invariant. Here IGG' is the subgroup of $U(1)$ describing the fusion rule of chargons. Quite generally for a Z_n topological order, $IGG' = Z_n$.

A PEPS with $IGG = Z_n$ can describe a deconfined phase with a Z_n topological order. We will only consider this case and we do have $IGG' = IGG$. So IGG tells us that when we implement the global symmetry transformation on chargons, it is

perfect fine to have a phase ambiguity, if this phase ambiguity is an element in IGG . Consequently, a single quasiparticle could form a projective representation of SG with coefficient in IGG , which is classified by second cohomology $H^2(SG, IGG)$.

Now, let us translate the above discussion into the PEPS language. The main task is to construct the local symmetry transformation operators for a small patch of PEPS with a nontrivial IGG . Here we focus on $IGG = Z_2$ case. Without loss of generality, we assume that tensors of the PEPS are all Z_2 even. Then we cut a small patch \mathcal{A} from the PEPS. We can view the tensor associated with patch \mathcal{A} as a linear map from boundary virtual legs to physical legs living in the bulk of the patch, which is labeled as $\hat{T}_{\mathcal{A}}^0$. Here 0 denotes that there is no quasiparticles inside \mathcal{A} . Namely,

$$\hat{T}_{\mathcal{A}}^0 = \sum_{I,V} (T_{\mathcal{A}}^0)_{IV} |I\rangle \langle V| \quad (3.67)$$

where $|I\rangle$ labels ket states of all physical legs inside \mathcal{A} , while $\langle V|$ labels bra states of all boundary virtual legs.

Before studying excitations inside \mathcal{A} , we firstly discuss properties of $\hat{T}_{\mathcal{A}}^0$. As a tensor, $\hat{T}_{\mathcal{A}}^0$ is Z_2 even. Namely, action of the nontrivial Z_2 element g on the boundary legs of $\hat{T}_{\mathcal{A}}^0$ leaves the tensor invariant. This property implies that $\hat{T}_{\mathcal{A}}^0$, as a linear map, can never be injective. To see this, consider an arbitrary boundary state $|V\rangle$, we have

$$\hat{T}_{\mathcal{A}}^0 |V\rangle = \hat{T}_{\mathcal{A}}^0 |g \circ V\rangle \quad (3.68)$$

So, the inverse map of $\hat{T}_{\mathcal{A}}^0$ is not well defined. To have a reasonable definition of the inverse map, one observes that an arbitrary boundary state $|V\rangle$ can be rewritten as

$$\begin{aligned} |V\rangle &= \frac{1}{2}(|V\rangle + |g \circ V\rangle) + \frac{1}{2}(|V\rangle - |g \circ V\rangle) \\ &= \Pi_{\mathcal{U}} |V\rangle + (1 - \Pi_{\mathcal{U}}) |V\rangle \end{aligned} \quad (3.69)$$

where \mathcal{U} is the Z_2 even sector of boundary legs. Namely, $\forall |V\rangle \in \mathcal{U}$, we have $|g \circ V\rangle = |V\rangle$. $\Pi_{\mathcal{U}}$ is a projection operator which projects a boundary state into \mathcal{U} . Under $\hat{T}_{\mathcal{A}}^0$,

the second term in the above equation is mapped to zero. For a generic PEPS with $IGG = Z_2$, we can further assume that $\hat{T}_{\mathcal{A}}^0$ is injective on the subspace \mathcal{U} when the patch \mathcal{A} is not too small. This is because the dimension of the physical Hilbert space increases parametrically faster than the dimension of the boundary virtual Hilbert space as the patch size increases. Such a PEPS is named as a Z_2 injective PEPS in Ref.[117]. Namely, generically one can find a linear map $(\hat{T}_{\mathcal{A}}^0)^{-1}$ from bulk physical legs to boundary virtual legs, such that

$$(\hat{T}_{\mathcal{A}}^0)^{-1} \cdot \hat{T}_{\mathcal{A}}^0 = \Pi_{\mathcal{U}} \quad (3.70)$$

Next, let us study the case with topological excitations inside patch \mathcal{A} . One could create odd number of chargons near the center of the patch \mathcal{A} by modifying $\hat{T}_{\mathcal{A}}^0$ to some Z_2 odd tensor $\hat{T}_{\mathcal{A}}^e$. Opposite to the previous case, we have

$$\hat{T}_{\mathcal{A}}^e |V\rangle = 0, \quad \forall |V\rangle \in \mathcal{U} \quad (3.71)$$

Generically we can further assume $\hat{T}_{\mathcal{A}}^e$ is injective on the Z_2 odd sector of boundary legs. Namely, one can construct $(\hat{T}_{\mathcal{A}}^e)^{-1}$ as linear map from bulk legs to Z_2 odd sector of boundary legs, such that

$$(\hat{T}_{\mathcal{A}}^e)^{-1} \cdot \hat{T}_{\mathcal{A}}^e = \Pi_{\bar{\mathcal{U}}} \quad (3.72)$$

where $\Pi_{\bar{\mathcal{U}}} \equiv 1 - \Pi_{\mathcal{U}}$.

Similarly, one can construct patch tensors with even number chargons inside the patch by modifying $\hat{T}_{\mathcal{A}}^0$ to any other Z_2 even and Z_2 injective tensors. For example, let us assume $\hat{T}_{\mathcal{A}}^1$ to be such a tensor. Then, one can find its inverse $(\hat{T}_{\mathcal{A}}^1)^{-1}$ on the subspace \mathcal{U} , such that $(\hat{T}_{\mathcal{A}}^1)^{-1} \cdot \hat{T}_{\mathcal{A}}^1 = \Pi_{\mathcal{U}}$.

In the following, we will study the local physical operator acting on small patches for a symmetry R . Starting with a PEPS wavefunction $|\Psi\rangle$ with topological excitations inside small patches $\mathcal{A}, \mathcal{B}, \dots$, while the region outside these patches share the same tensors as the ground state wavefunction $|\Psi_0\rangle$. The action of the symmetry R

on $|\Psi\rangle$ is obtained by acting R on all tensors, which is defined in Eq.(3.6,3.10,3.12). Since we try to construct local symmetry operators only on patches $\mathcal{A}, \mathcal{B}, \dots$, we can apply gauge transformations W_R on all virtual legs in the region *outside* all small patches as well as on the boundaries of all small patches, but leave virtual legs inside small patches untouched. Note that this gauge transformation does *not* modify the R -transformed physical wavefunction at all. Because tensors outside small patches are the same as tensors of ground state, the following relations still hold for them:

$$\begin{aligned} T^s &= \Theta_R W_R R \circ T^s \\ B_b &= W_R R \circ B_b \end{aligned} \tag{3.73}$$

Thus, under the symmetry R together with the gauge transformation W_R defined above, tensors outside patches will be invariant up to an “*locally accumulated*” phase $\prod_{s \in \text{outside}} \Theta_R(s)$. We emphasize that this actually provides the sharp *definition* of the “locally accumulated” phases mentioned earlier in this section. As discussed in the previous subsection, $\Theta_R(s)$ ’s exactly capture the local phases picked up after applying a global symmetry transformation. Without the tool of PEPS, it is actually difficult to sharply define this object.

For tensors inside patches, we have

$$\hat{T}_{\mathcal{A}}^R = W_R R \circ \hat{T}_{\mathcal{A}} \tag{3.74}$$

Here, $\hat{T}_{\mathcal{A}}$ is the linear map associated with patch \mathcal{A} , which is obtained by contraction of all tensors inside \mathcal{A} patch. And W_R in Eq.3.74 is defined to *only* act on boundary virtual legs of $\hat{T}_{\mathcal{A}}$. Note that $\hat{T}_{\mathcal{A}}$ is either Z_2 even or Z_2 odd, which corresponds to even number charginos or odd number charginos inside \mathcal{A} . Note that we should always choose the patch that is large enough so that all quasiparticles exist in the patch before the transformation keep staying in the patch after the transformation. The above equation can be viewed as the *definition* of $\hat{T}_{\mathcal{A}}^R$.

In fact, Eq.(3.74) is a very general result which is applicable even when the con-

dition of symmetry fractionalizations breaks down. For example, it is possible that certain symmetry transformation interchanges quasiparticle superselection sectors. In the PEPS formulation this happens when \hat{T}_A^R and \hat{T}_A describes distinct quasiparticle species, and consequently there is no way to use a local physical operator in \mathcal{A} to send \hat{T}_A to \hat{T}_A^R . For the kagome example this would never happen. For example, we showed that W_R matrices all commute with the nontrivial IGG element $g = J$, and therefore the parity of the number of chargons would be the same in \hat{T}_A^R and \hat{T}_A . But in a symmetric PEPS with a larger IGG (e.g. $IGG = Z_2 \times Z_2$), we expect that it is possible that W_R does not commute with a $g \in IGG$. In this case the R may interchange quasiparticle species.

Below we only consider the situation that \hat{T}_A^R and \hat{T}_A support the same superselection sector and consequently share the same Z_2 parity. This allows us to construct the fractionalized local *physical* operator \hat{L}_R^A for the symmetry R acting on patch \mathcal{A} that realizes Eq.(3.74); namely:

$$\hat{L}_R^A \circ \hat{T}_A = W_R R \circ \hat{T}_A, \quad (3.75)$$

at least for those \hat{T}_A describing the relevant low energy states. One should keep in mind that L_R^A only acts on physical legs, without touching boundary legs; i.e.,

$$\hat{L}_R^A = \sum_{I,I'} (L_R^A)_{I,I'} |I\rangle \langle I'|. \quad (3.76)$$

To obtain the explicit form of this local operator, let us consider a particular tensor \hat{T}_A^e , which supports an odd number of chargons in \mathcal{A} . We have

$$\hat{T}_A^{e,R} = [\hat{T}_A^{e,R} \cdot (\hat{T}_A^e)^{-1}] \cdot \hat{T}_A^e \quad (3.77)$$

where $\hat{T}_A^{e,R} \equiv W_R R \circ \hat{T}_A^e$, and $(\hat{T}_A^e)^{-1}$ is defined in Eq.(3.72). In the above equation we assume that both \hat{T}_A^e and $\hat{T}_A^{e,R}$ is Z_2 odd as well as injective in the Z_2 odd subspace of boundary legs, which is expected to be generically true. Note that $[\hat{T}_A^{e,R} \cdot (\hat{T}_A^e)^{-1}]$ can be viewed as an operator acting only on physical legs.

To study the transformation rules for a number of chargon excitations, let us consider a finite set Λ of tensors: $\Lambda \equiv \{\hat{T}_{\mathcal{A}}^{(i)}, i = 0, 1, \dots\}$ in the patch \mathcal{A} . These tensors may describe states with chargon number equal to zero, one, two, etc, and are injective in the corresponding boundary Z_2 sectors respectively. But tensors in Λ contain *no* fluxon excitations in \mathcal{A} . (we will study the symmetry fractionalization of fluxons later in this chapter.) We assume that any symmetry transformation as shown in Eq.(3.74) transform within the linear space spanned by Λ .

In addition, we assume the tensors in Λ to satisfy $(\hat{T}_{\mathcal{A}}^{(j)})^{-1} \cdot \hat{T}_{\mathcal{A}}^{(i)} = \mathbf{0}, \forall i \neq j$. Physically, this can be achieved by choosing Λ so that all tensor states in it can be sharply distinguished from each other by a set of mutually commuting local physical measurements. Mathematically these local physical measurements are Hermitian operators acting near the center of the patch where quasiparticles live. For instance, these measurements could include a measurement of the locations of chargons by inserting small fluxon loops. Then $\{\hat{T}_{\mathcal{A}}^{(i)}\}$ are chosen to be the eigenstates of these measurements with distinct eigenvalues. Since these measurements are locally near the center of the patch, the boundary condition (i.e., the virtual boundary state) will not affect the measurement when the patch is large enough, and the condition $(\hat{T}_{\mathcal{A}}^{(j)})^{-1} \cdot \hat{T}_{\mathcal{A}}^{(i)} = \mathbf{0}, \forall i \neq j$ is expected to hold.

We then can construct a local operator to transform states in Λ under a symmetry R :

$$\hat{L}_R^{\mathcal{A}} = \sum_i [\hat{T}_{\mathcal{A}}^{(i),R} \cdot (\hat{T}_{\mathcal{A}}^{(i)})^{-1}] \quad (3.78)$$

as shown in Fig.(3-5b). One can easily verify, $\hat{L}_R^{\mathcal{A}}$ defined above indeed satisfies Eq.(3.75) for all states in Λ . Moreover, such local operators in patches $\mathcal{A}, \mathcal{B}, \dots$ satisfy the symmetry fractionalization condition Eq.(3.66) up to the “locally accumulated” phase outside these patches $\prod_{s \in \text{outside}} \Theta_R(s)$.

After the local symmetry operator is defined, we are able to study the symmetry fractionalization of chargons. Consider a relation between symmetry group elements

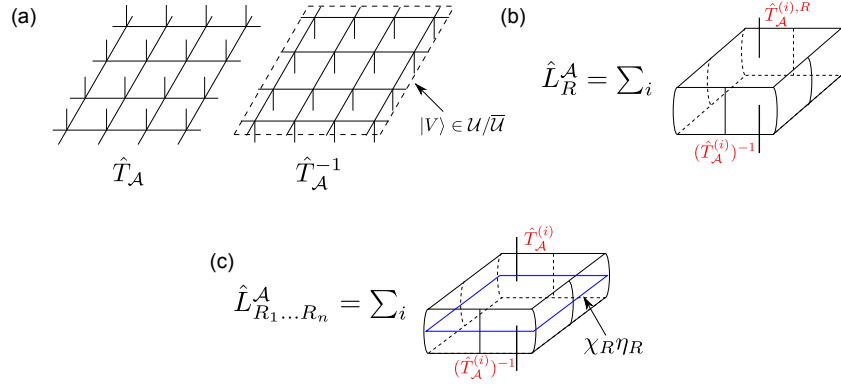


Figure 3-5: (a): Tensor \hat{T}_A and its “generalized inverse” \hat{T}_A^{-1} associated with patch \mathcal{A} . \hat{T}_A is obtained by contracting all bond tensors and site tensors inside patch \mathcal{A} . As a linear map from boundary legs to bulk legs, \hat{T}_A is either Z_2 even or Z_2 odd. (b): The local R -symmetry operator on patch \mathcal{A} . $\{\hat{T}_A^{(i)}\}$ is an orthonormal basis, where every state in the basis is either Z_2 even or Z_2 odd. (c): The local symmetry operator for a series symmetry operations $R_1 \dots R_n$, where $R_1 \dots R_n = I$. If η_R is nontrivial, action of this operator on Z_2 even or Z_2 odd tensor gives different phase factor. This indicates symmetry fractionalization of chargons.

$R_1 R_2 \dots R_n = e$, we can construct a local symmetry operators $\hat{L}_{R_1 \dots R_n}^A$ as

$$\hat{L}_{R_1 \dots R_n}^A \equiv \hat{L}_{R_1}^A \cdots \hat{L}_{R_n}^A \quad (3.79)$$

By inserting Eq.(3.78) into the above equation, we get

$$\hat{L}_{R_1 \dots R_n}^A = \sum_i [(\hat{T}_A^{(i), R_1 \dots R_n}) \cdot (\hat{T}_A^{(i)})^{-1}] \quad (3.80)$$

where

$$\begin{aligned} \hat{T}_A^{(i), R_1 \dots R_n} &\equiv W_{R_1} R_1 \dots W_{R_n} R_n \circ \hat{T}_A^{(i)} \\ &= \chi_R \eta_R \circ \hat{T}_A^{(i)} \end{aligned} \quad (3.81)$$

Here, the Z_2 element η_R and the phase factor χ_R act on boundary virtual legs, as shown in Fig.(3-5c). The second line of the above equation is obtained by the following

fact:

$$\eta_R(s, i)\chi_R(s, i) = W_{R_1}(s, i) \dots W_{R_n}(R_{n-1}^{-1} \dots R_1^{-1}(s, i)) \quad (3.82)$$

When $\eta_R = \mathbb{I}$, the action of $\hat{L}_{R_1 \dots R_n}^A$ on an arbitrary tensor $\hat{T}_A \in \Lambda$ gives the same phase. When η_R is the nontrivial Z_2 element, a Z_2 odd tensor \hat{T}_A^e picks up an extra -1 comparing to a Z_2 even tensor \hat{T}_A^1 under the action of $\hat{L}_{R_1 \dots R_n}^A$. This is exactly the phenomena for symmetry fractionalization of chargons: for nontrivial η_R , under symmetry $R_1 \dots R_n$, a single chargon picks up an extra -1 comparing to a topologically trivial excitations.

Note that χ_R only serves as a global phase, thus does not contribute to the symmetry fractionalization of chargons. It appears in Eq.(3.81) even for the ground state tensor patch. In fact, this result is expected and is consistent with the physical interpretation of χ discussed in the previous subsection. One way to see this is to repeat the above analysis *only* for the ground states of the 1d spin-1 AKLT model on an open chain, with the patch \mathcal{A} covering one end of the chain. Here one should instead consider an injective matrix project state since the *IGG* here is trivial. The appearance of χ in this example can be simply interpreted as the projective representation of the edge states in the AKLT model.

3.5 Discussion and Conclusions

In this chapter we attempt to construct generic symmetric ground state wavefunctions for integer or fractionally filled correlated systems using PEPS, under certain assumptions. Here we review the assumptions that we made and discuss the limitations and generalizations of our results.

Our assumption is that the on-site symmetry is implemented as the simple tensor product of local representations or projective representations on the virtual legs in PEPS. For instance, this is the origin of the minimal required Z_2 *IGG* in the half-integer spin systems on the kagome lattice.

This assumption is known to have problems when attempting to describe SPT phases as well as phases with chiral edge states. For instance, let's attempt to construct a $U(1)$ charge-conserving Chern insulator using the fermionic version of PEPS (fPEPS)[7, 35, 84, 106]. Here the exact constructions of free fermion states with a nonzero Chern number using Gaussian fPEPS[40, 142], in which the virtual legs transform as $U(1)$ representations, are shown to host power law correlation functions in the real space. It has been pointed by Hastings[62] that for a general $U(1)$ symmetric PEPS with a bounded bond dimension D which is a fully gapped ground state of a local Hamiltonian, the assumption that the virtual legs transform as $U(1)$ representations and the assumption that the PEPS carries nonzero Chern number generically lead to contradictions.

In the next chapter, by relaxing this assumption, we are able to construct all the cohomological SPT phases using PEPS. In particular, our formulation allows us to classify SPT phases protected by both on-site and lattice symmetries.

We made a second assumption: we study only those symmetric quantum ground states that can be represented by a single tensor network on the infinite lattice. This assumption is made here mainly for technical simplicity rather than fundamental difficulty. Note that this assumption is weaker than the assumption that the ground state sector is composed of one-dimensional representations of the symmetry group on any finite size samples. For instance consider a Z_2 QSL studied in this chapter with a four-fold ground state sector on torus. When considering a finite size torus, some of them could form multi-dimensional irreducible representations of the space group.

This assumption could be violated in general model simulations. As a trivial example we could consider a ferromagnetic state in an $SU(2)$ symmetric model. In this case the number of degenerate ground states scale linearly as the number of sites, which certainly cannot be represented by one or few PEPS.

As a slightly nontrivial example, we refer to the chiral-spin-charge-Chern liquid (SCCL) in Ref.[74]. The spin dynamics in SCCL is described by a chiral Z_2 QSL, which is a Z_2 QSL breaking the time reversal symmetry and has nonzero spin-chirality

order parameter (e.g., $\langle \vec{S}_i \cdot \vec{S}_j \times \vec{S}_k \rangle \neq 0$ for three nearby spins i, j, k). This state breaks both time-reversal and mirror reflection symmetries, but leaves the combination of the two respected. In this situation, we found $8 = 4 \times 2$ ground states on symmetric torus samples (compatible with the PSG transformations). The factor of 4 is related to the topological degeneracy of Z_2 gauge theory. And the extra factor of 2 is due to the fact that the time reversal, the mirror reflection and the lattice rotation form nontrivial 2-dimensional irreducible representations. The latter fact dictates that it is impossible to represent such chiral liquids by a single symmetric PEPS, in which case the extra factor of 2 degeneracy cannot be captured.

The simple way to proceed is to instead only consider the combination of the time reversal and the mirror reflection as a symmetry, which allows a description of one of the two time-reversal images using PEPS. The PEPS description of the other state can be obtained by the time-reversal transformation.

We now comment on another fact in our construction. In the half-integer spin systems on the kagome lattice, we show that a spin-singlet symmetric PEPS has an IGG that at least contains a Z_2 subgroup. If $IGG = Z_2$ for a PEPS, and if the PEPS is describing a fully gapped QSL, we showed that the topological order is toric-code-like in Sec.3.2.4. This remains to be true if we construct some Z_2 QSL in the absence of the time-reversal symmetry, using our formulation. However, there are known constructions[13, 111, 71] of gapped Z_2 QSL on the kagome lattice in the absence of the time-reversal symmetry whose topological order is the same as the one in the double-semion model, fundamentally different from toric-code.

Interestingly, in a PEPS construction of the double semion QSL[71], in which spin rotation is still implemented as representations on the virtual legs, the constructed tensors are actually Z_4 invariant. Naively, such a state should have a 16-fold degenerate ground state sector on torus, but it was shown that only 4 of them are linearly independent.

Next we comment on the connection between our work with previous works. For readers that are familiar with the parton constructions and projective symmetry group analysis of parton wavefunctions[153, 147, 93], clearly part of our results can be viewed

as generalizations of these analyses into PEPS wavefunctions. In particular, in the kagome half-integer spin S example presented here, every crude class contains a distinct Z_2 QSL as a member phase. Part of our results can be viewed as a classification of Z_2 QSL on the kagome lattice. Comparing with previous investigations on this topic specifically for $S = 1/2$, based on parton constructions[147, 93], we find that our result captures every phase present in the Schwinger-boson construction[147], and finer than that. Basically the previous PSG analysis of the Schwinger boson construction is related to the η -indices and Θ -indices in our formulation, while in this work χ -indices are revealed.

However, comparing with the classification based on the Abrikosov-fermion construction of Z_2 QSL on the kagome lattice[93], we find that some of them cannot be described in our result. Similar observation was made by Ref.[92] when directly comparing Schwinger-boson and Abrikosov-fermion constructions. We currently do not have a full understanding of the physics behind this phenomenon. But it is worth pointing out that the missing Abrikosov-fermion Z_2 QSL are all found to be gapless (at least perturbatively) on the mean-field level[93].

Finally we comment on the hierarchical structure of the crude classes. Sometimes there are physical reasons to believe that the IGG needs to be larger than the minimal required one in order to correctly capture certain quantum phases. The double semion PEPS mentioned above may be viewed as such an example.

As one can see from the above discussions, the current work, which is based on the point of view of diagnosing ground state wavefunctions using symmetric PEPS, brings up many open questions and needs future investigations to clarify. In addition, the algorithms proposed here for simulating strongly interacting models need benchmark tests to have a understanding of its practical performance. Nevertheless we believe that separating the short-range part of the physics from the long-range part is a useful idea in investigating quantum phase diagrams of strongly correlated systems. While generally the long-range part is still a difficult task, we expect that the method introduced here can be used to provide sharp information for the short-range physics efficiently.

3.6 Symmetry group of the kagome lattice

As shown in Fig.(3-4), we label the three lattice sites in each unit cell with sublattice index $\{s = u, v, w\}$. Further, we specify the virtual index $\{i = a, b, c, d\}$ of a given site. We choose Bravais unit vector as $\vec{a}_1 = \hat{x}$ and $\vec{a}_2 = \frac{1}{2}(\hat{x} + \sqrt{3}\hat{y})$. Thus, we are able to specify the virtual degrees of freedom of site tensors as (x, y, s, i) . The symmetry group of such a two-dimensional kagome lattice is generated by the following operations

$$\begin{aligned}
T_1 &: (x, y, s, i) \rightarrow (x + 1, y, s, i), \\
T_2 &: (x, y, s, i) \rightarrow (x, y + 1, s, i), \\
\sigma &: (x, y, u, i) \rightarrow (y, x, u, i_{\sigma 1}), \\
& \quad (x, y, v, i) \rightarrow (y, x, w, i_{\sigma 2}), \\
& \quad (x, y, w, i) \rightarrow (y, x, v, i_{\sigma 2}), \\
C_6 &: (x, y, u, i) \rightarrow (-y + 1, x + y - 1, v, i), \\
& \quad (x, y, v, i) \rightarrow (-y, x + y, w, i), \\
& \quad (x, y, w, i) \rightarrow (-y + 1, x + y, u, i_{C_6}).
\end{aligned} \tag{3.83}$$

together with time reversal \mathcal{T} . Here,

$$\begin{aligned}
\{a_{\sigma 1}, b_{\sigma 1}, c_{\sigma 1}, d_{\sigma 1}\} &= \{d, c, b, a\} \\
\{a_{\sigma 2}, b_{\sigma 2}, c_{\sigma 2}, d_{\sigma 2}\} &= \{c, d, a, b\} \\
\{a_{C_6}, b_{C_6}, c_{C_6}, d_{C_6}\} &= \{b, a, d, c\}
\end{aligned} \tag{3.84}$$

The symmetry group of a kagome lattice is defined by the following algebraic

relations between its generators:

$$\begin{aligned}
T_2^{-1}T_1^{-1}T_2T_1 &= e, \\
\sigma^{-1}T_1^{-1}\sigma T_2 &= e, \\
\sigma^{-1}T_2^{-1}\sigma T_1 &= e, \\
C_6^{-1}T_2^{-1}C_6T_1 &= e, \\
C_6^{-1}T_2^{-1}T_1C_6T_2 &= e, \\
\sigma^{-1}C_6\sigma C_6 &= e, \\
C_6^6 = \sigma^2 = \mathcal{T}^2 &= e, \\
g^{-1}\mathcal{T}^{-1}g\mathcal{T} &= e, \forall g = T_{1,2}, \sigma, C_6
\end{aligned} \tag{3.85}$$

where e stands for the identity element in the symmetry group.

Further, consider system with spin rotation symmetry operator $R_{\theta\vec{n}}$, which means spin rotation about axis \vec{n} through angle θ . We mainly consider half-integer spins ($SU(2)$ symmetry) in this chapter. The spin rotation symmetry commutes with all lattice symmetries as well as time reversal symmetry:

$$g^{-1}R_{\theta\vec{n}}^{-1}gR_{\theta\vec{n}} = e, \forall g = T_{1,2}, \sigma, C_6, \mathcal{T} \tag{3.86}$$

Chapter 4

Symmetry protected topological phases and tensor network states

4.1 Introduction

Recently the interplay between symmetry and topology in condensed matter physics attract considerable interest both theoretically and experimentally. After the discovery of topological insulators[78, 9, 100, 51, 114, 110, 59], it is theoretically recognized that there exist many new types of symmetric topological states of matter. In the absence of topological order, symmetry could protect different topological phases, which are often referred to as symmetry protected topological (SPT) phases[118, 24, 48, 108, 20, 25, 32]. In particular, the bosonic SPT phases require strong interactions to realize.

Previously SPT phases have been theoretically investigated using various different theoretical frameworks[20, 94, 141]. In particular, a wide range of SPT phases protected by onsite symmetry groups have been systematically classified and investigated[20], based on a definition of short-range-entangled quantum phases. These SPT phases are found to be directly related to the group cohomology theory, which we will refer to as cohomological SPT phases.

Generally in condensed matter systems spatial symmetries (e.g., lattice space group) are present. It is known that such symmetries could protect topological

phases such as the topological crystalline insulators in fermionic systems[33, 50]. In bosonic systems, analogous but correlation-driven SPT phases protected by spatial symmetries have been investigated recently, for instance, using topological field theory analysis[34, 167] and dimension reduction techniques[126]. However, so far the systematic understanding of spatial-symmetry-protected SPT phases is still lacking.

Apart from classification problems, it is certainly very important to understand whether these SPT phases can be realized in experimental systems. However, although it is known that there exist a vast number of correlation-driven SPT phases in two and higher spatial dimensions, very few of them are shown to be realized in more or less simple and realistic quantum models[120].

The challenge here, at least to some extent, is due to the lack of physical guidelines and suitable numerical methods. In history, the successful discovery of topological insulators very much benefits from the band-inversion picture[51], which is a very useful physical guideline. In this sense, it is highly desirable to develop more physical guidelines for realizing correlation-driven SPT phases.

In addition, in order to search for SPT phases in correlated models, intensive numerical simulations are inevitable. It is also desirable to develop new numerical methods suitable for simulating SPT phases. In particular, for realistic models, one usually has to perform variational simulations based on certain choice of variational wavefunctions. Can one construct generic wavefunctions for SPT phases that are suitable for numerical simulations?

In this chapter, we further develop a symmetric tensor-network theoretical framework that is powerful to address the conceptual and practical issues raised above. Let us firstly describe the results of this chapter. We mainly focus on the bosonic cohomological SPT phases. The major new results of this work are two-fold. First, we identify the interpretation of cohomological SPT phases in a general tensor-network formulation, which allows us to construct generic tensor-network wavefunctions for SPT phases protected by onsite symmetries and/or spatial symmetries (see Sec.4.3.2). Such generic tensor-network wavefunctions are suitable to perform variational numerical simulations in searching for SPT phases in practical model systems. Second, this

interpretation shows that, for a general symmetry group SG , which may involve both onsite symmetries and spatial symmetries, these cohomological SPT phases can be classified by $H^{d+1}(SG, U(1))$. Here the $(d+1)$ -th cohomology group $H^{d+1}(SG, U(1))$ are defined such that *the time-reversal symmetry and any mirror reflection symmetries act on the $U(1)$ group in the anti-unitary fashion, while other symmetries act on the $U(1)$ group in the unitary fashion.*

We would like to point out that the cohomological SPT phases classified by $H^{d+1}(SG, U(1))$ may or may not host gapless boundary states, related to whether one can choose a physical edge such that the symmetry protecting the SPT phase is still preserved along the boundary. For instance, in 2+1D, the inversion symmetry (equivalent to 180° spatial rotation) generate a Z_2 unitary group. Because $H^3(Z_2, U(1)) = Z_2$, according to our main result, there is one nontrivial SPT phase protected by inversion symmetry alone in 2+1D. However, near the edge the inversion symmetry is always broken and gapless edge states are not expected to present. This phenomenon is similar to the inversion symmetry protected topological insulators in weakly interacting fermionic systems, e.g., axion insulators[134].

Previously progresses on analytically understanding SPT phases with onsite symmetries based on the tensor-network formulation in 2+1D were made[158]. Comparing with earlier results, the current construction captures general spatial symmetries and applies in one, two and three spatial dimensions, and therefore is more general. In addition, in the current construction, the information of the SPT phases are encoded in certain *local* constraints on the building block tensors, i.e., the local tensors are living inside certain specific sub-Hilbert spaces. Such local constraints can be easily implemented in practical numerical simulations. We will provide some concrete examples of such SPT tensor-network wavefunctions in Sec.4.3.5.

There are several by-products that are related to the special cases of the more general results above. For instance, when SG involves translation symmetries in two and higher spatial dimensions d , our construction related to $H^{d+1}(SG, U(1))$ clearly demonstrates so-called “weak topological indices”, whose physical origin is related to lower dimensional SPT phases. As a concrete example, previously we demonstrated

that there are 4 distinct featureless Mott insulators on the honeycomb lattice at half-filling[79]. These distinct featureless Mott insulators now can be nicely interpreted as the consequence of two weak topological indices.

An more important by-product is a generic relation in 2+1D between the SPT phases and symmetry enriched topological (SET) phases via an anyon condensation mechanism, which provides new physical guidelines realizing SPT phases. SET phases are symmetric phases featuring topological order and anyon excitations. The interplay between symmetry and the topological order gives rise to so-called symmetry enriched phenomena such as symmetry fractionalization[153, 44, 98, 70, 69, 95, 6, 112, 128, 130].

One can consider an SET phase characterized by a usual abelian discrete gauge theory, in which gauge charges feature nontrivial symmetry fractionalizations. Such an SET phase can be quite conventional in the sense that there is no robust gapless edge states, and can be realized in rather simple model systems[99, 5]. It turns out that after the gauge fluxes boson-condense and destroy the topological order, the resulting confined phase must be SPT phase if the condensed gauge fluxes carry nontrivial quantum numbers and certain Criterion (see Sec.4.2) is satisfied.

This by-product signals that the traditional treatment on confinement-deconfinement phase transitions[49] may worth being revisited when physical symmetries are implemented. Although the general Criterion on the relation between SPT and SET phases is obtained using the tensor-network formulation in Sec.4.3.2, a major advantage of this by-product is that it can be understood using more conventional formulations which we will discuss below.

4.2 The connection between SET phases and SPT phases via anyon condensation

In this section we discuss a by-product of our general results obtained in Sec.4.3.2. Instead of using tensor-network formulation, here we use (topological) field theoretical languages, which does not require the readers to be familiar with tensor-network for-

mulations. The discussions in this section suggest that the confinement-deconfinement phase transitions of gauge theories, e.g. a usual Z_2 gauge theory need to be reconsidered when symmetries are present, because different ways to confine the gauge fields may lead to different SPT phases. For instance, it is well-known that valence bond solids(VBS) in quantum spin systems can be viewed as the confined phases of gauge theories. At the end of this section, we discuss the possible realizations of SPT VBS phases.

Previously a related physical route to realize SPT phases has been discussed[141, 120, 54], which states that condensing vortices in superfluid carrying $U(1)$ quantum numbers could lead to SPT phases. The current discussion can be viewed as analogous phenomena but in the context of topologically ordered phases. In addition, in the current work, general spatial and onsite symmetries are considered and systematic results are obtained.

4.2.1 A criterion to generate general cohomological SPT phases via anyon condensation

The connection between SET phases and SPT phases via anyon condensation can be quite general. In fact, the original study understanding the so-called E_8 state was achieved by condensing bosonic anyons coupled with multi-layers of $p+ip$ topological superconductors[82]. Later on it was understood that quite systematically, starting from a fermionic SPT phase, after coupling with a dynamical gauge field and condense the appropriate bosonic anyon, one could confine the fermionic degrees of freedom and obtain a bosonic SPT phase[168].

However, in those previous constructions of SPT phases, before anyon condensation, the SET phases themselves already feature gapless edge states. Indeed, before coupling to the dynamical gauge fields, the systems are already in fermionic SPT phases. In this chapter, we study a different type of generic connections between SET and SPT phases via anyon condensations. Namely, the SET phases themselves contain *no* symmetry protected edge states. In fact we will consider particularly sim-

ple SET phases: the usual discrete abelian gauge theories with certain symmetries. Here by “usual” we mean that, for instance, for a Z_2 gauge theory we only consider the toric-code type topological order and do not consider the double-semion topological order. At the superficial level, it is unclear how these simple SET phases are connected with SPT phases.

We will state a Criterion to obtain cohomological SPT phases via condensing (self-statistics) bosonic anyons in these simple SET phases. A proof of this Criterion based on tensor-network construction will be given in Sec.4.3.3. Before providing this tensor-network based argument, in Sec.4.2.2 we present several examples demonstrating the application of this criterion using the K -matrix Chern-Simons effective theories[151].

The topological quasiparticles in a usual Z_n gauge theory include the gauge charges and the gauge fluxes, both are self-statistics bosonic. They can generate all other quasiparticles via fusion. Let’s consider a $Z_{n_1} \times Z_{n_2} \times \dots \times Z_{n_k}$ finite abelian gauge theory, in the presence of a symmetry group SG that could be a combination of onsite symmetries and spatial symmetries. In the following discussion, we denote a general gauge flux as an m -quasiparticle, and a general gauge charge as an e -quasiparticle (they do not have to be unit gauge charge/flux). SG can be a combination of onsite and spatial symmetries. It turns out that SG may transform the topological quasiparticles according to certain projective representations — a phenomenon that has been called symmetry fractionalization.

It is known that the symmetry fractionalization pattern in the above SET phase can be characterized by the following mathematical expression:

$$\Omega_{g_1}\Omega_{g_2} = \lambda(g_1, g_2)\Omega_{g_1g_2}, \quad (4.1)$$

where $g_1, g_2 \in SG$, and Ω_g is the symmetry transformation on the quasiparticles, while $\lambda(g_1, g_2)$ is an abelian quasiparticle in the theory. Physically, it means that the operation $\Omega_{g_1}\Omega_{g_2}$ on some quasiparticle- a are different from the operation $\Omega_{g_1g_2}$ on quasiparticle- a by a full braiding phase between quasiparticle- a and $\lambda(g_1, g_2)$. The

associative condition of symmetry operations dictates the following fusing relation:

$$\lambda(g_1, g_2)\lambda(g_1g_2, g_3) = \lambda(g_2, g_3)\lambda(g_1, g_2g_3). \quad (4.2)$$

Here we particularly focus on situations in which symmetry operations would *not* change anyon types of $\lambda(g_1, g_2)$. Because Ω_g can be redefined by a braiding phase factor with a quasiparticle b_g , $\lambda(g_1, g_2)$ is well-defined up to a fusion with the quasiparticle $b_{g_1}b_{g_2}b_{g_1g_2}^{-1}$ (inverse means antiparticle.). Mathematically Eq.(4.2) indicates that $\lambda(g_1, g_2)$ is a 2-cocycle in the second-cohomology group $H^2(SG, \mathcal{A})$, where \mathcal{A} is the fusion group of the abelian quasiparticles in the SET phase.

For instance, consider a Z_2 gauge theory with an onsite Ising symmetry group $Z_2^{onsite} = \{I, g\}$, in which only the e -particle features nontrivial symmetry fractionalization: although $g^2 = I$, when acting on the e -particle $g(e)^2 = -1$. The -1 phase factor here can be interpreted as the braiding phase between the e particle with an m -particle. Consequently this SET phase can be described using the formulation in Eq.(4.1) by $\lambda(g, g) = m$, while all other λ 's are trivial.

Starting from the SET phase, *our goal is to destroy the topological order completely by boson-condensing all the m -particles, while leaving the physical symmetry unbroken.* It is straightforward to show that as long as one of the condensed m -particles hosts non-trivial symmetry fractionalization, the m -condensed phase would spontaneously break the symmetry.¹ Therefore, in order to be able to preserve the symmetry, all the m -particles must have trivial symmetry fractionalization. *Namely $\lambda(g_1, g_2)$ in Eq.(4.1) can be chosen such that all $\lambda(g_1, g_2)$ do not contain e -quasiparticles, while they may contain m -particles and their bound states* (meaning that the e -particles could have non-trivial symmetry fractionalization).

All the condensed m -quasiparticles have trivial symmetry fractionalization, but they may or may not carry non-trivial usual symmetry representations (i.e., usual quantum numbers). One may worry that condensing bosons carrying non-trivial

¹One way to see this is that the nontrivial projective representations can always fuse into nontrivial representations of the identity particle. Consequently one can always construct gauge invariant order parameters breaking symmetry in the boson condensed phase, if the bosons feature nontrivial symmetry fractionalization.

quantum numbers would also break the physical symmetry. However, because the m -quasiparticles are topological excitations, symmetry breaking does not have to happen. In fact, as long as the quantum numbers carried by the condensed m -quasiparticles are such that the identity quasiparticles generated by fusing them (a local physical excitation) always carry trivial quantum number, the symmetry is preserved even after the m -condensation.

Consequently, if we try to preserve the symmetry in the m -condensation, the quantum numbers carried by condensed m -particles cannot be arbitrary. First, they need to be one-dimensional representations of the symmetry since higher dimensional representations can always fuse into nontrivial representations for the identity quasiparticle. Let us denote the one-dimensional representation for an m -quasiparticle by χ_m , and $\forall g \in SG$, $\chi_m(g) \in U(1)$. We have:

$$\chi_m(g_1 g_2) = \chi_m(g_1) \cdot \chi_m(g_2)^{s(g_1)}, \forall g_1, g_2 \in SG. \quad (4.3)$$

Here $s(g) = 1$ if g is a unitary symmetry and $s(g) = -1$ if g is an anti-unitary symmetry.

In order to preserve symmetry in the m -condensate (i.e., all condensed identity particles carry trivial quantum numbers), we have the following constraint on χ : if two gauge-flux quasiparticles m and m' fuse into the quasiparticle $m \cdot m'$, then the quantum numbers carried by all the three quasiparticles must satisfy

$$\chi_m(g) \cdot \chi_{m'}(g) = \chi_{m \cdot m'}(g), \forall g \in SG. \quad (4.4)$$

For example, this condition dictates that $\chi_m(g) \in Z_n$ if m is the gauge flux in the Z_n gauge theory.

The question is, what is the symmetric phase after the m -condensation?

Criterion: The above m -condensed phase is a cohomological SPT phase char-

acterized by a 3-cocycle:

$$\omega_\lambda^x(g_1, g_2, g_3) \equiv \chi_{\lambda(g_2, g_3)}(g_1) \in H^3(SG, U(1)) \quad (4.5)$$

From Eq.(4.5), in order to realize a nontrivial SPT phase, two ingredients are required in this anyon-condensation mechanism: (1)the e -quasiparticles have some nontrivial symmetry fractionalizations so that λ 's are formed by nontrivial m -quasiparticles; and (2) the quantum numbers carried by the condensed m -particles χ are nontrivial. We will justify this Criterion using tensor-network formulation in 4.3.2. Here, let us only show three facts confirming that the Criterion is self-consistent. These facts are also useful to keep in mind in our discussions on examples.

(i): $\omega_\lambda^x(g_1, g_2, g_3)$ is necessarily a 3-cocycle, which means that it satisfies:

$$\begin{aligned} & \omega_\lambda^x(g_1 g_2, g_3, g_4) \cdot \omega_\lambda^x(g_1, g_2, g_3 g_4) \\ &= \omega_\lambda^x(g_2, g_3, g_4)^{s(g_1)} \cdot \omega_\lambda^x(g_1, g_2 g_3, g_4) \cdot \omega_\lambda^x(g_1, g_2, g_3). \end{aligned} \quad (4.6)$$

But this 3-cocycle condition directly follows from the fusion rule Eq.(4.2), Eq.(4.3), and the symmetry-preserving condition Eq.(4.4).

(ii): Choosing equivalent 2-cocycle $\lambda(g_1, g_2)$ in Eq.(4.2) to represent the same physical symmetry fractionalization would at most modify $\omega_\lambda^x(g_1, g_2, g_3)$ by a 3-coboundary and thus would not change its equivalence class. This fact is straightforward to show realizing $\lambda(g_1, g_2)$ in Eq.(4.2) is well defined only up to a 2-coboundary, i.e.:

$$\lambda(g_1, g_2) \rightarrow \lambda(g_1, g_2) \cdot \epsilon(g_1) \cdot \epsilon(g_2) \cdot \epsilon^{-1}(g_1 g_2). \quad (4.7)$$

(iii): The quantum number $\chi_m(g)$ in Eq.(4.3) is also well-defined up to a 1-coboundary: $\chi_m(g) \rightarrow \chi_m(g) \cdot \frac{\alpha_m^{s(g)}}{\alpha_m}$, where α_m like a gauge choice. It is straightforward to also show that, if this modification of $\chi_m(g)$ preserve the relation Eq.(4.4), then it can only induce a change of $\omega_\lambda^x(g_1, g_2, g_3)$ by a 3-coboundary.

Remark-I: *Time-reversal symmetry, mirror symmetries and the anti-unitary transformation.* The above Criterion need to be used with the following caution in mind.

The Criterion has a straightforward interpretation when SG only involves unitary symmetries, including usual onsite symmetries, translational/rotational spatial symmetries and their combinations. However, the time-reversal \mathcal{T} and mirror symmetries \mathcal{P} need to be treated as anti-unitary transformations. Namely, $s(g) = -1$ if $g = \mathcal{T}$ or $g = \mathcal{P}$. And generally if one counts the total number of \mathcal{T} operation *and* mirror symmetry operations in g , then $s(g) = -1$ iff this total number is an odd number. For instance, the product of two different mirror planes is a rotational symmetry and should be treated as a unitary transformation.

More precisely, if we consider the creation operator of an m -particle as $m^\dagger \sim e^{i\phi_m}$, then in order to use the Criterion, we *assume* that the transformation rules for the phase variable ϕ_m as: $g : \phi_m \rightarrow -\phi_m + \theta_g$ if $g = \mathcal{T}$ or $g = \mathcal{P}$, where $e^{i\theta_g}$ is a $U(1)$ phase. Because \mathcal{T} involves the complex conjugation while \mathcal{P} does not, this leads to: $\mathcal{T} : m^\dagger \rightarrow e^{-i\theta_{\mathcal{T}}} m^\dagger$, and $\mathcal{P} : m^\dagger \rightarrow e^{i\theta_{\mathcal{P}}} m^\dagger$.

Clearly, with these transformation rules, the \mathcal{T} quantum number $\chi_m(\mathcal{T})$ carried by an m -particle alone is only a gauge choice and is not well-defined. But, for instance, the combination of the two transformations: $\mathcal{T} \cdot \mathcal{P}$ should be treated as a unitary transformation and its quantum number carried by an m -particle is well-defined.

These transformation rules can be physically interpreted as follows. In the usual discrete Abelian gauge theories, the e -particles and m -particles are dual variables, and it is a matter of choice to call which particles as gauge charges(fluxes). However, if one treats e 's as particles, then the m 's need to be treated as vortices. Under either \mathcal{T} or \mathcal{P} , if a particle transforms into a particle (an anti-particle), then its vortex transforms into an anti-vortex (a vortex). We assign the above transformation rules for the m -particles in order for the e -particles to have well-defined symmetry fractionalizations. We will come back to this issue with a detailed field-theoretical discussion shortly in Sec.4.2.2.

Remark-II: *Definition of quantum numbers carried by m -particles.* In Eq.(4.3,4.5) we introduce the quantum numbers carried by an m -particle $\chi_m(g), \forall g \in SG$. We firstly emphasize the fact that, apart from the antiunitary transformations like \mathcal{T}, \mathcal{P} , these quantum numbers are numerically measurable for a low energy m -particle using

tensor-network algorithms (see Sec.4.3.2 for details). However, it would be useful to sharply define these quantum numbers in a way that is independent of the tensor-network formulation. Below we provide such a definition using a symmetry-defect argument for on-site unitary symmetries only.

The subtleties to define these quantum numbers for a given m -particle arise from the fact that an anyon m is not a local excitation. To define how an m -particle transforms under a symmetry g , one has to find a way to define a local symmetry operator Ω_g acting on a finite region A covering the m -particle. It has been argued that [6, 18], for an onsite unitary g , Ω_g can be interpreted as the following physical transformation of the wavefunction: (1) creating a pair of symmetry- g defects; (2) adiabatically braiding one of the symmetry defect around the m -particle and finally annihilating with the other symmetry defect (the path of the moving symmetry defect encloses a region A covering the m -particle); (3) applying the symmetry transformation g for the physical degrees of freedom within A only. The quantum number carried by the m -particle is the Berry's phase accumulated over this process, relative to the Berry's phase obtained via the same process in the ground state.

The ambiguity in defining quantum numbers of the m -particle using the above symmetry-defect argument can now be understood. The symmetry defects created in pair may or may not contain other anyons, e.g., an e -particle, which have non-trivial braiding statistics with the m -particle being studied. Different choices of the symmetry defects used in the above process may lead to different quantum numbers due to braiding statistics between the e -particle in the symmetry defects and the m -particle being studied. Therefore, to well-define the $\chi_m(g)$ quantum number, one needs to make a particular choice of the symmetry defects. As will be proved in Sec.4.3.3 and 4.3.4, it turns out that *the quantum numbers $\chi_m(g)$ in the Criterion are defined such that the symmetry defects in the above process have trivial symmetry fractionalizations*. We denote this choice of the symmetry defect as the canonical choice of symmetry defect. The canonical choice of symmetry defects rules out the possibility that the g_1 -symmetry-defects contain extra e -particles having nontrivial statistics with $\lambda(g_2, g_3)$ in Eq.(4.5), and thus well-define the $\chi_{\lambda(g_2, g_3)}(g_1)$.

However, for spatial symmetries and the time-reversal symmetry, it is unclear how to systematically create symmetry defects. For these symmetries, unfortunately we currently do not know to define the quantum numbers $\chi_m(g)$'s independent of the tensor-network formulation. We will provide the measurable meaning of these quantum numbers in the tensor-network language in Sec.4.3.4.

4.2.2 Examples: anyon condensation induced SPT phases in the Chern-Simons K -matrix formalism

The purpose of this subsection is to demonstrate the application of the Criterion Eq.(4.5) in some simple examples, within a convenient field-theory description: the multi-component Chern-Simons theory, or the K -matrix formulation. In particular, this formulation has been further developed by Lu and Vishwanath to successfully describe the SPT phases and their gapless edge states[94]. All the SPT phases studied here can be realized by condensing visons in a usual Z_2 gauge theory, which may be useful to motivate microscopic model realizations of them.

The topological Lagrangian of a general multi-component Chern-Simons theory is:

$$\mathcal{L} = -\frac{1}{4\pi} \sum_{I,J} K_{IJ} \epsilon^{\mu\nu\lambda} a_\mu^I \partial_\nu a_\lambda^J + \sum_I a_\mu^I j_I^\mu, \quad (4.8)$$

where j_I^μ for $I = 1, 2, \dots, N$ are the currents of quasiparticles coupling with gauge fields a_μ^I . For the usual Z_2 gauge theory, the K -matrix can be chosen to be: $K^{Z_2} = \begin{pmatrix} 0 & 2 \\ 2 & 0 \end{pmatrix}$.

Physically, this mutual-Chern-Simons theory can be interpreted as follows. Let us start from a boson superfluid phase, formed by boson b , and consider the vortices. For the purpose of physical arguments below, it is convenient to introduce the boson number conservation $U(1)$ symmetry which can be removed later. The well-known boson-vortex duality states that one can describe the system as:

$$\mathcal{L} = -\frac{1}{2\kappa} (\epsilon^{\mu\nu\lambda} \partial_\nu a_\lambda)^2 - a_\mu j_b^\mu, \quad (4.9)$$

where j_v^μ is the current of the vortices. We will use Ψ_v to denote the single vortex operator. The gauge flux of a_μ is the density of the original boson b : $j_b^\mu = \frac{1}{2\pi}\epsilon^{\mu\nu\lambda}\partial_\nu a_\lambda$. In the superfluid phase the vortices are gapped and the $U(1)$ Goldstone mode is described by the photon mode of a_μ (i.e., the Maxwell-like dynamics in the first term in Eq.(4.9)).

Now let us consider the vortex condensed phase (i.e., the Mott insulator phase of the boson b). One way to describe the vortex condensation is to introduce an additional gauge field a^v to describe the vortex current: $j_v^\mu = \frac{1}{2\pi}\epsilon^{\mu\nu\lambda}\partial_\nu a_\lambda^v$. In order to have vortex condensation captured, the dynamics of a^v should be Maxwell-like. Consequently the vortex condensed phase is described by:

$$\begin{aligned} \mathcal{L}_{\text{v-cond.}} = & -\frac{1}{2\kappa}(\epsilon^{\mu\nu\lambda}\partial_\nu a_\lambda)^2 - \frac{1}{2\kappa^v}(\epsilon^{\mu\nu\lambda}\partial_\nu a_\lambda^v)^2 \\ & - \frac{1}{2\pi}\epsilon^{\mu\nu\lambda}a_\mu\partial_\nu a_\lambda^v \end{aligned} \quad (4.10)$$

If one ignores the higher order Maxwell dynamics, and only focus on the topological terms, the Chern-Simons description of the vortex condensate is found to have the form of Eq.(4.8) with $K^{\text{triv.}} = \begin{pmatrix} 0 & 1 \\ 1 & 0 \end{pmatrix}$. The two component gauge fields can be identified: $a_\mu^1 = a_\mu$ and $a_\mu^2 = a_\mu^v$. Equations of motion tell that the quasiparticle current j_1^μ should be identified with that of 2π - a_μ^v -flux (i.e., vortex Ψ_v), and the quasiparticle current j_2^μ is that of the 2π - a_μ -flux (the original boson b). As explained in Ref.[94], these quasiparticles could transform nontrivially under global symmetry, and many SPT phases can be described by this $K^{\text{triv.}}$ effective theory by demonstrating the existence of symmetry protected gapless edge states.

One can now view a Z_2 topologically ordered state described by $K^{Z_2} = \begin{pmatrix} 0 & 2 \\ 2 & 0 \end{pmatrix}$ as an intermediate phase between the superfluid phase and the vortex condensed phase. Instead of directly condensing Ψ_v , one could firstly condense the double-vortices Ψ_v^2 . Such double-vortex condensate can be again formulated by introducing the double-vortex current $j_{dv}^\mu = \frac{1}{2\pi}\epsilon^{\mu\nu\lambda}\partial_\nu a_\lambda^{dv}$ carrying two unit a_μ gauge charges (a term $-2a_\mu j_{dv}^\mu$

in the Lagrangian), and add some Maxwell dynamics for a^{dv} ,

$$\mathcal{L}_{\text{dv-cond.}} = -\frac{1}{\pi}\epsilon^{\mu\nu\lambda}a_\mu\partial_\nu a_\lambda^{dv} + \dots \quad (4.11)$$

where ... include Maxwell dynamics for a_μ and a_μ^{dv} . The mutual Chern-Simons term here is just the K^{Z_2} in the K -matrix formulations. In such a gauge-charge-2 condensate, the bosonic topological quasiparticles include the unpaired single-vortex: Ψ_v , or the π -flux of a_μ^{dv} (labelled as quasiparticle- m), and the quantized π -flux vortex of a_μ (labelled as quasiparticle- e). Note that in this continuum theory, the π -flux and $-\pi$ -flux are microscopically distinct, and we label e^\dagger as the creation operator the π -flux of a_μ . Consequently e is the operator creating the $-\pi$ -flux. In addition, $e^\dagger e^\dagger = b^\dagger$.

Remark-III: In this formulation, the relation between the symmetry transformation laws of the quasiparticles e, m in the double-vortex condensate and the quasiparticles Ψ_v, b the single-vortex condensate is now established: *the quantum numbers carried by Ψ_v is the same as those carried by m , and the quantum numbers carried by b is twice of those carried by e .*²

The bulk Chern-Simons effective theory Eq.4.8 is accompanied with an effective edge theory:

$$S_{\text{edge}} = \sum_{I,J} \int \frac{dt dx}{4\pi} K_{IJ} \partial_t \phi_I \partial_x \phi_J - V_{IJ} \partial_x \phi_I \partial_x \phi_J + \dots \quad (4.12)$$

where the K_{IJ} term is the universal Berry's phase, leading to the Kac-Moody algebra $[\partial_x \phi_I(x), \partial_y \phi_J(y)] = 2\pi i K_{IJ}^{-1} \partial_x \delta(x-y)$. The V_{IJ} term is non-universal and depends on details of the edge, and “...” represents other symmetry allowed terms describing local dynamics.

The phase variables ϕ_I 's in Eq.(4.12) can be interpreted as the phases of quasiparticles: $e^{i\phi_I}$ can be identified with the quasiparticle creation operator for the current j_I^μ in Eq.(4.8). For example, in the double-vortex condensate, one has $K = K^{Z_2}$, $\phi_1 = \phi_m$

²The first half of this statement is in fact implicitly related to our definition of the quantum numbers carried by the m -particle as explained in Remark-II. The canonical symmetry defects in measuring these quantum numbers for onsite unitary symmetries do not contain e -particles, and consequently would not be affected by the confinement phase transition.

and $\phi_2 = \phi_e$, where $m^\dagger \sim e^{i\phi_m}$, $e^\dagger \sim e^{i\phi_e}$. On the other hand, in the single-vortex condensate, we have $K = K^{triv.}$, $\phi_1 = \phi_v$ and $\phi_2 = \phi_b$, where $\Psi_v^\dagger \sim e^{i\phi_v}$, $b^\dagger \sim e^{i\phi_b}$.

As explained in Ref.[94, 95], in the absence of symmetry, cosine terms describing local dynamics $\sum_I C_I \cos(\sum_J K_{IJ}\phi_J + \chi_I)$ are allowed in the “...” in Eq.(4.12) (we only consider bosonic systems). And when these terms are large, often the edge states can be fully gapped by pinning the phase variables to their classical minima. However, in the presence of symmetry, the transformation rules of ϕ_I sometimes dictate that the edge states can only be gapped out after spontaneously breaking the symmetry. When this happens for systems without topological order, i.e. $K = K^{triv.}$, the bulk state can be identified as an SPT phase with symmetry protected edge states.

We will apply the Criterion Eq.(4.5) for the symmetry groups (SG) in Table 4.1 in 2+1D. Here σ is an onsite unitary Ising symmetry, \mathcal{T} is the time-reversal, \mathcal{P} is a mirror

SG	$H^3(SG, U(1))$
$Z_2^{onsite} \equiv \{I, \sigma\}$	Z_2
$Z_2^{TP} \equiv \{I, \mathcal{T} \cdot \mathcal{P}\}$	Z_2
$Z_2^{onsite} \times Z_2^T \equiv \{I, \sigma\} \times \{I, \mathcal{T}\}$	Z_2^2
$Z_2^{onsite} \times Z_2^P \equiv \{I, \sigma\} \times \{I, \mathcal{P}\}$	Z_2^2
$Z_2^{TP} \times Z_2^T \simeq Z_2^P \times Z_2^T$	Z_2^2

Table 4.1: Five examples of SPT phases studied in this section.

reflection symmetry, and $\mathcal{T} \cdot \mathcal{P}$ is their combination. According to the Criterion and Remark-I, \mathcal{T} and \mathcal{P} should be both treated as anti-unitary, but $\mathcal{T} \cdot \mathcal{P}$ is unitary. One can see that although the SG 's of the former two examples (latter three examples) in Table 4.1 are physically very different, at the mathematical group theoretical level, they are identical.

The explicit forms of the inequivalent 3-cocycles can be obtained by direct calculations. In these simple examples, it turns out that one can always choose the 3-cocycle ω such that $\omega(g_1, g_2, g_3) = -1$ for certain g_1, g_2, g_3 , while all other $\omega(g_1, g_2, g_3) = 1$. We list the nontrivial cocycles in Table 4.2, 4.3. The trivial cocycle can be chosen such that $\omega(g_1, g_2, g_3) = 1, \forall g_1, g_2, g_3$.

Remark-IV: time-reversal and mirror symmetries In order for the 2-component mutual Chern-Simons theories of either $K^{triv.}$ or K^{Z_2} to be symmetric under \mathcal{T} or

cocycle ω	$\omega(g_1, g_2, g_3) = -1$ iff
ω_1	$g_1 = g_2 = g_3 = u$

Table 4.2: $SG = Z_2^{onsite} = \{I, \sigma\}$ or $SG = Z_2^{TP} = \{I, \mathcal{T} \cdot \mathcal{P}\}$. Denoting $Z_2^{onsite}/Z^{TP} = \{I, u\}$, two inequivalent 3-cocycles ω_0 (trivial) and ω_1 form a Z_2 group.

cocycle ω	$\omega(g_1, g_2, g_3) = -1$ iff
$\omega_{[1,0]}$	g_1, g_2, g_3 all contain u
$\omega_{[0,1]}$	g_1 contains u and g_2, g_3 both contain η .
$\omega_{[1,1]}$	g_1 contains u and g_2, g_3 both contain either u or η except for $g_2 = g_3 = u \cdot \eta$.

Table 4.3: $SG = Z_2^{onsite} \times Z_2^T$, or $SG = Z_2^{onsite} \times Z_2^P$, or $SG = Z_2^{TP} \times Z_2^T$. Denoting $Z_2^{onsite}/Z^{TP} = \{I, u\}$ and $Z_2^T/Z_2^P = \{I, \eta\}$, the four inequivalent 3-cocycles $\omega_{[0,0]}$ (trivial), $\omega_{[1,0]}$, $\omega_{[0,1]}$, $\omega_{[1,1]}$ form a Z_2^2 group. Note that u is a unitary transformation and η is an anti-unitary transformation.

\mathcal{P} , it is required that the a_μ^1 and a_μ^2 to transform oppositely under these symmetries. Consequently, denoting the densities of the two types of quasiparticles coupled with $a_\mu^1(a_\mu^2)$ as $\rho_1(\rho_2)$, if one has $\mathcal{T} : \rho_1 \rightarrow \rho_1$ ($\mathcal{P} : \rho_1 \rightarrow \rho_1$), one must also have $\mathcal{T} : \rho_2 \rightarrow -\rho_2$ ($\mathcal{P} : \rho_2 \rightarrow -\rho_2$), and vice versa.

For instance, if one requires $\mathcal{P} : e^\dagger \rightarrow e^{i\alpha_e} e^\dagger$, then $\mathcal{P} : m^\dagger \rightarrow e^{i\alpha_m} m$, where $e^{i\alpha_e}, e^{i\alpha_m}$ are phase factors. After choosing a \mathcal{P} symmetric edge along the x -direction, these leads to the following rules in the effective theory Eq.(4.12): $\mathcal{P} : \phi_e(t, x, y) \rightarrow \phi_e(t, -x, y) + \alpha_e$; $\phi_m(t, x, y) \rightarrow -\phi_m(t, -x, y) + \alpha_m$. As discussed in Remark-I, to use the Criterion, we always require that under either \mathcal{P} or \mathcal{T} , ϕ_m flips sign but ϕ_e does not.

All SPT phase examples discussed in this section can be realized via the anyon condensation Criterion starting from a SET phase with usual Z_2 topological order. Our strategy is two-step. For a given SPT 3-cocycle $\omega(g_1, g_2, g_3)$, using the Criterion, we look for the Z_2 topologically ordered SET phase with desired symmetry properties $\chi_m(g_1)$ and $\lambda(g_2, g_3)$. Second, we condense the m -particle and demonstrate the resulting phase is indeed an SPT phase by studying its edge effective theory Eq.(4.12).

$$SG = Z_2^{onsite}$$

As the simplest example of the Criterion, let us consider the SPT phase corresponds to the 3-cocycle ω_1 for $SG = Z_2^{onsite} = \{I, g\}$ in Table 4.2. The desired Z_2 topologically ordered SET phase can be easily identified:

$$\begin{aligned} \chi_{\lambda(g_2, g_3)}(g_1) &= \omega_1(g_1, g_2, g_3) \\ \Rightarrow \chi_m(g) &= -1, \lambda(g, g) = m, \end{aligned} \tag{4.13}$$

while all other χ, λ 's are trivial. Namely this is an SET phase in which the gauge charge e features nontrivial symmetry fractionalization: $g(e)^2 = -1$, and the gauge flux m has no nontrivial symmetry fractionalization but carries a nontrivial Ising quantum number $\chi_m(g) = -1$.

These symmetry transformation properties can be implemented in the K -matrix formulation with $K = K^{Z_2}$ and $g : m^\dagger \rightarrow -m^\dagger; e^\dagger \rightarrow i \cdot e^\dagger$. In the corresponding edge theory Eq.(4.12), these lead to:

$$g : \phi_m \rightarrow \phi_m + \pi; \quad \phi_e \rightarrow \phi_e + \pi/2 \tag{4.14}$$

In this SET phase, it is perfectly fine to have a gapped edge without breaking physical symmetry. For example, symmetry allows $C \cdot \cos(2\phi_m + \chi_m)$ term in the "...". When this term is large enough the edge states will be gapped out by pinning $2\phi_m$ to a semiclassical minimum, which does *not* break the physical symmetry. Note that $e^{i\phi_m}$ itself is an anyon operator and does not correspond to a local order parameter.

Next, we condense the m -particles (the remaining single-vortices) to destroy the topological order without breaking the symmetry. The resulting single-vortex condensate is described by $K = K^{triv}$. According to Remark-III, we have $g : \Phi_v^\dagger \rightarrow -\Phi_v^\dagger; b^\dagger \rightarrow -b^\dagger$. In the corresponding edge theory Eq.(4.12), these lead to:

$$g : \phi_v \rightarrow \phi_v + \pi; \quad \phi_b \rightarrow \phi_b + \pi. \tag{4.15}$$

3-cocycle	SET bulk	SPT edge
ω_1	$g : m^\dagger \rightarrow -m^\dagger$ $e^\dagger \rightarrow i \cdot e^\dagger$	$g : \phi_v \rightarrow \phi_v + \pi$ $\phi_b \rightarrow \phi_b + \pi$

Table 4.4: The symmetry properties of the nontrivial SPT phase protected by $SG = Z_2^{onsite} = \{I, g\}$, and the SET phase before the anyon condensation.

This is exactly the symmetry properties of the Z_2^{onsite} SPT phase studied in Ref.[94], where it is shown that it is impossible to gap out the edge states without spontaneously breaking the Z_2^{onsite} symmetry. In Ref.[94], Eq.(4.15) was obtained by systematically investigating all possible self-consistent transformation rules and searching for symmetry protected gapless edge states. But here, with the help of the Criterion and knowledge of the 3-cocycle ω_1 , Eq.(4.15) is directly obtained. These results are summarized in Table 4.4.

$$SG = Z_2^{onsite} \times Z_2^T$$

There are three nontrivial cohomological SPT phases protected by $SG = Z_2^{onsite} \times Z_2^T = \{I, g\} \times \{I, \mathcal{T}\}$, whose corresponding nontrivial 3-cocycles are listed in Table 4.3. We discuss them separately:

- $\omega_{[1,0]}$: We need $\chi_m(g) = -1$ and $\lambda(g, g) = m$ in the SET phase (all other λ 's are trivial). After condensing m -particles gapless edge states are protected by g alone, as already discussed in Eq.(4.15).

- $\omega_{[0,1]}$: We again need an SET phase with $\chi_m(g) = -1$, but $\lambda(\mathcal{T}, \mathcal{T}) = m$ (all other λ 's are trivial). The latter condition dictates that the e -particles are Kramer doublets because they form projective representations under time reversal: $\mathcal{T}(e)^2 = -1$. The symmetry transformation rules in the bulk effective theory can be implemented as: $g : m^\dagger \rightarrow -m^\dagger; e^\dagger \rightarrow e^\dagger$, while $\mathcal{T} : m^\dagger \rightarrow m^\dagger; e^\dagger \rightarrow -i \cdot e^\dagger$. In the corresponding edge theory:

$$\begin{aligned}
g : \phi_m &\rightarrow \phi_m + \pi; \quad \phi_e \rightarrow \phi_e, \\
\mathcal{T} : \phi_m &\rightarrow -\phi_m; \quad \phi_e \rightarrow \phi_e + \pi/2.
\end{aligned} \tag{4.16}$$

More precisely, for example, the first rule should be interpreted as $\phi_m(t, x, y) \rightarrow \phi_m(-t, x, y) + \pi$ and we have been ignoring the space-time coordinates to save notations. After condensing m -particles, the resulting phase is described by $K = K^{triv}$. with the following symmetry transformations on the edge degrees of freedom:

$$\begin{aligned} g : \phi_v &\rightarrow \phi_v + \pi; \quad \phi_b \rightarrow \phi_b, \\ \mathcal{T} : \phi_v &\rightarrow -\phi_v; \quad \phi_b \rightarrow \phi_b + \pi. \end{aligned} \tag{4.17}$$

Clearly the cosine terms $\cos(\phi_v + \chi_v)$ and $\cos(\phi_b + \chi_b)$ are not allowed by symmetry and gapless edge states are protected. This is indeed the symmetry properties of another $SG = Z_2^{onsite} \times Z_2^T$ SPT phase studied in Ref.[94].

• $\omega_{[1,1]}$: We need an SET phase in which $\chi_m(g) = -1$, and both $\lambda(g, g) = \lambda(\mathcal{T}, \mathcal{T}) = m$ (i.e. both $g(e)^2 = \mathcal{T}(e)^2 = -1$). In the edge theory of this SET phase:

$$\begin{aligned} g : \phi_m &\rightarrow \phi_m + \pi; \quad \phi_e \rightarrow \phi_e + \pi/2, \\ \mathcal{T} : \phi_m &\rightarrow -\phi_m; \quad \phi_e \rightarrow \phi_e + \pi/2. \end{aligned} \tag{4.18}$$

After condensing m -particles, the resulting phase is described by $K = K^{triv}$. with the following symmetry transformations on the edge degrees of freedom:

$$\begin{aligned} g : \phi_v &\rightarrow \phi_v + \pi; \quad \phi_b \rightarrow \phi_b + \pi, \\ \mathcal{T} : \phi_v &\rightarrow -\phi_v; \quad \phi_b \rightarrow \phi_b + \pi. \end{aligned} \tag{4.19}$$

The edge theory of this SPT phase was also pointed out in Ref.[94]. Again, using the Criterion, all these SPT phases are directly obtained. The results of this part are summarized in Table 4.5.

3-cocycle	SET bulk	SPT edge
$\omega_{[1,0]}$	$g : m^\dagger \rightarrow -m^\dagger$ $e^\dagger \rightarrow i \cdot e^\dagger$ $\mathcal{T} : m^\dagger \rightarrow m^\dagger$ $e^\dagger \rightarrow e$	$g : \phi_v \rightarrow \phi_v + \pi$ $\phi_b \rightarrow \phi_b + \pi$ $\mathcal{T} : \phi_v \rightarrow -\phi_v$ $\phi_b \rightarrow \phi_b$
$\omega_{[0,1]}$	$g : m^\dagger \rightarrow -m^\dagger$ $e^\dagger \rightarrow e^\dagger$ $\mathcal{T} : m^\dagger \rightarrow m^\dagger$ $e^\dagger \rightarrow -i \cdot e$	$g : \phi_v \rightarrow \phi_v + \pi$ $\phi_b \rightarrow \phi_b$ $\mathcal{T} : \phi_v \rightarrow -\phi_v$ $\phi_b \rightarrow \phi_b + \pi$
$\omega_{[1,1]}$	$g : m^\dagger \rightarrow -m^\dagger$ $e^\dagger \rightarrow i \cdot e^\dagger$ $\mathcal{T} : m^\dagger \rightarrow m^\dagger$ $e^\dagger \rightarrow -i \cdot e$	$g : \phi_v \rightarrow \phi_v + \pi$ $\phi_b \rightarrow \phi_b + \pi$ $\mathcal{T} : \phi_v \rightarrow -\phi_v$ $\phi_b \rightarrow \phi_b + \pi$

Table 4.5: The symmetry properties of the three nontrivial SPT phases protected by $SG = Z_2^{onsite} \times Z_2^T = \{I, g\} \times \{I, \mathcal{T}\}$, together with those of the corresponding SET phases before anyon condensations.

$$SG = Z_2^{onsite} \times Z_2^P$$

Again there are three nontrivial cohomological SPT phases as listed in Table 4.3. Because the analysis is similar to the previous case, we only list the results in Table 4.6. Note that we will choose a \mathcal{P} symmetric edge along the x -direction, and will again ignore the space-time coordinates to save notations: e.g., $\mathcal{P} : \phi \rightarrow \pm\phi + \alpha$ really means $\mathcal{P} : \phi(t, x, y) \rightarrow \pm\phi(t, -x, y) + \alpha$. We find that the three nontrivial SPT phases obtained here are consistent with earlier results in Ref.[167] obtained by directly studying the symmetry transformations in the K^{triv} effective theory without resorting to group cohomology.

$$SG = Z_2^{TP} \times Z_2^T \simeq Z_2^P \times Z_2^T \text{ and } SG = Z_2^{TP}$$

As mentioned before, both \mathcal{T}, \mathcal{P} send ϕ_m to $-\phi_m$ up to phase shifts. These phase shifts are changing under gauge transformation $\phi_m \rightarrow \phi_m + \delta$ and are not well-defined. But their combination $\mathcal{T} \cdot \mathcal{P}$ should be treated as a unitary transformation sending ϕ_m to ϕ_m up to a well-defined phase shift, whose possible values are limited to 0 and π since $(\mathcal{T} \cdot \mathcal{P})^2 = I$ assuming m -particles have trivial symmetry fractionalization.

3-cocycle	SET bulk	SPT edge
$\omega_{[1,0]}$	$g : m^\dagger \rightarrow -m^\dagger$ $e^\dagger \rightarrow i \cdot e^\dagger$ $\mathcal{P} : m^\dagger \rightarrow m$ $e^\dagger \rightarrow e^\dagger$	$g : \phi_v \rightarrow \phi_v + \pi$ $\phi_b \rightarrow \phi_b + \pi$ $\mathcal{P} : \phi_v \rightarrow -\phi_v$ $\phi_b \rightarrow \phi_b$
$\omega_{[0,1]}$	$g : m^\dagger \rightarrow -m^\dagger$ $e^\dagger \rightarrow e^\dagger$ $\mathcal{P} : m^\dagger \rightarrow m$ $e^\dagger \rightarrow i \cdot e^\dagger$	$g : \phi_v \rightarrow \phi_v + \pi$ $\phi_b \rightarrow \phi_b$ $\mathcal{P} : \phi_v \rightarrow -\phi_v$ $\phi_b \rightarrow \phi_b + \pi$
$\omega_{[1,1]}$	$g : m^\dagger \rightarrow -m^\dagger$ $e^\dagger \rightarrow i \cdot e^\dagger$ $\mathcal{P} : m^\dagger \rightarrow m$ $e^\dagger \rightarrow i \cdot e^\dagger$	$g : \phi_v \rightarrow \phi_v + \pi$ $\phi_b \rightarrow \phi_b + \pi$ $\mathcal{P} : \phi_v \rightarrow -\phi_v$ $\phi_b \rightarrow \phi_b + \pi$

Table 4.6: The symmetry properties of the three nontrivial SPT phases protected by $SG = Z_2^{\text{onsite}} \times Z_2^P = \{I, g\} \times \{I, \mathcal{P}\}$, together with those of the corresponding SET phases before anyon condensations.

Using the anyon condensation mechanism (the Criterion) and the cocycles listed in Table 4.3 and Table 4.2, one can straightforwardly obtain the three nontrivial SPT phases protected by $SG = Z_2^{TP} \times Z_2^T \simeq Z_2^P \times Z_2^T$ and the one nontrivial SPT phase protected by $SG = Z_2^{TP} = \{I, \mathcal{T} \cdot \mathcal{P}\}$. After choosing a \mathcal{P} symmetric edge along the x -direction, we list the results in Table 4.7 and 4.8. One can easily check that indeed the cosine terms $\cos(\phi_v + \chi_v)$ or $\cos(\phi_b + \chi_b)$ are forbidden by symmetry, and the symmetry allowed terms like $\cos(2\phi_v + \chi_v)$ or $\cos(2\phi_b + \chi_b)$ would spontaneously break the symmetry after gapping out the edge modes. These SPT phases, to our knowledge, have not been pointed out before.

4.2.3 Possible realizations — SPT Valence Bond Solids

Valence Bond Solids(VBS) can be realized in quantum spin-1/2 model systems[113, 99, 121, 116]. They spontaneously break the lattice translational symmetry but preserve the spin-rotational symmetry/time-reversal symmetry. The characteristic of a VBS phase is the long-range bond-bond correlation function. It is quite popular to visualize these phases as if the neighboring spin-1/2's form static spin-singlet valence

3-cocycle	SET bulk	SPT edge
$\omega_{[1,0]}$	$\mathcal{P} : m^\dagger \rightarrow -m$ $e^\dagger \rightarrow i \cdot e^\dagger$ $\mathcal{T} : m^\dagger \rightarrow m^\dagger$ $e^\dagger \rightarrow e$	$\mathcal{P} : \phi_v \rightarrow -\phi_v + \pi$ $\phi_b \rightarrow \phi_b + \pi$ $\mathcal{T} : \phi_v \rightarrow -\phi_v$ $\phi_b \rightarrow \phi_b$
$\omega_{[0,1]}$	$\mathcal{P} : m^\dagger \rightarrow -m$ $e^\dagger \rightarrow i \cdot e^\dagger$ $\mathcal{T} : m^\dagger \rightarrow m^\dagger$ $e^\dagger \rightarrow -i \cdot e$	$\mathcal{P} : \phi_v \rightarrow -\phi_v + \pi$ $\phi_b \rightarrow \phi_b + \pi$ $\mathcal{T} : \phi_v \rightarrow -\phi_v$ $\phi_b \rightarrow \phi_b + \pi$
$\omega_{[1,1]}$	$\mathcal{P} : m^\dagger \rightarrow -m$ $e^\dagger \rightarrow e^\dagger$ $\mathcal{T} : m^\dagger \rightarrow m^\dagger$ $e^\dagger \rightarrow -i \cdot e$	$\mathcal{P} : \phi_v \rightarrow -\phi_v + \pi$ $\phi_b \rightarrow \phi_b$ $\mathcal{T} : \phi_v \rightarrow -\phi_v$ $\phi_b \rightarrow \phi_b + \pi$

Table 4.7: The symmetry properties of the three nontrivial SPT phases protected by $SG = Z_2^{TP} \times Z_2^T \simeq Z_2^P \times Z_2^T = \{I, \mathcal{P}\} \times \{I, \mathcal{T}\}$, together with those of the corresponding SET phases before anyon condensations.

3-cocycle	SET bulk	SPT edge
ω_1	$\mathcal{T} \cdot \mathcal{P} : m^\dagger \rightarrow -m^\dagger$ $e^\dagger \rightarrow -i \cdot e$	$\mathcal{T} \cdot \mathcal{P} : \phi_v \rightarrow \phi_v + \pi$ $\phi_b \rightarrow \phi_b + \pi$

Table 4.8: The symmetry properties of the nontrivial SPT phase protected by $SG = Z_2^{TP}$, and the SET phase before the anyon condensation.

bond patterns, which suggests that they may be adiabatically connected to a limit in which the global wavefunctions are simply direct products of all the valence bonds.

However, from a general point of view, this picture of VBS may be misleading: the long-range bond-bond correlation function does not imply that the wavefunction can be always adiabatically connected to a direct product state. Motivated by the examples studied in Table 4.7, below we propose new types of SPT-VBS phases protected by a mirror symmetry \mathcal{P} and the time-reversal symmetry \mathcal{T} . In fact, it is even unclear whether these SPT-VBS phases are already realized in existing models featuring VBS phases.

One could understand a VBS phase in spin models with a half-integer spin per unit-cell by starting from a Z_2 quantum spin liquid(QSL) phase. Quite generally, in a Z_2 QSL, the e -particles are the Kramer-doublet spinons, and the m -particles are the spinless visons. Namely the fact that the e -particles are Kramer-doublets basically comes for free. It is well-known that the half-integer spin per unit-cell would dictate that the visons have nontrivial translational symmetry fractionalization. Consequently condensing the visons would break translational symmetry but preserve the spin-rotational symmetry, resulting in a VBS phase. But the VBS phase can be still symmetric under certain mirror reflection. For instance, the columnar VBS pattern on the square lattice is symmetric under the mirror reflection around the line crossing the bond centers along a column. The vison would certainly have trivial symmetry fractionalization under the \mathcal{T} and \mathcal{P} defined here.

Let us particularly pay attention to the two SPT phases characterized by $\omega_{[0,1]}$ and $\omega_{[1,1]}$ in Table 4.7. Before the m -particle condensation, the corresponding two SET phases both have Kramer-doublet e -particles, and their difference lies in the presence/absence of symmetry fractionalization of \mathcal{P} . In both case, one could realize the corresponding SPT phases by condensing the m -particle (vison) which is odd under the combination $\mathcal{T} \cdot \mathcal{P}$: $m^\dagger \rightarrow -m$.

Namely, whether the topological trivial VBS or the SPT-VBS is realized completely depends on which vison is condensed: the $\mathcal{T} \cdot \mathcal{P}$ even vison or the $\mathcal{T} \cdot \mathcal{P}$ odd vison. This is an energetic question and one need to numerically measure this quan-

tum number for the low energy visons near the condensation. However, as mentioned before, such measurement is nontrivial to perform and we currently only know how to do it using tensor-network-based algorithms (see Sec.4.3.3 for details).

Note that although we propose the SPT-VBS phases using the anyon-condensation mechanism from Z_2 QSLs, one does not have to realize the Z_2 QSL in spin models in order to realize the SPT-VBS phases. The anyon-condensation mechanism is simply one route to ensure that SPT-VBS phase can be obtained. As stable phases, SPT-VBS phases may be obtained via other routes³, or even first-order phase transitions, which do not involve QSLs.

4.3 Symmetric tensor-network constructions in 2+1D

In this section, we develop a general formulation to construct/classify 2+1D cohomological bosonic SPT phases protected by both on-site symmetries as well as spatial symmetries by Projected Entangled Pair States (PEPS). For each class we provide generic tensor wavefunctions, which are useful for numerical simulations.

4.3.1 A simple example: Z_2 SPT

Before developing a general formulation, we will study a simple example: the SPT phase protected by onsite Z_2 symmetry[25].

Let us first focus on the fixed point wavefunction of the nontrivial Z_2 SPT phase. Here, we follow the convention in Ref.[28]. The system lives on a honeycomb lattice, where each lattice site contains three qubits, as shown in Fig. 4-1 as three circles. The six spin $\frac{1}{2}$'s around a plaquette are either all in the $|0\rangle$ state or all in the $|1\rangle$ state, forming Z_2 domains. The fixed point wavefunction for the nontrivial Z_2 SPT phase

³for instance, the VBS phase in the context of the easy-plane deconfined criticality is obtained by condensing magnetic vortices coupling with a $U(1)$ gauge field. It would be interesting to understand whether the $\mathcal{T} \cdot \mathcal{P}$ quantum number discussed here can be generalized to these vortex-like objects.

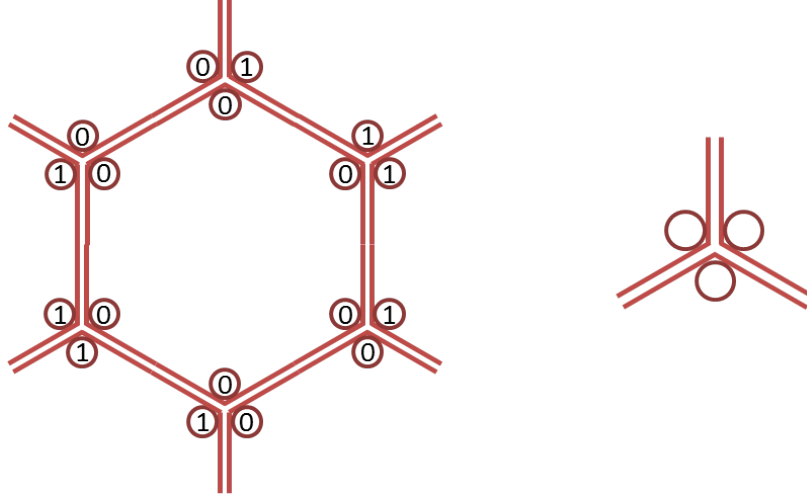


Figure 4-1: The Z_2 symmetric wavefunction on the honeycomb lattice. Each site contains three qubits. The six qubits around each plaquette are all in the same spin state. The Z_2 symmetry flips spins, which acts as σ_x .

is

$$|\psi\rangle = \sum_{\mathcal{C}} (-1)^{N_{\mathcal{C}}} |\mathcal{C}\rangle \quad (4.20)$$

where \mathcal{C} denotes Z_2 domain configurations and $N_{\mathcal{C}}$ is the number of domain walls in \mathcal{C} .

The nontrivial SPT state can be represented with tensors given in Fig. 4-2. A site tensor has six internal (virtual) legs, where each internal leg represents a qubit. Here, we choose tensors to be the same for both sub-lattices. Notice that a physical leg and the two inner indices connected to it are always in the same state. So after contraction, physical legs within one plaquette share the same state. Further, the extra $\pm i$ phase contributes -1 for each domain wall loop. In this way, one can easily check that the tensor network state indeed represents the wavefunction defined in Eq.(4.20).

It is instructive to see how the Z_2 symmetry acts on local tensors. A local tensor is not invariant under g action, but the transformed tensor differ from the original one by some gauge transformation on internal legs, labeled as W_g (W_g^{-1}), as shown in

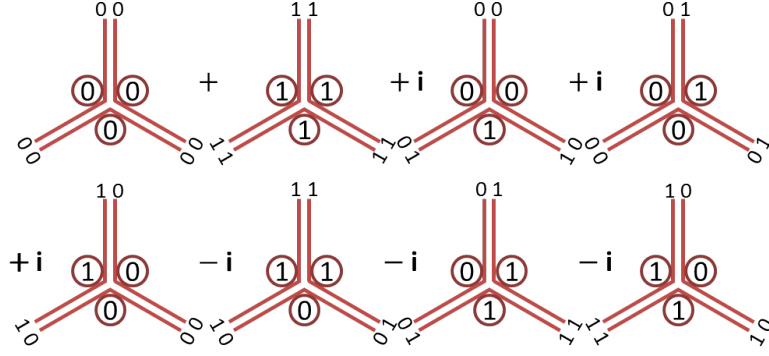


Figure 4-2: The tensor state representing the nontrivial Z_2 SPT wavefunction defined in Eq.(4.20). An internal leg support two dimensional Hilbert space. Physical states are labeled by numbers in the circle, while virtual states are labeled by numbers at the end of internal legs.

Fig. 4-3. For tensors defined on Fig. 4-2), we obtain that

$$W_g = |11\rangle\langle 00| + i|10\rangle\langle 01| + i|01\rangle\langle 10| + |00\rangle\langle 11| \quad (4.21)$$

We point out here, W_g does not form a Z_2 group. Instead, we have

$$W_g^2 = \sigma_z \otimes \sigma_z \quad (4.22)$$

So, after applying Ising symmetry twice, we are left with the σ_z action on all internal legs, and trivial action on all physical legs. Notice, the σ_z action on every internal leg is a special kind of gauge transformation, which leaves every single tensor invariant, as indicated by tensor equations on Fig. 4-4(a). This kind of gauge transformations form a group, named as the *invariant gauge group* (IGG). IGG is essential for tensor network constructions of nontrivial phases.

Here, IGG is a Z_2 group, since $\sigma_z^2 = I$. In general, a nontrivial Z_2 IGG leads to the Z_2 toric code topological order[127, 117, 76]. However, we claim that the Z_2 topological order is killed due to tensor equations in Fig. 4-4. To see this, we first point out that a site tensor is invariant under single-leg σ^z action on internal legs of one plaquette. Notice that the single-leg σ_z action anticommutes with W_g , while

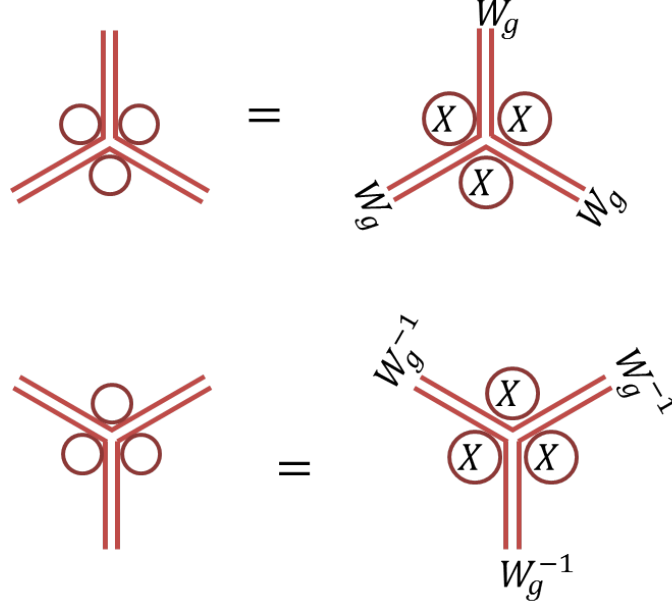


Figure 4-3: Symmetry conditions for the Z_2 symmetric state. Here, X is short for σ_x , and W_g (W_g^{-1}) denotes the associated gauge transformation. For the wavefunction defined in Eq.(4.20), $W_g = |11\rangle\langle 00| + i|10\rangle\langle 01| + i|01\rangle\langle 10| + |00\rangle\langle 11|$.

double-leg $\sigma_z \otimes \sigma_z$ action commutes with W_g :

$$W_g \sigma_z = -\sigma_z W_g \quad (4.23)$$

The physical meaning of the single-leg σ_z action is to create a (topologically-trivial) Z_2 symmetry charge excitation. To see this, we first point out that action of Z_2 symmetry g on a local patch \mathcal{R} is naturally defined as acting g on physical sites of R and W_g on the boundary virtual legs of R . If R contains one tensor with a single-leg σ_z action, we get an extra minus sign due to Eq.(4.23), which is interpreted as a Z_2 symmetry charge inside R .

The fact that a site tensor is invariant under two single-leg σ_z action indicates the existence of a particular sub-group of IGG – the “plaquette IGG”, whose elements only have nontrivial action on internal legs within one plaquette. By multiplying all nontrivial plaquette IGG elements of all plaquettes, we recover the nontrivial element of the original Z_2 IGG, which is double-leg σ_z action on every internal leg. The decomposition of IGG element into plaquette IGG elements is essential for the

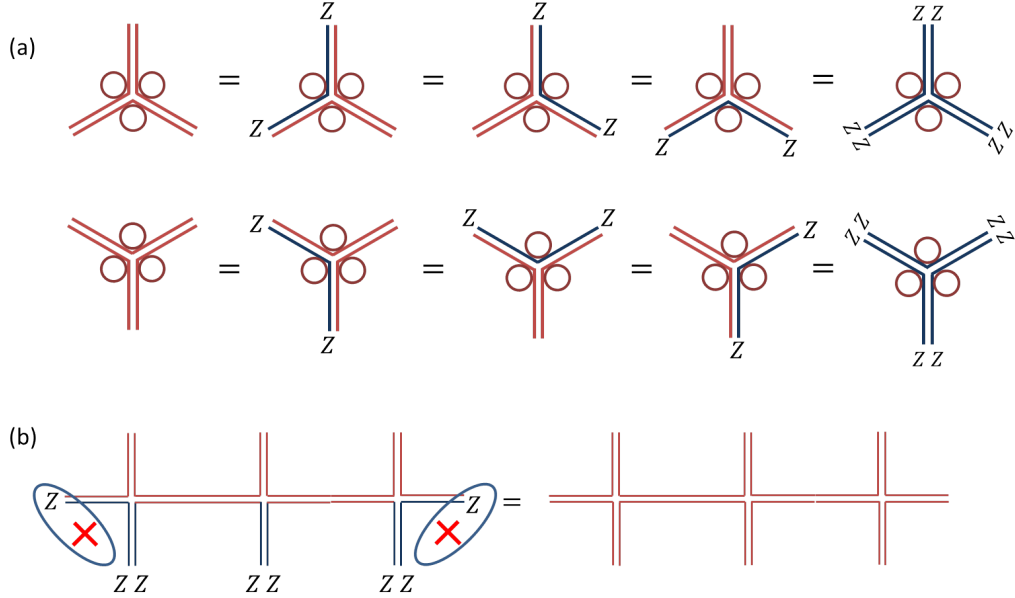


Figure 4-4: (a) Gauge transformations which leave local tensors invariant. Here, Z is short for σ_z . (b) The condensation of visons carrying Z_2 symmetry charge.

construction of generic wavefunctions of SPT phases.

As we will see, the toric code topological order is killed due to the presence of the plaquette IGG. We put the system on a torus. The topological degenerate ground states are captured by inserting the non-contractible σ_z loops. Since every tensor is invariant under two single-leg σ_z actions, the wavefunction with non-contractable σ_z loop turns out to be the same as the original wavefunction. So, there is no topological ground state degeneracy, and the state has no topological order.

The physical reason can be interpreted as vison (m) condensation. A pair of m -particles are created at two ends of a double-leg $\sigma_z \otimes \sigma_z$ string. As indicated in Fig. 4-4(b), the creation of a pair of bond states of Z_2 symmetry charges and visons leaves the wavefunction invariant. In other words, these bound states (m -particles carrying Z_2 odd quantum number) are condensed, thus killing the topological order.

There remains one question to be answered: what is the SET phase (Z_2 topological order with Z_2 symmetry) before condensation? To see this, let us re-examine Eq.(4.22): two Z_2 symmetry defects W_g fuse to a vison, which means e carries fractional Z_2 quantum number and m has the trivial symmetry fractionalization pattern.

Let us summarise the previous discussion. We start from an SET phase with Z_2^g

topological order, where e -particles carry fractional Z_2^s quantum number, as indicated in Eq.(4.22). Eq.(4.23) tells us that the single-leg σ_z action creates nontrivial Z_2^s symmetry charge⁴. The plaquette IGG defined on Fig. 4-4(a) leads to the condensation of visons carrying nontrivial Z_2 charges. In the following, we show that any state satisfying these tensor equations is either a nontrivial Z_2 SPT phase, or a spontaneously symmetry breaking phase in the thermodynamic limit.

One way to see this is to gauge the Z_2^s symmetry. It is known that gauging the nontrivial Z_2^s SPT phase gives us the double semion topological order[87]. Let us verify it in the tensor network formulation. As shown in Fig. 4-5, for the gauged Z_2 SPT state, physical degrees of freedom live on links. The physical state on the link is determined by the “difference” of the two internal legs. The Z_2 symmetric condition for g and W_g in Fig. 4-3 becomes a new IGG element, as indicated in Fig. 4-6. Similar to the ungauged theory, W_g also satisfies Eq.(4.22) and Eq.(4.23).

According to Eq.(4.22), the gauged tensor state actually holds an Z_4 global IGG: $\{I, W_g, \sigma_z \otimes \sigma_z, W_g \cdot (\sigma_z \otimes \sigma_z)\}$. Z_4 flux, labeled as m_0 (m_0^\dagger), are created at ends of W_g strings. And ends of $\sigma_z \otimes \sigma_z$ strings are double Z_4 flux, labeled as m_0^2 . To see the physical meaning of single leg action of σ_z , we first note that it is a self boson. And braiding m_0 around it, one obtain π phase according to Eq.(4.23). So, the single leg action of σ_z corresponds to a double Z_4 charge e_0^2 . Due to the existence of nontrivial plaquette IGG elements, bound states of m_0^2 and e_0^2 are condensed, as shown in Fig. 4-4(b). And all other particles sharing nontrivial braiding statistics with $m_0^2 e_0^2$ are confined. Then, the remaining topological order can be determined by the following table:

⁴One may wonder whether the local Z_2^s charge of an m -particle is well defined, since we can always attach e particle to the symmetry defect W_g , which will change the result of local symmetry action due to the nontrivial braiding phase between e and m . However, if we always require that *symmetry defects have the trivial symmetry fractionalization pattern*, quantum numbers of m -particles are well defined

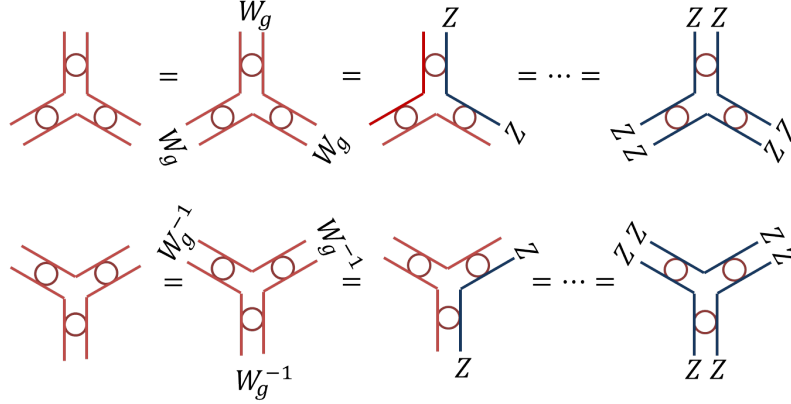


Figure 4-6: IGG for double semion topological order

- the symmetry transformation rules and IGG elements are interplaying with each other, as given in Eq.(4.22) and Eq.(4.23).

We will follow the above strategy in this part and develop a general framework for SPT phases on tensor networks. The three cohomology classification naturally emerges from tensor equations.

Symmetries

Let us first discuss how to impose symmetries on tensor networks[104, 171, 123, 124, 125, 8, 149, 76]. We focus on the case where the state is a 1D representation of symmetry group SG :

$$g \circ |\Psi\rangle = e^{i\theta_g} |\Psi\rangle, \forall g \in SG \quad (4.24)$$

Here SG includes both onsite symmetries as well as lattice symmetries.

Consider a PEPS state formed by site tensors. We assume that *for a symmetric PEPS state, the symmetry transformed tensors and the original tensors are related by a gauge transformation (up to a $U(1)$ phase factor)*:

$$\Theta_g W_g g \circ \mathbb{T} = \mathbb{T} \quad (4.25)$$

Here, \mathbb{T} represents the tensor states *with all internal legs uncontracted*. Namely $\mathbb{T} =$

$\bigotimes_a T^a$, where T_a represents a local tensor at site a . W_g is a gauge transformation, which acts on all internal legs of the tensor network:

$$W_g = \bigotimes_{(a,i)} W_g(a,i) \quad (4.26)$$

where (a, i) labels a leg of site a . If leg (a, u) and (b, v) are connected, according to the definition of gauge transformation, $W_g(a, u) \cdot W_g^t(b, v) = \mathbb{I}$. Θ_g is a tensor-dependent $U(1)$ phase. In the following, we will focus on systems defined on an infinite lattice, for which we can always absorb Θ_g to W_g . So, the symmetric condition for a tensor wavefunction can be expressed as

$$W_g g \circ \mathbb{T} = \mathbb{T} \quad (4.27)$$

To be more clear, we can write the above equation explicitly as

$$\begin{aligned} & (W_g(a, u))_{\alpha\alpha'} \cdot (W_g(a, v))_{\beta\beta'} \dots g \circ (T_{uv\dots}^a)_{\alpha'\beta'\dots}^i \\ & = (T_{uv\dots}^a)_{\alpha'\beta'\dots}^i \end{aligned} \quad (4.28)$$

where T_a labels a tensor at site a , and $u, v \dots$ labels legs of tensor T^a .

Invariant gauge group

The invariant gauge group (IGG) is a sub-group of gauge transformations, *whose element leaves every tensor – or equivalently the tensor state before contraction (\mathbb{T}) – completely invariant*[127, 117, 76]. Notice that a general gauge transformation only leaves the physical wavefunction invariant, while could transform the site tensors nontrivially. To make the discussion below clear, we denote any element in IGG as a *global* IGG element, since by definition this element is a gauge transformation involving all virtual legs on the tensor network.

We also introduce a special type of IGG elements – the plaquette IGG element λ_p , where λ_p acts nontrivially only on internal legs of plaquette p , as shown in Fig.

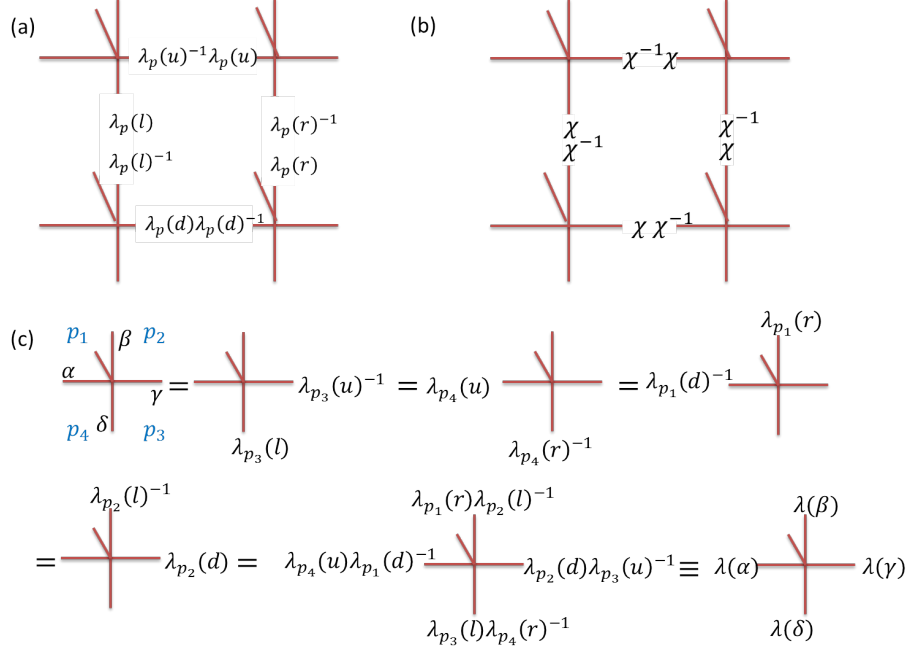


Figure 4-7: (a) An example of the plaquette IGG element λ_p . (b) The plaquette IGG element formed by complex number χ and χ^{-1} . This kind of plaquette IGG exists for any PEPS state. (c) A site tensor lives on the subspace which is invariant under action of IGGs. Here, p_1, p_2, p_3, p_4 are four neighbouring plaquettes around the tensor and $\alpha, \beta, \gamma, \delta$ denote legs of the tensor. The last equation indicates that a global IGG element is obtained from multiplication of plaquette IGG elements.

4-7(a). The plaquette IGG is a generalization of the single leg action of σ_z in Fig. 4-4. For any given plaquette p , the collection of plaquette IGG elements $\{\lambda_p\}$ acting on p forms a subgroup of IGG. To construct SPT, we further assume that *any global IGG element can always be decomposed into the product of plaquette IGG elements*, $\lambda = \prod_p \lambda_p$. Namely, plaquette IGG elements can generate the full IGG.

For SPT tensor wavefunctions, we have assumed that the decomposition from a global IGG element to the product of plaquette IGG elements always exist. One may ask whether the decomposition is unique. The answer is no. To see this, we consider the decomposition of the trivial action I on all internal legs. There is a special kind of plaquette IGG element: for every plaquette $\lambda_l = \lambda_u = \lambda_r = \lambda_d = \chi$, where χ is a complex number, as shown in Fig. 4-7(b). We also label this IGG element as χ_p . Then, $\prod_p \chi_p = I$. We assume that *this is the only way to decompose I*. Notice that the identity $\prod_p \chi_p = I$ directly leads to the fact that the phase factor χ in any

plaquette is the same. So, for any global IGG element, there is only one global phase ambiguity to decompose into the plaquette IGG elements λ_p reads

$$\lambda = \prod_p \lambda_p = \prod_p \chi_p \lambda_p \quad (4.29)$$

It turns out that this phase ambiguity is essential to get SPT phases, and naturally gives 3-cohomology classification.

Cohomology from symmetry equations on PEPS

For group elements g_1, g_2 , we have

$$\mathbb{T} = W_{g_1 g_1} W_{g_2 g_2} \circ \mathbb{T} = W_{g_1 g_2} g_1 g_2 \circ \mathbb{T}, \quad (4.30)$$

Since $W_{g_1 g_1} W_{g_2 g_2}$ and $W_{g_1 g_2} g_1 g_2$ only differ by a gauge transformation, and they both leave \mathbb{T} invariant. So, they should differ up to an IGG element, which we label as $\lambda(g_1, g_2)$,

$$W_{g_1 g_1} W_{g_2 g_2} = \lambda(g_1, g_2) W_{g_1 g_2} g_1 g_2 \quad (4.31)$$

which generalize Eq.(4.22). According to associativity

$$(W_{g_1 g_1} W_{g_2 g_2}) W_{g_3 g_3} = W_{g_1 g_1} (W_{g_2 g_2} W_{g_3 g_3}) \quad (4.32)$$

we get

$$\lambda(g_1, g_2) \lambda(g_1 g_2, g_3) = W_{g_1 g_1} \lambda(g_2, g_3) \lambda(g_1, g_2 g_3) \quad (4.33)$$

where we define ${}^a b \equiv a \cdot b \cdot a^{-1}$. Particularly, for a leg i , we have

$$(W_{g g} \lambda)(i) = W_g(i) \cdot \lambda^{s(g)}(g^{-1}(i)) \cdot [W_g(i)]^{-1} \quad (4.34)$$

where $s(g)$ is complex conjugate if g contains time reversal action.

One can decompose λ 's into λ_p 's, and due to the phase ambiguity Eq.(4.29), λ_p 's satisfy

$$\begin{aligned} \lambda_p(g_1, g_2)\lambda_p(g_1g_2, g_3) = \\ \omega_p(g_1, g_2, g_3)^{W_{g_1g_2}}\lambda_p(g_2, g_3)\lambda_p(g_1, g_2g_3) \end{aligned} \quad (4.35)$$

where $\omega_p(g_1, g_2, g_3)$ is the phase IGG satisfying $I = \prod_p \omega_p(g_1, g_2, g_3)$.

In Section 4.7, we prove ω_p satisfies three cocycle condition:

$$\begin{aligned} \omega_p(g_1, g_2, g_3)\omega_p(g_1, g_2g_3, g_4)^{g_1}\omega_p(g_2, g_3, g_4) \\ = \omega_p(g_1g_2, g_3, g_4)\omega_p(g_1, g_2, g_3g_4) \end{aligned} \quad (4.36)$$

And ω_p is defined up to a coboundary:

$$\omega_p(g_1, g_2, g_3) \sim \omega_p(g_1, g_2, g_3) \frac{\chi_p(g_1, g_2)\chi_p(g_1g_2, g_3)}{g_1\chi_p(g_2, g_3)\chi_p(g_1, g_2g_3)} \quad (4.37)$$

The action of g on $\omega_p(\chi_p)$ follows a very simple rule: for a leg i , we have $({}^g\omega_p)(i) = \omega_{g^{-1}(p)}^{s(g)}(g^{-1}(i))$, where $s(g)$ is complex conjugate if g contains time reversal. Then, consider ω_p , we have

- For unitary onsite symmetry g , ${}^g\omega_p = \omega_p$
- For time reversal symmetry \mathcal{T} , ${}^{\mathcal{T}}\omega_p = \omega_p^*$
- For translation and/or rotation symmetry T_i and C_i , ${}^{T_i}\omega_p = {}^{C_i}\omega_p = \omega_p$
- For reflection symmetry σ , ${}^{\sigma}\omega_p = \omega_p^{-1}$

Methods to construct generic SPT tensor wavefunctions

Now, we have developed a general way to write down tensor equations for SPT phases: Eq.(4.31), Eq.(4.33) and Eq.(4.35). The next step is to answer the following question: given a symmetry group SG and a cohomology class $[\omega]$, how do we construct generic

SPT wavefunctions from tensor equations? This problem actually can be decomposed to three parts:

1. Figure out the group structure for λ 's, λ_p 's and W_g 's to realize the SPT phase.
2. Obtain the representation of the IGG and symmetry on tensor networks.
3. Find subspace of tensors, which are invariant under IGG action on internal legs as well as symmetry actions on both physical legs and virtual legs.

The second part and the third part are relatively easy to solve, and we give examples in Sec.4.3.5. Here, we focus on the first part, and we provide two methods in the following.

The first way is to start from exact solvable models. If there exists an exact solvable model realizing some SPT phase, one can construct a fixed point wavefunction by PEPS. Then, one can extract tensor equations as well as the group structure for λ 's λ_p 's and W_g 's. For example, as we show in Sec.4.3.1, to realize a nontrivial Z_2^s SPT, λ 's form a Z_2^g group. λ_p 's form group $Z_2 \times U(1)$ for any plaquette p . And W_g is a projective representation with coefficient in Z_2 , which anticommutes with nontrivial λ_p .

Notice that the group structure for IGG and W_g does not depend on whether SG is onsite or spatial. So, we are also able to figure out IGG and W_g for spatial SPT phases. For example, as we will show in Sec.4.3.5, for the nontrivial inversion SPT phase, λ 's form a Z_2^g group, which is the same as the case for Z_2^s onsite SPT phase. The only difference is that for the inversion SPT and Z_2 onsite SPT, the IGGs have distinct representations on internal legs.

For every SPT phase protected by a discrete symmetry group and also some SPT phases protected by continuous symmetry groups, one can write down exact solvable models. So one is able to realize those generic SPT wavefunctions by tensors.

The second way is related to a mathematical object named as crossed module extensions. It is known in mathematical literatures that crossed module extensions of SG by $U(1)$ are classified by $H^3(SG, U(1))$. And as we show in Section 4.7, our

tensor constructions can be viewed as a representation of crossed module extensions. So, given a crossed module extension, we are able to figure out the group structure for IGG and W_g 's.

4.3.3 A by-product: the general anyon condensation mechanism for realizing SPT phases

Using the above results, here we prove the Criterion of the anyon condensation mechanism. We will start from an SET phase with discrete Abelian topological order and condense m -particles to confine the gauge field, and demonstrate the Criterion to realize SPT phases. For the purpose of presentation, we will consider Z_N topologically ordered SET phases with the symmetry group SG , but one can straightforwardly generalize the discussion below for SET phases with any discrete Abelian gauge groups $Z_{N_1} \times Z_{N_2} \dots$.

In order to represent a regular Z_N topological order in the tensor-network formulation, one needs to introduce a nontrivial *global* IGG[127, 117, 76], labeled as H . In particular, there is a nontrivial global IGG element $J \in H$ satisfying $J^N = \mathbf{I}$, and representing the Z_N gauge transformation. Here J is nontrivial means that it is not $U(1)$ -phase multiplications on the virtual legs. A J string is interpreted as a Z_N flux line, while the Z_N gauge flux and its antiparticle are created at two ends of the J string. Besides the nontrivial Z_N IGG, there is always “trivial” IGG X , whose elements are loops of phases. So, we start from tensor states with an abelian IGG $H \times X$.

In the presence of symmetry SG and IGG $H \times X$, the tensor equations read

$$W_{g_1 g_1} W_{g_2 g_2} = \xi(g_1, g_2) \eta(g_1, g_2) W_{g_1 g_2 g_1 g_2}, \quad \forall g_1, g_2 \in SG \quad (4.38)$$

where $\xi(g_1, g_2) \in X$, and $\eta(g_1, g_2) \in H$. ξ 's and η 's both satisfy the two-cocycle

condition:

$$\begin{aligned}\xi(g_1, g_2)\xi(g_1g_2, g_3) &= {}^{g_1}\xi(g_2, g_3)\xi(g_1, g_2g_3) \\ \eta(g_1, g_2)\eta(g_1g_2, g_3) &= {}^{W_{g_1g_1}}\eta(g_2, g_3)\eta(g_1, g_2g_3)\end{aligned}\tag{4.39}$$

We point out that η 's label the symmetry fractionalization pattern of Z_N charges.

How about the symmetry properties for fluxes? To see this, let us study the symmetry action on Z_N flux line J : ${}^{W_g}J \in H \times X$. Since we are studying phases featuring symmetry fractionalizations, we require that the anyon types are invariant under symmetry action:

$${}^{W_g}J = \chi_J(g) \cdot J\tag{4.40}$$

where $\chi_J(g) \in X$, and $(\chi_J(g))^N = 1$. Further, $\chi_J : SG \rightarrow Z_N$ is a representation of SG , since

$$\begin{aligned}{}^{W_{g_1g_1}W_{g_2g_2}}J &= \chi_J(g_1) {}^{g_1}\chi_J(g_2) \cdot J \\ &= \xi(g_1, g_2)\eta(g_1, g_2) {}^{W_{g_1g_2g_1g_2}}J = \chi_J(g_1g_2) \cdot J\end{aligned}\tag{4.41}$$

where we use the fact $\xi(g_1, g_2)\eta(g_1, g_2)$ commute with J . So,

$$\chi_J(g_1g_2) = \chi_J(g_1) {}^{g_1}\chi_J(g_2)\tag{4.42}$$

Notice that both time reversal \mathcal{T} and reflection P should be treated as antiunitary operations.

To proceed, we point out that the building blocks for X are plaquette phase IGGs:

$$\chi = \prod_p \chi_p, \forall \chi \in X\tag{4.43}$$

Here $\chi_p \in X_p$, where $X_p \subset X$ is the plaquette IGG of p , whose elements are loops of phases along virtual legs of plaquette p . As before, the decomposition to plaquette

phase IGG elements has a single phase ambiguity:

$$\chi = \prod_p \chi_p = \prod_p \epsilon_p \chi_p \quad (4.44)$$

Here $\epsilon_p(i) = \epsilon^{\pm 1}$, where ± 1 pattern follows as Fig. 4-7(b).

Then, according to Eq.(4.42) and Eq.(4.44), we obtain

$$\chi_{p,J}(g_1)^{g_1} \chi_{p,J}(g_2) = \omega_{p,J}(g_1, g_2) \chi_{p,J}(g_1 g_2) \quad (4.45)$$

where $\omega_{p,J}(g_1, g_2)(i) = \omega_J(g_1, g_2)^{\pm 1}$. Because $\chi_J(g)^N = 1$, clearly phase factors $\chi_{p,J}(g)$ and $\omega_{p,J}(g_1, g_2)$ can be chosen to be Z_N elements. It is straightforward to check that $\omega_{p,J}$ satisfies the two-cocycle condition:

$$\omega_{p,J}(g_1, g_2) \omega_{p,J}(g_1 g_2, g_3) = {}^{g_1} \omega_{p,J}(g_2, g_3) \omega_{p,J}(g_1, g_2 g_3) \quad (4.46)$$

It turns out that $\omega_J(g_1, g_2) \in Z_N$ labels the symmetry fractionalization pattern of Z_N fluxes.

For onsite symmetries, we can restrict to one internal leg i . Then, Eq.(4.45) becomes a relation for phase factors. We can always tune $\omega_{p,J}$ to be trivial by redefining $\chi_{p,J}(g) \rightarrow \epsilon_J(g) \cdot \chi_{p,J}(g)$. In other words, onsite symmetry fractionalization patterns for fluxes are always trivial for the case IGG equals $H \times X$. Notice, fluxes can carry fractional spatial symmetry quantum numbers in general.

Now, let us derive the Criterion to obtain SPT phases by condensing fluxes. In this tensor formulation, we require nontrivial plaquette IGG for every plaquette. And the plaquette IGG for p is labeled as $H_p \times X_p$.

To kill the topological order, we require the decomposition of J as

$$J = \prod_p J_p = \prod_p \epsilon_p J_p \quad (4.47)$$

where J_p is a nontrivial plaquette IGG element for plaquette p . Again, the decomposition has an $U(1)$ ambiguity $\epsilon_{p,J}$. As shown in Fig. 4-7(d), the bound state of Z_N

fluxes and J_p is condensed according to the above equation. Notice that there is a canonical choice for J_p such that $J_p^N = I$. So we can choose $H_p \cong Z_N$, and $H_p \times X_p$ is an abelian group. Further, as we prove in Section 4.7, elements of plaquette IGG for different plaquettes commute. Thus, we conclude, the whole IGG is abelian.

To see the symmetry action on J_p , or equivalently, the symmetry quantum number carried by J_p , we have

$$\begin{aligned} W_{gg}J &= \prod_p W_{gg}J_p \\ &= \chi_J(g) \cdot J = \prod_p \chi_{p,J}(g) J_p \end{aligned} \quad (4.48)$$

Due to the $U(1)$ ambiguity, we conclude

$$W_{gg}J_p = \epsilon_{p,J}(g) \chi_{p,J}(g) J_p \quad (4.49)$$

We further have

$$\begin{aligned} W_{g_1 g_1} W_{g_2 g_2} J_p &= \epsilon_{p,J}(g_1) \chi_{p,J}(g_1)^{g_1} \epsilon_{p,J}(g_2)^{g_1} \chi_{p,J}(g_2)^{g_1} \cdot J_p \\ &= \xi^{(g_1, g_2) \eta(g_1, g_2)} W_{g_1 g_2 g_1 g_2} J_p = \epsilon_{p,J}(g_1 g_2) \chi_{p,J}(g_1 g_2) \cdot J_p \end{aligned} \quad (4.50)$$

where we use the fact that $\xi\eta$ commutes with J_p . Comparing with Eq.(4.45), we conclude

$$\omega_{p,J}(g_1, g_2) = \frac{\epsilon_{p,J}(g_1 g_2)}{\epsilon_{p,J}(g_1)^{g_1} \epsilon_{p,J}(g_2)} \quad (4.51)$$

is a two-coboundary. Namely, in this tensor formulation, symmetry-preserving flux-condensation requires fluxes to have no symmetry fractionalization.

In the following, we focus on a simple case:

$$\chi_J(g) = 1, \forall g \in SG. \quad (4.52)$$

If instead $\chi_J(g)$ is nontrivial phase factor for symmetry g , the quantum number

carried by the flux will depend on the details of the region of local-symmetry action as well as the flux string configuration. Although this situation is not violating basic principles, it is rather unlikely in usual models. In addition, the main purpose of this section is to derive the Criterion for anyon condensation mechanism, where we assume the quantum numbers of the flux is independent of the details of local symmetry action. Consequently, in this section, we do not consider this situation and focus on the cases given by Eq.(4.52).

We choose a canonical gauge such that $J_p^N = I$, and $\eta_p = J_p^m$ for $\eta = J^m, \forall m$. In particular, we have

$$\eta_p \cdot \eta'_p = (\eta \cdot \eta')_p \quad (4.53)$$

Then, according to Eq.(4.39), we have

$$\eta_p(g_1, g_2)\eta_p(g_1g_2, g_3) = \eta_p(g_2, g_3)\eta_p(g_1, g_2g_3) \quad (4.54)$$

Let us define

$$\omega_1(g_1, g_2, g_3) = \frac{W_{g_1g_2}\eta_p(g_2, g_3)\eta_p(g_1, g_2g_3)}{\eta_p(g_1, g_2)\eta_p(g_1g_2, g_3)} = \frac{W_{g_1g_2}\eta_p(g_2, g_3)}{\eta_p(g_2, g_3)} \quad (4.55)$$

which is the quantum number of condensed fluxes. We also define

$$\omega_2(g_1, g_2, g_3) = \frac{W_{g_1g_2}\xi_p(g_2, g_3)\xi_p(g_1, g_2g_3)}{\xi_p(g_1, g_2)\xi_p(g_1g_2, g_3)} \quad (4.56)$$

Following Section 4.7, one can prove ω_1 and ω_2 are both three-cocycles. And the obtained SPT phase is characterized by $[\omega] = [\omega_1] \cdot [\omega_2]$, where $[\cdot]$ means equivalent class up to coboundary. Notice that even before anyon condensation (without nontrivial plaquette IGG H_p), ω_2 is still present – it is “background” SPT index unaffected by anyon condensation. However, because ω_2 is obtained from the algebra of phase factors (instead of matrices), ω_2 can be nontrivial only due to spatial translational symmetries (i.e. ω_2 is only describing a weak SPT indices). The strong SPT indices

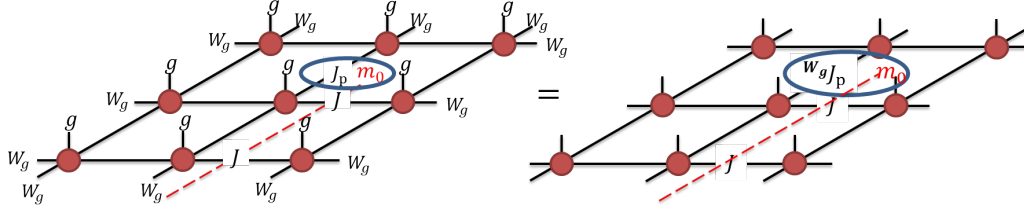


Figure 4-8: Measurement of the quantum number $\chi_{m_0}(g)$ carried by an m -particle for a local unitary symmetry g . According to Eq.(4.40,4.52), J commute with W_g , so we conclude that the quantum number is obtained by $\chi_{m_0}(g) \cdot J_p = W_{g^p} J_p$.

can only appear due to ω_1 . So we have proved the Criterion as in Sec. 4.2.

4.3.4 Algorithms to measure anyon quantum numbers

It would be useful to be able to numerically measure the quantum numbers carried by the low energy m -particles inside the SET phase near the condensation phase transition. Such measurements, together with the Criterion, would allow one to predict the nature of the resulting symmetric phases. Now let us present several “conceptual” algorithms to measure these quantum numbers. Although these algorithms could be implemented in the existing tensor-network algorithms[136] to practically measure these quantum numbers, here our focus is mainly to clarify conceptual issues. In particular, the quantum numbers introduced in the previous section may appear somewhat formal, and it would be ideal to explicitly demonstrate their measurable meanings.

We again focus on ordinary Z_N gauge theories. As discussed before, the two ends of an open string created by a sequence of J operations on the virtual bonds actually describe an elementary m -particle (coined m_0) and its anti-particle (coined m_0^\dagger). In order to simulate the low energy excitations within the topological sectors corresponding to m_0 and m_0^\dagger , one needs to further variationally optimize the tensors over finite regions (about correlation-length size) near the centers of these m -particles. Namely, a low energy excitation state $|\Psi_{ex}\rangle$ hosting m_0 and m_0^\dagger quasiparticles is obtained by only modifying these local tensors (coined excited-state-local-tensors) while leaving all other tensors in the network (coined ground-state-local-tensors) the

same as the ground state (apart from multiplying a sequence of J operations on the string).

Our basic scheme is to use the symmetry transformation rules on the ground-state-local-tensors to obtain the symmetry properties of m_0 and m_0^\dagger . Let us start from discussing the measurement of the quantum number of an onsite unitary symmetry $g \in SG$, as shown in Fig.(4-8). For example, let us focus on m_0 . The local action of g on m_0 is described by applying W_g on a loop of virtual legs enclosing m_0 (but *not* enclosing m_0^\dagger), together with applying the physical transformation g on the physical legs inside the region enclosed by the W_g -loop. Physically, such a tensor-network operation corresponds to braiding a g -symmetry-defect (described by the end point of the W_g -string) around m_0 . It turns out that the condition $W_g g J = J$ (i.e. Eq.(4.40,4.52)) dictates that *the g -symmetry-defect itself has no symmetry fractionalization*. It also dictates that the m_0 is transformed by this local action back to the same topological sector.

Now quantum number carried by m_0 : $\chi_{m_0}(g)$ has direct measurable meaning. After applying the local action of g on m_0 , one obtains a new physical state $|\Psi'_{ex}\rangle$, corresponding to applying symmetry g only on m_0 but not on m_0^\dagger . Due to symmetry, $|\Psi'_{ex}\rangle$ can at most differ from $|\Psi_{ex}\rangle$ by a phase factor, which is exactly the measurable meaning of $\chi_{m_0}(g)$. Note that the variationally determined excited-state-local-tensors around m_0 only introduces a common global phase ambiguity in the physical state $|\Psi_{ex}\rangle$ and $|\Psi'_{ex}\rangle$, and consequently not affecting their relative phase $\chi_{m_0}(g)$.

Similar discussion can be naturally extended to rotational spatial symmetries, which can be treated as unitary operations. The only modification is that one needs to choose the position m_0 to be invariant under the rotations in order to respect these symmetries.

The more interesting and nontrivial situation is the time-reversal \mathcal{T} and mirror reflection \mathcal{P} . It is straightforward to show that the assumption Eq. (4.40,4.52) leads to the following transformation rules: $\mathcal{T} : e \rightarrow e^\dagger, m \rightarrow m$, and $\mathcal{P} : e \rightarrow e, m \rightarrow m^\dagger$. And the quantum numbers $\chi_m(g)$ should be treated as an element in $H^1(SG, Z_N)$ but with \mathcal{T} and \mathcal{P} acting anti-unitarily on Z_N . However, their combination $\mathcal{T} \cdot \mathcal{P}$ should

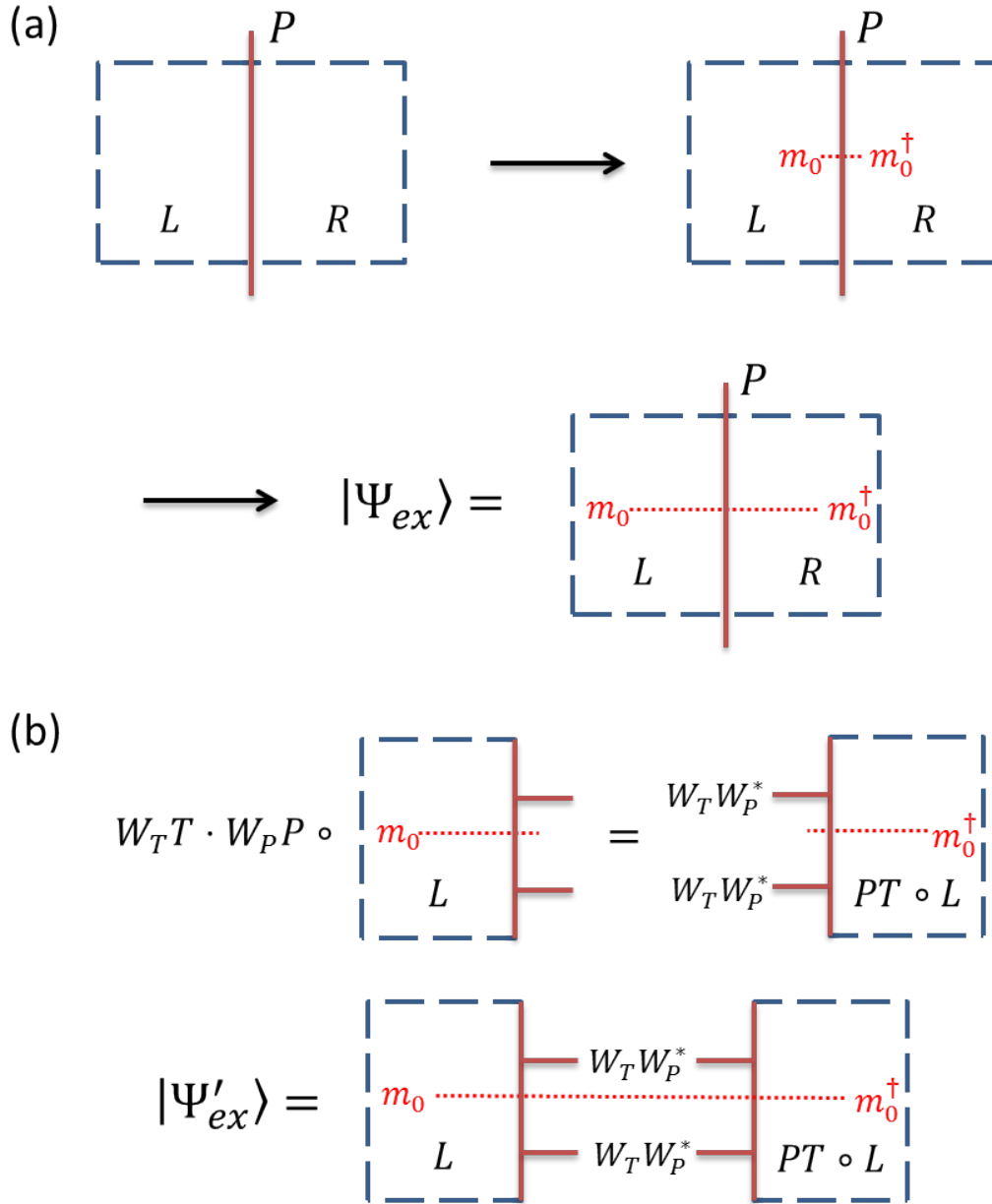


Figure 4-9: (a) The procedure to create $|\Psi_{ex}\rangle$ which is $\mathcal{T}\cdot\mathcal{P}$ invariant. One first creates a pair of m_0 and m_0^\dagger from ground state, and then move away from each other. The global phase of $|\Psi_{ex}\rangle$ by requiring the wavefunction overlap between adjacent states to be real and positive. (b) $|\Psi'_{ex}\rangle$ is obtained by gluing between the original left-half of the tensor-network with the $\mathcal{T}\cdot\mathcal{P}$ transformed left-half tensor-network. The $\mathcal{T}\cdot\mathcal{P}$ transformed left-half tensor-network is obtained by transforming the physical legs of the left-half via $\mathcal{T}\cdot\mathcal{P}$, together with applying $W_{\mathcal{T}}\mathcal{T}\cdot W_{\mathcal{P}}\cdot\mathcal{T}^{-1}$ on all the virtual legs cut by the mirror line. $\chi_{m_0}(\mathcal{T}\cdot\mathcal{P})$ is defined as phase difference between $|\Psi_{ex}\rangle$ and $|\Psi'_{ex}\rangle$.

be treated as unitary and the corresponding quantum number is sharply measurable. Below we present such an algorithm, which is depicted in Fig. 4-9.

Let us choose the positions of m_0 and m_0^\dagger to be \mathcal{P} image of each other. For example, we will consider the situation that $m_0(m_0^\dagger)$ is located in the left(right) half of the sample, and the mirror is the vertical line. Consequently $|\Psi_{ex}\rangle$ is $\mathcal{T}\cdot\mathcal{P}$ symmetric. Our goal is to measure the quantum number $\chi_{m_0}(\mathcal{T}\cdot\mathcal{P})$. This quantity may appear to be strange because we know that the combination $\mathcal{T}\cdot\mathcal{P}$ would send m_0 to m_0^\dagger — a different quasiparticle. But it turns out that this is exactly what is required to sharply measure $\chi_{m_0}(\mathcal{T}\cdot\mathcal{P})$.

Similar to previous example, our plan is to apply $\mathcal{T}\cdot\mathcal{P}$ only on m_0 and obtain a new excited physical state $|\Psi'_{ex}\rangle$. But because of the nature of \mathcal{P} , the $|\Psi'_{ex}\rangle$ should be obtained by gluing (i.e. contracting virtual legs) between the original left-half of the tensor-network with the $\mathcal{T}\cdot\mathcal{P}$ transformed left-half tensor-network (which is now on the right-half). Specifically, the $\mathcal{T}\cdot\mathcal{P}$ transformed left-half tensor-network is obtained by transforming the physical legs of the left-half via $\mathcal{T}\cdot\mathcal{P}$, together with applying $W_{\mathcal{T}}\mathcal{T}\cdot W_{\mathcal{P}}\cdot\mathcal{T}^{-1}$ on all the virtual legs cut by the mirror line. The procedure to obtain $|\Psi'_{ex}\rangle$ is shown in Fig. 4-9(b).

If one naively uses the phase difference between this $|\Psi'_{ex}\rangle$ and $|\Psi_{ex}\rangle$ to measure $\chi_{m_0}(\mathcal{T}\cdot\mathcal{P})$, one will find that it is not well-defined. The reason is that the global phase factor of $|\Psi_{ex}\rangle$ is not properly chosen yet. In order to sharply measure $\chi_{m_0}(\mathcal{T}\cdot\mathcal{P})$, one needs to fully determine the global phase factor of $|\Psi_{ex}\rangle$ relative to the ground state in the following sense. In order to construct $|\Psi_{ex}\rangle$, one can imagine to firstly create a pair of m_0 and m_0^\dagger near each other, and then further move them away from each other to a large distance, while *maintaining $\mathcal{T}\cdot\mathcal{P}$ over the whole process*, as shown in Fig. 4-9(a). This process would create a sequence of states, with ground state as the first one and $|\Psi_{ex}\rangle$ as the last one. The global phase factor of $|\Psi_{ex}\rangle$ is determined by requiring the *wavefunction overlap between adjacent states in this sequence to be positive and real*.

Because the global phase factor of $|\Psi_{ex}\rangle$ is fixed, the only ambiguity in the tensor-network construction of $|\Psi_{ex}\rangle$ is a global phase factor $e^{i\theta}$ on the left-half, and $e^{-i\theta}$ on

the right-half. But this relative phase ambiguity would not affect the phase difference between this $|\Psi'_{ex}\rangle$ and $|\Psi_{ex}\rangle$ discussed above. Namely the phase difference between this $|\Psi'_{ex}\rangle$ and $|\Psi_{ex}\rangle$ is now sharply measurable, which is nothing but $\chi_{m_0}(\mathcal{T} \cdot \mathcal{P})$.

4.3.5 Examples

We present some explicit examples for the 2+1D SPT. Let us consider square lattice with a $d = 2$ qubit on each site. For simplicity, we will focus on the case where all tensors are translationally invariant. We label the legs of a site tensor as $\alpha, \beta, \gamma, \delta$, and plaquette IGG elements act as $\lambda_l, \lambda_u, \lambda_r, \lambda_d$, as shown in Fig. 4-7.

SPT phases protected by inversion symmetry

Consider nontrivial SPT phases protected by inversion symmetry \mathcal{I} . According to the discussion in the previous part, the inversion protected SPT phases are classified by $H^2(Z_2^{\mathcal{I}}, U(1)) = Z_2$. Namely, there is only one nontrivial phase.

We start with a tensor network with Z_2 global IGG $\{I, \lambda\}$. Tensor equations for this nontrivial SPT phase are

$$\begin{aligned} W_{\mathcal{I}\mathcal{I}} &= \lambda \\ W_{\mathcal{I}\mathcal{I}}\lambda_p &= -\lambda_p \end{aligned} \tag{4.57}$$

where λ_p is the plaquette IGG element. For a single leg action, we have

$$\begin{aligned} \mathcal{I}W_{\mathcal{I}}(i) &= W_{\mathcal{I}}^{\dagger}(\mathcal{I}(i)), \quad i = \alpha, \beta, \gamma, \delta \\ \mathcal{I}\lambda_j &= \lambda_{\mathcal{I}(j)}^{\dagger}, \quad j = l, u, r, d \end{aligned} \tag{4.58}$$

Here, due to translational invariance, we define $\lambda_j \triangleq \lambda_p(j), \forall p$.

The simplest solution requires internal bond dimension $D = 6$. IGG elements are

represented as

$$\begin{aligned}
\lambda &= \sigma_0 \oplus (-\sigma_0 \otimes \sigma_0) \\
\lambda_l &= \lambda_u = \sigma_z \oplus (\sigma_z \otimes \sigma_z) \\
\lambda_r &= \lambda_d = \sigma_z \oplus (-\sigma_z \otimes \sigma_z)
\end{aligned} \tag{4.59}$$

and the inversion operation on internal legs is

$$W_{\mathcal{I}}(i) = \sigma_x \oplus (\sigma_y \otimes \sigma_x) \tag{4.60}$$

Now, let us determine the constraint Hilbert space for the nontrivial SPT phase. As shown in Fig. 4-7(c), we require that the single tensor lives in the subspace which is invariant under action of plaquette IGG elements, where the nontrivial plaquette IGG element in Eq.(4.59). Further, we require the single tensor to be inversion symmetric: $W_{\mathcal{I}}\mathcal{I} \circ T^a = T^a$, where $W_{\mathcal{I}}$ is given in Eq.(4.60). Then, by solving these linear equations, we obtain a $D_{\mathcal{I}} = 74$ dimensional (complex) Hilbert space. We point out that the original Hilbert space for a site tensor is $dD^4 = 2592$ dimensional.

It is also straightforward to check that the only nontrivial cocycle phase is $\omega(\mathcal{I}, \mathcal{I}, \mathcal{I}) = -1$, which cannot be tuned away.

SPT phases protected by time reversal and reflection symmetries

Now, we study a more interesting example: 2D SPT phases protected by $Z_2^P \times Z_2^T$ (reflection and time reversal) symmetry. The four group elements are $\{I, P, \mathcal{T}, P\mathcal{T}\}$, where $\mathcal{T} = \sigma_x \mathcal{K}$ and P is the reflection along y axis. As we mentioned above, both P and \mathcal{T} should be treated as ‘‘anti-unitary’’ action. Then, $P\mathcal{T}$ should be treated as a unitary action. Namely, we have

$$H^3(Z_2^P \times Z_2^T, U(1)) = H^3(Z_2 \times Z_2^T, U(1)) = Z_2 \times Z_2 \tag{4.61}$$

The tensor equations for these SPT phases are:

$$\begin{aligned}
W_{\mathcal{T}}\mathcal{T}W_{\mathcal{T}}\mathcal{T} &= \lambda(\mathcal{T}, \mathcal{T}) \\
W_P P W_P P &= \lambda(P, P) \\
W_P P W_{\mathcal{T}}\mathcal{T} &= W_{\mathcal{T}}\mathcal{T}W_P P \\
{}^{W_P P W_{\mathcal{T}}\mathcal{T}}\lambda_p &= -\lambda_p
\end{aligned} \tag{4.62}$$

where $\lambda(\mathcal{T}, \mathcal{T}), \lambda(P, P)$ belongs to the global Z_2 IGG. And different choice of λ 's gives different SPT phases.

By definition, the action of symmetry on W 's and λ 's are

$$\begin{aligned}
{}^{\mathcal{T}}W_R(i) &= W_R^*(i) \\
{}^P W_R(\alpha/\gamma) &= W_R^t(\gamma/\alpha) = (W_R^{-1}(\alpha/\gamma))^t \\
{}^P W_R(\beta/\delta) &= W_R(\beta/\delta)
\end{aligned} \tag{4.63}$$

as well as

$${}^{\mathcal{T}}\lambda_j = \lambda_j^*, \quad {}^P\lambda_{l/r} = \lambda_{r/l}^{-1}, \quad {}^P\lambda_{u/d} = (\lambda_{u/d}^{-1})^t \tag{4.64}$$

To realize these SPT phases, we start from $D = 6$ PEPS. Without any constraint, a single tensor lives in a $dD^4 = 2592$ dimensional (complex) Hilbert space. IGG elements are chosen as

$$\begin{aligned}
\lambda &= \sigma_0 \oplus (-\sigma_0 \otimes \sigma_0) \\
\lambda_l &= \sigma_z \oplus (\sigma_z \otimes \sigma_z), \quad \lambda_r = \sigma_z \oplus (-\sigma_z \otimes \sigma_z) \\
\lambda_u &= \sigma_z \oplus (\sigma_z \otimes \sigma_0), \quad \lambda_d = \sigma_z \oplus (-\sigma_z \otimes \sigma_0)
\end{aligned} \tag{4.65}$$

In the following, we discuss each class in $Z_2 \times Z_2$ separately.

1. $\lambda(\mathcal{T}, \mathcal{T})$ and $\lambda(P, P)$ are both trivial. We get a trivial symmetric phase in this case.

2. $\lambda(\mathcal{T}, \mathcal{T}) = \text{I}$, $\lambda(P\mathcal{T}, P\mathcal{T})$ is nontrivial. Time reversal and reflection symmetries on internal legs are represented as

$$\begin{aligned}
W_{\mathcal{T}}(i) &= \sigma_x \oplus (\sigma_x \otimes \sigma_0) \\
W_P(\alpha) &= W_P(\beta) = \sigma_0 \oplus (\sigma_0 \otimes i\sigma_y) \\
W_P(\gamma) &= W_P(\delta) = \sigma_0 \oplus (\sigma_0 \otimes (-i\sigma_y))
\end{aligned} \tag{4.66}$$

The constrained sub-space is an 80 dimensional real Hilbert space.

3. $\lambda(P, P) = \text{I}$, $\lambda(\mathcal{T}, \mathcal{T})$ is nontrivial. Time reversal and reflection symmetries are represented as

$$\begin{aligned}
W_{\mathcal{T}}(\alpha) &= W_{\mathcal{T}}(\beta) = \sigma_x \oplus (i\sigma_y \otimes \sigma_0) \\
W_{\mathcal{T}}(\gamma) &= W_{\mathcal{T}}(\delta) = \sigma_x \oplus (i\sigma_y \otimes \sigma_0) \\
W_P(i) &= \sigma_0 \oplus (\sigma_0 \otimes \sigma_x)
\end{aligned} \tag{4.67}$$

The constrained sub-space is an 88 dimensional real Hilbert space.

4. $\lambda(\mathcal{T}, \mathcal{T})$ and $\lambda(P\mathcal{T}, P\mathcal{T})$ are both nontrivial. Time reversal and reflection symmetries are represented as

$$\begin{aligned}
W_{\mathcal{T}}(\alpha) &= W_{\mathcal{T}}(\beta) = \sigma_x \oplus (i\sigma_y \otimes \sigma_0) \\
W_{\mathcal{T}}(\gamma) &= W_{\mathcal{T}}(\delta) = \sigma_x \oplus (-i\sigma_y \otimes \sigma_0) \\
W_P(\alpha) &= W_P(\beta) = \sigma_0 \oplus (i\sigma_0 \otimes \sigma_y) \\
W_P(\gamma) &= W_P(\delta) = \sigma_0 \oplus (-i\sigma_0 \otimes \sigma_y)
\end{aligned} \tag{4.68}$$

The constrained sub-space is an 80 dimensional real Hilbert space.

Weak SPT phases protected by lattice group

In this part, we consider the interplay of translation with point group. It is known that in the presence of translation, there are more SPT phases, which are named

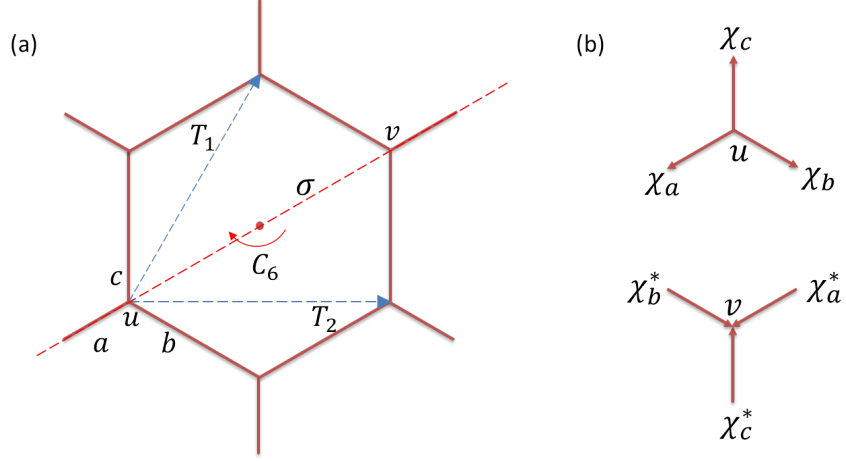


Figure 4-10: (a) The honeycomb lattice and generators the lattice symmetry group. u, v labels sites while a, b, c labels bonds in one unit cell. (b) The IGG element formed by phases. We require $\chi_a \cdot \chi_b \cdot \chi_c = 1$.

as weak indices[22]. In Ref.[31], the authors find that weak indices can be elegantly incorporated into the cohomology formulation by treating translation in the same way as the on-site symmetry. Weak indices can be explicitly calculated using Künneth formula. In (2+1)D, assuming the symmetry group $SG = \mathbb{Z}^2 \times G$, where \mathbb{Z}^2 denotes translational symmetry on the plane, the formula reads

$$H^3[\mathbb{Z}^2 \times G, U(1)] = H^3[G, U(1)] \times (H^2[G, U(1)])^2 \times H^1[G, U(1)] \quad (4.69)$$

where $H^3[G, U(1)]$ classify the strong indices, $(H^2[G, U(1)])^2$ are weak indices capture (1+1)D SPT phases and $H^0[G, U(1)]$ simply captures different charges in a unit cell.

In our tensor construction of SPT phases, we show that it is indeed natural to treat lattice symmetry in the same way as on-site symmetry. Not surprising, the interplay between translation and point group leads to new “weak SPT” phases.

Let us consider a spin system in a honeycomb lattice, as shown in Fig.4-10. In Ref.[79], the authors obtain four classes of featureless insulators, which can be captured by two Z_2 indices χ_{C_6} and χ_σ . The $Z_2 \times Z_2$ classification can actually be understood as weak indices, which comes from the interplay between C_6 , σ and translation T_1, T_2 .

4.4 SPT phases in 3+1D

It is natural to generalize tensor construction of SPT phases to 3+1D. Before going into this higher dimensions, we would like to mention that in Section 4.6 we go to the lower dimensions and prove our results on 1+1D SPT.

As the same in 2+1D, the symmetric tensor condition reads

$$W_g g \circ \mathbb{T} = \mathbb{T} \quad (4.70)$$

where \mathbb{T} labels the 3+1D tensor network before contraction, and W_g is the gauge transformation associated to symmetry g .

Then, $W_g g$ satisfies the group multiplication rules up to an IGG element:

$$W_{g_1 g_1} W_{g_2 g_2} = \lambda(g_1, g_2) W_{g_1 g_2 g_1 g_2} \quad (4.71)$$

Due to associativity, $\lambda(g_1, g_2)$ satisfies the two cocycle condition:

$$\lambda(g_1, g_2) \lambda(g_1 g_2, g_3) = {}^{W_{g_1 g_1}} \lambda(g_2, g_3) \lambda(g_1, g_2 g_3) \quad (4.72)$$

In general, the nontrivial IGG leads to nontrivial topological order in 3+1D. In order to kill the topological order, we introduce cubic IGG $\{\lambda_c\}$, where λ_c only acts nontrivially on the internal legs of cubic c . We further assume, any IGG element λ can be decomposed to product of cubic IGG elements:

$$\lambda = \prod_c \lambda_c \quad (4.73)$$

Let us discuss the uniqueness of the above decomposition. We introduce the plaquette IGG $\{\xi_p\}$, which acts nontrivially only on legs belonging to plaquette p . Then, we can define a special kind of cubic IGG $\{\eta_c\}$, where any η_c can be decomposed

as multiplication of plaquette IGG elements,

$$\eta_c = \prod_{p \in c} \xi_p^c \quad (4.74)$$

If we further require $\xi_p^{c_1} = (\xi_p^{c_2})^{-1}$ for $p = c_1 \cap c_2$, then, we get the decomposition of I as

$$I = \prod_c \eta_c \quad (4.75)$$

In other words, the decomposition of a given IGG element λ is not unique. We can always attach such kind of η_c to get new decomposition. Then, roughly speaking, the cubic IGG element $\lambda_c(g_1, g_2)$ should satisfy a “twist” two cocycle condition, where the “twist factors” take value in $\{\eta_c\}$.

We can further prove $\eta_c(g_1, g_2, g_3)$ satisfies condition similar to three cocycles. We notice that the decomposition of η_c to plaquette IGG elements ξ_p 's is also not unique, we can always attach some phase factor to ξ_p such that the multiplication of ξ_p is invariant. Then, ξ_p should satisfy a “twist” three cocycle equation, where the “twist factor” is labeled as ω_p . As shown in Ref.[77], through some tedious calculations, we prove that ω_p satisfies the four cocycle condition, where time reversal and/or reflection symmetries are treated as antiunitary.

$$\begin{aligned} \omega_p(g_1, g_2, g_3, g_4) \omega_p(g_1, g_2, g_3 g_4, g_5) \omega_p(g_1 g_2, g_3, g_4, g_5) = \\ {}^{g_1} \omega_p(g_2, g_3, g_4, g_5) \omega_p(g_1, g_2 g_3, g_4, g_5) \omega_p(g_1, g_2, g_3, g_4 g_5) \end{aligned} \quad (4.76)$$

and ω_p are defined up to coboundary.

$$\begin{aligned} \omega_p(g_1, g_2, g_3, g_4) \sim \\ \omega_p(g_1, g_2, g_3, g_4) \frac{\chi_p(g_1, g_2, g_3) \cdot \chi_p(g_1, g_2 g_3, g_4) \cdot {}^{g_1} \chi_p(g_2, g_3, g_4)}{\chi_p(g_1 g_2, g_3, g_4) \cdot \chi_p(g_1, g_2, g_3 g_4)} \end{aligned} \quad (4.77)$$

4.5 Discussion

In summary, by using tensor networks, we develop a general framework to (partially) classify bosonic SPT phases in any dimension, as well as construct generic tensor wavefunctions for each class. We find that for a general symmetry group SG , which include both on site symmetries as well as lattice symmetries, the cohomological bosonic SPT phases can be classified by $H^{d+1}(SG, U(1))$, where $d + 1$ is the space-time dimension. Here, time reversal and reflection symmetries should be treated as antiunitary. An important by-product is a generic relation between SET phases and SPT phases: SPT phases can be obtained from SET phases by condensing anyons carrying integer quantum numbers.

This work leaves several interesting future directions. On the conceptual side, it is known there are bosonic SPT phases beyond group cohomology classification. Famous examples include time reversal[141, 146, 15] (or reflection[126]) SPT phases in 3+1D, which has a $Z_2 \times Z_2$ classification. However, group cohomology only capture a Z_2 class: $H^4(Z_2^T, U(1)) = H^4(Z_2^P, U(1)) = Z_2$. The other Z_2 is beyond our framework. It would be interesting to understand whether our framework can be further generalized to capture this missing index.

It is also interesting to generalize our formulation to construct generic wavefunctions for topological ordered phases as well as SET phases. We first point out that it is straightforward to “(dynamically) gauge” the on-site unitary discrete symmetries on tensor networks[57]. Tensor networks invariant under symmetry g satisfy the tensor equation $\mathbb{T} = W_g g \circ \mathbb{T}$. By gauging symmetry g , the new tensor equation becomes $\mathbb{T} = W_g \circ \mathbb{T}$, where W_g is interpreted as gauge flux. Namely, for topological phases, we require additional global IGG elements, which cannot be decomposed into plaquette IGG elements. By gauging onsite unitary symmetries of SPT phases[87], we are able to write down generic wavefunctions for Dijkgraaf-Witten type[39] of topological ordered phases. Similarly, some SET phases can be obtained by gauging part of the symmetries[98, 70, 30, 64].

As shown in Ref.[11, 158], the SPT phases protected by onsite symmetries can also

be classified by MPO injective PEPS. It would be interesting to see the connection between these two approaches.

As conjectured in Ref.[91], all topological ordered phases in 2+1D with gapped boundaries can be realized by exactly solvable models – string-net models, which have natural PEPS representations[56, 12, 83, 14, 122, 96], and are described by tensor equations involving matrix product operators rather than gauge transformations. Our formulation is incapable to construct string-net models beyond the cohomological classes, such as the double Ising theory. Can we generalize our formulation to capture all string-net models? In addition, it would be interesting to generalize our formulation to fermionic cases using fermionic tensor network[84, 35, 36, 143, 164, 159, 157]. We leave all these questions to future work.

On the practical side, it would be interesting to perform variational numerical simulations based on the symmetric tensor-network wavefunctions proposed here, and to test their performance. In particular, efficient gradient-based variational algorithms on tensor-network wavefunctions have been proposed[135], which are exactly suitable to carry out these simulations.

4.6 SPT phases in 1+1D

In this part, we rederive the classification of 1D SPT[118, 23, 24, 108] using the formulation we set in the main text. In particular, it is clear that time reversal and reflection symmetries act nontrivially on the two cohomology phase.

Consider an infinite MPS state with symmetry SG , then we can express the symmetric condition for a local tensor as4-11

$$\mathbb{T} = W_g g \circ \mathbb{T} \tag{4.78}$$

where \mathbb{T} represents a tensor network before contraction, $g \in SG$ and W_g is the gauge transformation associated with g .

Now, let us identify the IGG element. A single tensor is invariant if we multiply

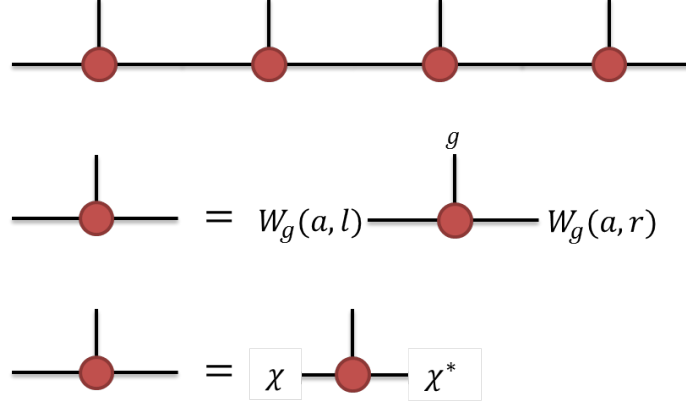


Figure 4-11: Symmetries and IGG in matrix product states.

a phase χ to its left leg and χ^* to its right leg. Therefore, we at least have a $U(1)$ IGG for a generic MPS. In the following, we will focus on the $U(1)$ IGG.

Given the symmetry condition as well as the $U(1)$ IGG, we are able to list the tensor equation as following:

$$W_{g_1 g_1} W_{g_2 g_2} = \omega(g_1, g_2) W_{g_1 g_2} g_1 g_2 \quad (4.79)$$

where $\omega(g_1, g_2)$ is an IGG element, which acts $\omega(g_1, g_2)$ ($\omega^*(g_1, g_2)$) on the left (right) leg. Due to associativity condition, we obtain the two cocycle condition for ω as

$$\omega(g_1, g_2) \omega(g_1 g_2, g_3) = {}^{g_1} \omega(g_2, g_3) \omega(g_1, g_2 g_3) \quad (4.80)$$

where ${}^{g_1} \omega \triangleq g_1 \cdot \omega \cdot g_1^{-1}$. For onsite unitary g_1 , the action is trivial. If g_1 is some anti-unitary operator, such as time reversal symmetry, ${}^{g_1} \omega = \omega^*$. For reflection symmetry σ , it maps the right (left) leg to the left (right) leg, so ${}^{\sigma} \omega = \omega^*$.

Notice, the symmetry operation is defined up to an IGG element. Namely, we have

$$\mathbb{T} = W_g g \circ \mathbb{T} = \epsilon(g) W_g g \circ \mathbb{T} \quad (4.81)$$

So, the equivalence condition for $\omega(g_1, g_2)$ is

$$\omega \sim \omega \cdot \frac{\epsilon(g_1 g_2)}{\epsilon(g_1)^{g_1} \epsilon(g_2)} \quad (4.82)$$

In other words, ω is defined up to a coboundary. In summary, the 1D symmetric phase is classified by $H^2[SG, U(1)]$, where time reversal and reflection symmetries impose complex conjugation on the $U(1)$ phase factor.

4.7 The three cohomology classification from tensor equations in 2+1D

First, we discuss commutation relations between the IGG elements of plaquette p_1 and p_2 for later convenience:

$$v_{p_1 p_2} \equiv (\lambda_{p_1}^1)^{-1} (\lambda_{p_2}^2)^{-1} \lambda_{p_1}^1 \lambda_{p_2}^2 \quad (4.83)$$

$v_{p_1 p_2}$ still belongs to IGG according to the definition. Apparently, for the case where $p_1 \cap p_2 = \emptyset$ or they share only a common site, $\lambda_{p_1}^1$ and $\lambda_{p_2}^2$ commute. When p_1 and p_2 share a common edge v , $v_{p_1 p_2}$ can only have nontrivial action on v . However, there is no such kind of nontrivial IGG, so $\lambda_{p_1}^1$ and $\lambda_{p_2}^2$ still commute. When $p_1 = p_2 \equiv p$, $v_p \equiv v_{p_1 p_2}$ can act nontrivially on legs of p . So v_p belongs to IGG of the plaquette p . To conclude, we have

$$(\lambda_{p_1}^1)^{-1} (\lambda_{p_2}^2)^{-1} \lambda_{p_1}^1 \lambda_{p_2}^2 = \lambda'_{p_1} \delta_{p_1 p_2} \quad (4.84)$$

As shown in the main text, λ 's satisfy the two cocycle relation:

$$\lambda(g_1, g_2) \lambda(g_1 g_2, g_3) = W_{g_1 g_2} \lambda(g_2, g_3) \lambda(g_1, g_2 g_3) \quad (4.85)$$

According to Eq.(4.29) and Eq.(4.84), we can decompose IGG elements as

$$\begin{aligned}\lambda(g_1, g_2)\lambda(g_1g_2, g_3) &= \prod_p \lambda_p(g_1, g_2)\lambda_p(g_1g_2, g_3) \\ W_{g_1g_1}\lambda(g_2, g_3)\lambda(g_1, g_2g_3) &= \prod_p W_{g_1g_1}\lambda_p(g_2, g_3)\lambda_p(g_1, g_2g_3)\end{aligned}\quad (4.86)$$

Further, due to the phase ambiguity in Eq.(4.29), we conclude

$$\begin{aligned}\lambda_p(g_1, g_2)\lambda_p(g_1g_2, g_3) &= \\ \omega_p(g_1, g_2, g_3) W_{g_1g_1}\lambda_p(g_2, g_3)\lambda_p(g_1, g_2g_3)\end{aligned}\quad (4.87)$$

Now, we prove $\omega_p(g, g', g'')$ satisfies the 3-cocycle condition. We implement two ways to calculate the expression $\lambda_p(g_1, g_2)\lambda_p(g_1g_2, g_3)\lambda_p(g_1g_2g_3, g_4)$:

$$\begin{aligned}&\lambda_p(g_1, g_2)\lambda_p(g_1g_2, g_3)\lambda_p(g_1g_2g_3, g_4) \\ &= \omega_p(g_1, g_2, g_3) W_{g_1g_1}\lambda_p(g_2, g_3)\lambda_p(g_1, g_2g_3)\lambda_p(g_1g_2g_3, g_4) \\ &= \omega_p(g_1, g_2, g_3) W_{g_1g_1}\lambda_p(g_2, g_3)\omega_p(g_1, g_2g_3, g_4) \cdot \\ &\quad W_{g_1g_1}\lambda_p(g_2g_3, g_4)\lambda_p(g_1, g_2g_3g_4) \\ &= \omega_p(g_1, g_2, g_3)\omega_p(g_1, g_2g_3, g_4) {}^{g_1}\omega_p(g_2, g_3, g_4) \cdot \\ &\quad W_{g_1g_1}W_{g_2g_2}\lambda_p(g_3, g_4) W_{g_1g_1}\lambda_p(g_2, g_3g_4)\lambda_p(g_1, g_2g_3g_4)\end{aligned}\quad (4.88)$$

where we use Eq.(4.87) to obtain the result. Notice that in the last line, we use the fact that W_g always commutes with ω_p , so $W_g{}^q\omega_p = {}^q\omega_p$. Using another way to

calculate, we get

$$\begin{aligned}
& \lambda_p(g_1, g_2)\lambda_p(g_1g_2, g_3)\lambda_p(g_1g_2g_3, g_4) \\
&= \lambda_p(g_1, g_2)\omega_p(g_1g_2, g_3, g_4)^{W_{g_1g_2g_1g_2}}\lambda_p(g_3, g_4)\lambda_p(g_1g_2, g_3g_4) \\
&= \omega_p(g_1g_2, g_3, g_4)^{\lambda_p(g_1, g_2)W_{g_1g_2g_1g_2}}\lambda_p(g_3, g_4)\lambda_p(g_1, g_2) \cdot \\
& \quad \lambda_p(g_1g_2, g_3g_4) \\
&= \omega_p(g_1g_2, g_3, g_4)\omega_p(g_1, g_2, g_3g_4)^{\lambda_p(g_1, g_2)W_{g_1g_2g_1g_2}}\lambda_p(g_3, g_4) \cdot \\
& \quad W_{g_1g_1}\lambda_p(g_2, g_3g_4)\lambda(g_1, g_2g_3g_4) \\
&= \omega_p(g_1g_2, g_3, g_4)\omega_p(g_1, g_2, g_3g_4)^{W_{g_1g_1}W_{g_2g_2}}\lambda_p(g_3, g_4) \cdot \\
& \quad W_{g_1g_1}\lambda_p(g_2, g_3g_4)\lambda(g_1, g_2g_3g_4)
\end{aligned} \tag{4.89}$$

Comparing the above results, we conclude ω_p satisfies three cocycle equation:

$$\begin{aligned}
& \omega_p(g_1, g_2, g_3)\omega_p(g_1, g_2g_3, g_4)^{g_1}\omega_p(g_2, g_3, g_4) \\
&= \omega_p(g_1g_2, g_3, g_4)\omega_p(g_1, g_2, g_3g_4)
\end{aligned} \tag{4.90}$$

The action of g on ω_p follows a very simple rule: for a leg i , we have $({}^g\omega_p)(i) = \omega_{g^{-1}(p)}^{s(g)}(g^{-1}(i))$, where $s(g)$ is trivial (complex conjugate) for unitary (anti-unitary) symmetry.

According to Eq.(4.29). We note that $\lambda_p(g, g')$ is defined up to a complex number. We can define $\lambda'_p(g, g') = \chi_p(g, g')\lambda_p(g, g')$. Then, we have

$$\begin{aligned}
& \lambda'_p(g_1, g_2)\lambda'_p(g_1g_2, g_3) = \\
& \omega'_p(g_1, g_2, g_3)^{W_{g_1g_1}}\lambda'_p(g_2, g_3)\lambda'_p(g_1, g_2g_3)
\end{aligned} \tag{4.91}$$

Thus, we can always tune ω to be some $U(1)$ phase factor. In the following, we will restrict ourselves for the case where ω 's and χ 's are phase factors. Now, let us

calculate $\omega'_p(g_1, g_2, g_3)$:

$$\begin{aligned}
& \lambda'_p(g_1, g_2)\lambda'_p(g_1g_2, g_3) \\
&= \chi_p(g_1, g_2)\lambda_p(g_1, g_2)\chi_p(g_1g_2, g_3)\lambda_p(g_1g_2, g_3) \\
&= \chi_p(g_1, g_2)\chi_p(g_1g_2, g_3)\omega_p(g_1, g_2, g_3)^{W_{g_1g_1}}\lambda_p(g_2, g_3) \cdot \\
& \quad \lambda_p(g_1, g_2g_3) \\
&= \frac{\chi_p(g_1, g_2)\chi_p(g_1g_2, g_3)}{g_1\chi_p(g_2, g_3)\chi_p(g_1, g_2g_3)}\omega_p(g_1, g_2, g_3)^{W_{g_1g_1}}\lambda'_p(g_2, g_3) \cdot \\
& \quad \lambda'_p(g_1, g_2g_3) \tag{4.92}
\end{aligned}$$

where we use the fact that $W_g\chi_p = \chi_p$ in the last line. Comparing the above two equations, we conclude

$$\omega'_p(g_1, g_2, g_3) = \omega_p(g_1, g_2, g_3) \frac{\chi_p(g_1, g_2)\chi_p(g_1g_2, g_3)}{g_1\chi_p(g_2, g_3)\chi_p(g_1, g_2g_3)} \tag{4.93}$$

It is straightforward to check that ω'_p also satisfies three cocycle condition in Eq.(4.36). In other words, the ω_p is well defined up 3-coboundary constructed by 2-cochain χ . So, ω_p are classified by 3-cohomology $H^3(SG, U(1))$, where the symmetry group SG may have nontrivial action on coefficient $U(1)$.

Notice that the physical wavefunction is invariant under gauge transformation V as well as the IGG transformation $\widetilde{W}_g = \epsilon(g)W_g$, where $\epsilon(g) \in \text{IGG}$. If ω_p classify the PEPS wavefunctions, ω_p should be invariant (up to coboundary) under these two kinds of transformations.

For any gauge transformation V , $W_g \rightarrow VW_ggV^{-1}g^{-1}$. Then it is straightforward to prove that ω_p is invariant.

Now, let us consider IGG transformation. For $\widetilde{W}_g = \epsilon(g)W_g$, we have

$$\widetilde{W}_{g_1g_1}\widetilde{W}_{g_2g_2} = \widetilde{\lambda}(g_1, g_2)\widetilde{W}_{g_1g_2g_1g_2} \tag{4.94}$$

where $\widetilde{\lambda}(g_1, g_2) = \epsilon(g_1)^{W_{g_1g_1}}\epsilon(g_2)\lambda(g_1, g_2)\epsilon^{-1}(g_1g_2)$.

Restrict to one plaquette, we calculate

$$\begin{aligned}
& \tilde{\lambda}_p(g_1, g_2) \tilde{\lambda}_p(g_1 g_2, g_3) \epsilon_p(g_1 g_2 g_3) \\
&= \epsilon_p(g_1) W_{g_1 g_1} \epsilon_p(g_2) \lambda_p(g_1, g_2) W_{g_1 g_2 g_1 g_2} \epsilon_p(g_3) \lambda_p(g_1 g_2, g_3) \\
&= \epsilon_p(g_1) W_{g_1 g_1} \epsilon_p(g_2) W_{g_1 g_1} W_{g_2 g_2} \epsilon_p(g_3) \lambda_p(g_1, g_2) \lambda_p(g_1 g_2, g_3)
\end{aligned} \tag{4.95}$$

where we use Eq.(4.94) several times. In second line, we have used the fact that $\lambda_p \epsilon_p = \lambda_{\epsilon_p}$ as well as Eq.(4.31). On the other hand,

$$\begin{aligned}
& \tilde{W}_{g_1 g_1} \tilde{\lambda}_p(g_2, g_3) \tilde{\lambda}_p(g_1, g_2 g_3) \epsilon_p(g_1 g_2 g_3) \\
&= \epsilon_p(g_1) W_{g_1 g_1} (\epsilon_p(g_2) W_{g_2 g_2} \epsilon_p(g_3) \lambda_p(g_2, g_3) \epsilon_p^{-1}(g_2 g_3)) \epsilon_p(g_1) \cdot \\
& \quad W_{g_1 g_1} \epsilon_p(g_2, g_3) \lambda_p(g_1, g_2 g_3) \\
&= \epsilon_p(g_1) W_{g_1 g_1} \epsilon_p(g_2) W_{g_1 g_1} W_{g_2 g_2} \epsilon_p(g_3) W_{g_1 g_1} \lambda_p(g_2, g_3) \lambda_p(g_1, g_2 g_3)
\end{aligned} \tag{4.96}$$

According to Eq.(4.35), we conclude that

$$\begin{aligned}
& \tilde{\lambda}_p(g_1, g_2) \tilde{\lambda}_p(g_1 g_2, g_3) = \\
& \omega_p(g_1, g_2, g_3) \tilde{W}_{g_1 g_1} \tilde{\lambda}_p(g_2, g_3) \tilde{\lambda}_p(g_1, g_2 g_3)
\end{aligned} \tag{4.97}$$

So, one obtains the same 3-cocycle for ϵ_p transformation.

We now make a general remark: our tensor construction for SPT phases in 2+1D is related to *crossed module extension* known in the mathematical literature.

Let us first review the SPT phases in 1+1D with symmetry group SG , which are classified by different projective representations of SG , or equivalently, by different central extensions of SG :

$$1 \rightarrow U(1) \rightarrow E \rightarrow SG \rightarrow 1 \tag{4.98}$$

In the tensor network construction, the center $U(1)$ is mapped to the $U(1)$ phase IGG, and symmetry actions on all legs of the tensor network $W_g g$ together with the $U(1)$ IGG form the extended group E . So, the construction of 1+1D SPT phases by MPS can be viewed as a realization of the central extension.

A crossed module extension is an exact sequence:

$$1 \rightarrow U(1) \rightarrow N \xrightarrow{\varphi} E \rightarrow SG \rightarrow 1 \quad (4.99)$$

with a left action of E on N , represented by $n \mapsto {}^e n$, such that $\varphi({}^e n) = e \varphi(n) e^{-1}$, for all $n, n' \in N$ and $e \in E$. It is well known[65, 67, 131, 10, 43] that the crossed module extensions of SG by $U(1)$ are classified by $H^3(SG, U(1))$, which is the same object classifies the 2+1D SPT phases protected by SG . As in the 1+1D case, our construction can be viewed as a realization of a crossed module extension by tensor networks. Namely, given a crossed module extension characterized by a three cohomology $[\omega]$, we can write down tensor equations realize this crossed module extension and construct generic tensor wavefunctions for the SPT phase characterized by $[\omega]$. This fact also indicates that our tensor constructions are able to capture all cohomological bosonic SPT phases in 2+1D.

Now, let us describe the procedure to obtain tensor equations from a crossed module extension. Given a crossed module extension in Eq.(4.99), one can decompose it to two short exact sequences as following:

$$\begin{aligned} 1 \rightarrow U(1) \rightarrow N \xrightarrow{\phi} M \rightarrow 1 \\ 1 \rightarrow M \xrightarrow{i} E \rightarrow SG \rightarrow 1 \end{aligned} \quad (4.100)$$

where M is identified as $\phi(N)$, and $i : M \hookrightarrow E$ is an inclusion map. Apparently $\varphi = i \circ \phi$.

We can write down tensor equations to realize these two short exact sequence. As shown in Eq.(4.31), symmetry actions on all legs of tensor networks $\{W_g g | \forall g \in SG\}$ form a projective representation with coefficient in group $\{\lambda\}$, which we identify as

M . In the anyon condensation context, M is the gauge group characterizing the topological order before condensation. M together with $\{W_g g | \forall g\}$ form the extended group E , which captures the SET physics before anyon condensation. According to the assumption, $\forall \lambda \in M$ can be decomposed to plaquette IGG elements: $\lambda = \prod_p \lambda_p$. An element $n \in N$ is identified as a set of plaquette IGG elements: $n = \{\lambda_p | \forall p\}$, which satisfies $\prod_p \lambda_p = \lambda$. Then, $N = \left\{ \{\lambda_p | \forall p\} \mid \prod_p \lambda_p = \lambda \in M \right\}$. And mapping ϕ is defined as

$$\begin{aligned} \phi : N &\mapsto M, \\ \phi(n) &= \prod_p \lambda_p \end{aligned} \tag{4.101}$$

It is easy to see that the kernel of ϕ forms a $U(1)$ group: $\left\{ \{\chi_p | \forall p\} \mid \prod_p \chi_p = I \right\} \cong U(1)$.

Now, let us consider the action of E on N . Set $n = \{\lambda_p | \forall p\}$, $n' = \{\lambda'_p | \forall p\}$ and $e = \lambda^{(e)} W_g g \in E$, we define the action as

$$\begin{aligned} \varphi^{(n)} n' &\triangleq \{\lambda \lambda'_p | \forall p\} = \{\lambda_p \cdot \lambda'_p \cdot \lambda_p^{-1} | \forall p\} = n \cdot n' \cdot n^{-1} \\ \varphi(\lambda^{(e)} n) &= \prod_p \lambda^{(e) W_g g} \lambda_p = \lambda^{(e) W_g g} \lambda = e \cdot \varphi(n) \cdot e^{-1} \end{aligned} \tag{4.102}$$

which indeed satisfies the crossed module condition. In summary, from a crossed module extension, we are able to construct tensor equations for SPT phases and vice versa.

Bibliography

- [1] Ian Affleck, Tom Kennedy, Elliott H. Lieb, and Hal Tasaki. Rigorous results on valence-bond ground states in antiferromagnets. *Phys. Rev. Lett.*, 59:799–802, Aug 1987.
- [2] John C Baez, Derek K Wise, Alissa S Crans, et al. Exotic statistics for strings in 4d bf theory. *Advances in Theoretical and Mathematical Physics*, 11(5):707–749, 2007.
- [3] F Alexander Bais, Peter van Driel, and Mark de Wild Propitius. Anyons in discrete gauge theories with chern-simons terms. *Nuclear Physics B*, 393:547, 1993.
- [4] FA Bais and JC Romers. The modular s-matrix as order parameter for topological phase transitions. *New Journal of Physics*, 14(3):035024, 2012.
- [5] L. Balents, M. P. A. Fisher, and S. M. Girvin. Fractionalization in an easy-axis kagome antiferromagnet. *Phys. Rev. B*, 65:224412, May 2002.
- [6] Maissam Barkeshli, Parsa Bonderson, Meng Cheng, and Zhenghan Wang. Symmetry, defects, and gauging of topological phases. *arXiv preprint arXiv:1410.4540*, 2014.
- [7] Thomas Barthel, Carlos Pineda, and Jens Eisert. Contraction of fermionic operator circuits and the simulation of strongly correlated fermions. *Phys. Rev. A*, 80:042333, Oct 2009.
- [8] B Bauer, P Corboz, R Orús, and M Troyer. Implementing global abelian symmetries in projected entangled-pair state algorithms. *Physical Review B*, 83(12):125106, 2011.
- [9] B. Andrei Bernevig, Taylor L. Hughes, and Shou-Cheng Zhang. Quantum spin hall effect and topological phase transition in hgte quantum wells. *Science*, 314(5806):1757–1761, 2006.
- [10] Kenneth S Brown. *Cohomology of groups*, volume 87. Springer Science & Business Media, 2012.
- [11] Oliver Buerschaper. Twisted injectivity in projected entangled pair states and the classification of quantum phases. *Annals of Physics*, 351:447–476, 2014.

- [12] Oliver Buerschaper, Miguel Aguado, and Guifré Vidal. Explicit tensor network representation for the ground states of string-net models. *Phys. Rev. B*, 79:085119, Feb 2009.
- [13] Oliver Buerschaper, Siddhardh C. Morampudi, and Frank Pollmann. Double semion phase in an exactly solvable quantum dimer model on the kagome lattice. *Phys. Rev. B*, 90:195148, Nov 2014.
- [14] Mehmet Burak Sahinoglu, Dominic Williamson, Nick Bultinck, Michael Mariën, Jutho Haegeman, Norbert Schuch, and Frank Verstraete. Characterizing topological order with matrix product operators. *arXiv preprint arXiv:1409.2150*, 2014.
- [15] F. J. Burnell, Xie Chen, Lukasz Fidkowski, and Ashvin Vishwanath. Exactly soluble model of a three-dimensional symmetry-protected topological phase of bosons with surface topological order. *Phys. Rev. B*, 90:245122, Dec 2014.
- [16] J. Scott Carter, Daniel Jelsovsky, Seiichi Kamada, and Masahico Saito. Quandle homology groups, their betti numbers, and virtual knots. *J. Pure Appl. Algebra*, 157(2-3):135–155, 2001.
- [17] Scott Carter, Seiichi Kamada, and Masahico Saito. *Surfaces in 4-space*. Springer-Verlag, 2004.
- [18] Xie Chen, F. J. Burnell, Ashvin Vishwanath, and Lukasz Fidkowski. Anomalous symmetry fractionalization and surface topological order. *Phys. Rev. X*, 5:041013, Oct 2015.
- [19] Xie Chen, Fiona J Burnell, Ashvin Vishwanath, and Lukasz Fidkowski. Anomalous symmetry fractionalization and surface topological order. *arXiv*, cond-mat.str-el, Mar 2014.
- [20] Xie Chen, Zheng-Cheng Gu, Zheng-Xin Liu, and Xiao-Gang Wen. Symmetry-protected topological orders in interacting bosonic systems. *Science*, 338(6114):1604–1606, 2012.
- [21] Xie Chen, Zheng-Cheng Gu, Zheng-Xin Liu, and Xiao-Gang Wen. Symmetry protected topological orders and the group cohomology of their symmetry group. *Physical Review B*, 87:155114, Apr 2013.
- [22] Xie Chen, Zheng-Cheng Gu, Zheng-Xin Liu, and Xiao-Gang Wen. Symmetry protected topological orders and the group cohomology of their symmetry group. *Phys. Rev. B*, 87:155114, Apr 2013.
- [23] Xie Chen, Zheng-Cheng Gu, and Xiao-Gang Wen. Classification of gapped symmetric phases in one-dimensional spin systems. *Phys. Rev. B*, 83:035107, Jan 2011.

- [24] Xie Chen, Zheng-Cheng Gu, and Xiao-Gang Wen. Complete classification of one-dimensional gapped quantum phases in interacting spin systems. *Phys. Rev. B*, 84:235128, Dec 2011.
- [25] Xie Chen, Zheng-Xin Liu, and Xiao-Gang Wen. Two-dimensional symmetry-protected topological orders and their protected gapless edge excitations. *Phys. Rev. B*, 84:235141, Dec 2011.
- [26] Xie Chen, Yuan-Ming Lu, and Ashvin Vishwanath. Symmetry protected topological phases from decorated domain walls. *Nature Communications*, 5:3507, Mar 2014.
- [27] Xie Chen and Ashvin Vishwanath. 'gauging' time reversal symmetry in tensor network states. *arXiv*, cond-mat.str-el, Jan 2014.
- [28] Xie Chen and Ashvin Vishwanath. Towards gauging time-reversal symmetry: A tensor network approach. *Phys. Rev. X*, 5:041034, Nov 2015.
- [29] Xie Chen, Bei Zeng, Zheng-Cheng Gu, Isaac L. Chuang, and Xiao-Gang Wen. Tensor product representation of a topological ordered phase: Necessary symmetry conditions. *Phys. Rev. B*, 82:165119, Oct 2010.
- [30] Meng Cheng, Zheng-Cheng Gu, Shenghan Jiang, and Yang Qi. Exactly solvable models for symmetry-enriched topological phases. *arXiv preprint arXiv:1606.08482*, 2016.
- [31] Meng Cheng, Michael Zaletel, Maissam Barkeshli, Ashvin Vishwanath, and Parsa Bonderson. Translational symmetry and microscopic constraints on symmetry-enriched topological phases: a view from the surface. *arXiv preprint arXiv:1511.02263*, 2015.
- [32] Ching-Kai Chiu, Jeffrey C. Y. Teo, Andreas P. Schnyder, and Shinsei Ryu. Classification of topological quantum matter with symmetries. *Rev. Mod. Phys.*, 88:035005, Aug 2016.
- [33] Ching-Kai Chiu, Hong Yao, and Shinsei Ryu. Classification of topological insulators and superconductors in the presence of reflection symmetry. *Phys. Rev. B*, 88:075142, Aug 2013.
- [34] Gil Young Cho, Chang-Tse Hsieh, Takahiro Morimoto, and Shinsei Ryu. Topological phases protected by reflection symmetry and cross-cap states. *Phys. Rev. B*, 91:195142, May 2015.
- [35] Philippe Corboz, Román Orús, Bela Bauer, and Guifré Vidal. Simulation of strongly correlated fermions in two spatial dimensions with fermionic projected entangled-pair states. *Phys. Rev. B*, 81:165104, Apr 2010.
- [36] Philippe Corboz and Guifré Vidal. Fermionic multiscale entanglement renormalization ansatz. *Phys. Rev. B*, 80:165129, Oct 2009.

- [37] Mark de Wild Propitius. Topological interactions in broken gauge theories. *arXiv*, hep-th, Nov 1995.
- [38] Stefan Depenbrock, Ian P. McCulloch, and Ulrich Schollwöck. Nature of the spin-liquid ground state of the $s = 1/2$ heisenberg model on the kagome lattice. *Phys. Rev. Lett.*, 109:067201, Aug 2012.
- [39] Robbert Dijkgraaf and Edward Witten. Topological gauge theories and group cohomology. *Comm. Math. Phys.*, 129(2):393–429, 1990.
- [40] J Dubail and N Read. Tensor network trial states for chiral topological phases in two dimensions. *arXiv preprint arXiv:1307.7726*, 2013.
- [41] A. Einstein, B. Podolsky, and N. Rosen. Can quantum-mechanical description of physical reality be considered complete? *Phys. Rev.*, 47:777–780, May 1935.
- [42] Jens Eisert, Marcus Cramer, and Martin B Plenio. Colloquium: Area laws for the entanglement entropy. *Reviews of Modern Physics*, 82(1):277, 2010.
- [43] Dominic V. Else and Chetan Nayak. Classifying symmetry-protected topological phases through the anomalous action of the symmetry on the edge. *Phys. Rev. B*, 90:235137, Dec 2014.
- [44] Andrew M. Essin and Michael Hermele. Classifying fractionalization: Symmetry classification of gapped F_2 spin liquids in two dimensions. *Phys. Rev. B*, 87:104406, Mar 2013.
- [45] Mark Fannes, Bruno Nachtergaele, and Reinhard F Werner. Finitely correlated states on quantum spin chains. *Communications in mathematical physics*, 144(3):443–490, 1992.
- [46] Zili Feng, Zheng Li, Xin Meng, Wei Yi, Yuan Wei, Jun Zhang, Yan-Cheng Wang, Wei Jiang, Zheng Liu, Shiyan Li, et al. Gapped spin-1/2 spinon excitations in a new kagome quantum spin liquid compound $\text{Cu}_3\text{Zn}(\text{OH})_6\text{FBr}$. *arXiv preprint arXiv:1702.01658*, 2017.
- [47] Lukasz Fidkowski. Entanglement spectrum of topological insulators and superconductors. *Phys. Rev. Lett.*, 104:130502, Apr 2010.
- [48] Lukasz Fidkowski and Alexei Kitaev. Topological phases of fermions in one dimension. *Phys. Rev. B*, 83:075103, Feb 2011.
- [49] Eduardo Fradkin and Stephen H. Shenker. Phase diagrams of lattice gauge theories with higgs fields. *Phys. Rev. D*, 19:3682–3697, Jun 1979.
- [50] Liang Fu. Topological crystalline insulators. *Phys. Rev. Lett.*, 106:106802, Mar 2011.
- [51] Liang Fu, C. L. Kane, and E. J. Mele. Topological insulators in three dimensions. *Phys. Rev. Lett.*, 98:106803, Mar 2007.

- [52] Yohei Fuji, Frank Pollmann, and Masaki Oshikawa. Distinct trivial phases protected by a point-group symmetry in quantum spin chains. *arXiv preprint arXiv:1409.8616*, 2014.
- [53] Artur Garcia-Saez, Valentin Murg, and Tzu-Chieh Wei. Spectral gaps of affleck-kennedy-lieb-tasaki hamiltonians using tensor network methods. *Phys. Rev. B*, 88:245118, Dec 2013.
- [54] Scott D. Geraedts and Olexei I. Motrunich. Exact realization of integer and fractional quantum hall phases in models in. *Annals of Physics*, 334:288 – 315, 2013.
- [55] Yuxiang Gu, Ling-Yan Hung, and Yidun Wan. A unified framework of topological phases with symmetry. *arXiv*, cond-mat.str-el, Feb 2014.
- [56] Zheng-Cheng Gu, Michael Levin, Brian Swingle, and Xiao-Gang Wen. Tensor-product representations for string-net condensed states. *Phys. Rev. B*, 79:085118, Feb 2009.
- [57] Jutho Haegeman, Karel Van Acoleyen, Norbert Schuch, J. Ignacio Cirac, and Frank Verstraete. Gauging quantum states: From global to local symmetries in many-body systems. *Phys. Rev. X*, 5:011024, Feb 2015.
- [58] Tian-Heng Han, Joel S Helton, Shaoyan Chu, Daniel G Nocera, Jose A Rodriguez-Rivera, Collin Broholm, and Young S Lee. Fractionalized excitations in the spin-liquid state of a kagome-lattice antiferromagnet. *Nature*, 492(7429):406–410, 2012.
- [59] M. Z. Hasan and C. L. Kane. *Colloquium* : Topological insulators. *Rev. Mod. Phys.*, 82:3045–3067, Nov 2010.
- [60] M. B. Hastings. Lieb-schultz-mattis in higher dimensions. *Phys. Rev. B*, 69:104431, Mar 2004.
- [61] M. B. Hastings. Sufficient conditions for topological order in insulators. *EPL (Europhysics Letters)*, 70(6):824, 2005.
- [62] M. B. Hastings. Notes on Some Questions in Mathematical Physics and Quantum Information. *ArXiv e-prints*, April 2014.
- [63] Huan He, Heidar Moradi, and Xiao-Gang Wen. Modular matrices as topological order parameter by a gauge-symmetry-preserved tensor renormalization approach. *Phys. Rev. B*, 90:205114, Nov 2014.
- [64] Chris Heinrich, Fiona Burnell, Lukasz Fidkowski, and Michael Levin. Symmetry enriched string-nets: Exactly solvable models for set phases. *arXiv preprint arXiv:1606.07816*, 2016.

- [65] Derek F Holt. An interpretation of the cohomology groups $h^n(g, m)$. *Journal of Algebra*, 60(2):307–318, 1979.
- [66] Yuting Hu, Yidun Wan, and Yong-Shi Wu. Twisted quantum double model of topological phases in two-dimension. *arXiv*, cond-mat.str-el, Nov 2012.
- [67] Johannes Huebschmann. Crossed n -fold extensions of groups and cohomology. *Commentarii Mathematici Helvetici*, 55(1):302–313, 1980.
- [68] Ling-Yan Hung and Yidun Wan. String-net models with zn fusion algebra. *Physical Review B*, 86:235132, Dec 2012.
- [69] Ling-Yan Hung and Yidun Wan. k matrix construction of symmetry-enriched phases of matter. *Phys. Rev. B*, 87:195103, May 2013.
- [70] Ling-Yan Hung and Xiao-Gang Wen. Quantized topological terms in weak-coupling gauge theories with a global symmetry and their connection to symmetry-enriched topological phases. *Phys. Rev. B*, 87:165107, Apr 2013.
- [71] Mohsin Iqbal, Didier Poilblanc, and Norbert Schuch. Semionic resonating valence-bond states. *Phys. Rev. B*, 90:115129, Sep 2014.
- [72] Chao-Ming Jian and Xiao-Liang Qi. Layer construction of 3d topological states and string braiding statistics. *Phys. Rev. X*, 4:041043, Dec 2014.
- [73] Hong-Chen Jiang, Zhenghan Wang, and Leon Balents. Identifying topological order by entanglement entropy. *Nature Physics*, 8(12):902–905, 2012.
- [74] Shenghan Jiang, Andrej Mesaros, and Ying Ran. Chiral spin-density wave, spin-charge-charge liquid, and $d + id$ superconductivity in 1/4-doped correlated electronic systems on the honeycomb lattice. *Phys. Rev. X*, 4:031040, Sep 2014.
- [75] Shenghan Jiang, Andrej Mesaros, and Ying Ran. Generalized modular transformations in $(3 + 1)$ D topologically ordered phases and triple linking invariant of loop braiding. *Phys. Rev. X*, 4:031048, Sep 2014.
- [76] Shenghan Jiang and Ying Ran. Symmetric tensor networks and practical simulation algorithms to sharply identify classes of quantum phases distinguishable by short-range physics. *Phys. Rev. B*, 92:104414, Sep 2015.
- [77] Shenghan Jiang and Ying Ran. Anyon condensation and a generic tensor-network construction for symmetry-protected topological phases. *Phys. Rev. B*, 95:125107, Mar 2017.
- [78] C. L. Kane and E. J. Mele. Quantum spin hall effect in graphene. *Phys. Rev. Lett.*, 95:226801, Nov 2005.
- [79] Panjin Kim, Hyunyong Lee, Shenghan Jiang, Brayden Ware, Chao-Ming Jian, Michael Zaletel, Jung Hoon Han, and Ying Ran. Featureless quantum insulator on the honeycomb lattice. *Phys. Rev. B*, 94:064432, Aug 2016.

- [80] Itamar Kimchi, SA Parameswaran, Ari M Turner, Fa Wang, and Ashvin Vishwanath. Featureless and nonfractionalized mott insulators on the honeycomb lattice at 1/2 site filling. *Proceedings of the National Academy of Sciences*, 110(41):16378–16383, 2013.
- [81] A Yu Kitaev. Fault-tolerant quantum computation by anyons. *Annals of Physics*, 303(1):2–30, 2003.
- [82] Alexei Kitaev. Anyons in an exactly solved model and beyond. *Annals of Physics*, 321(1):2–111, 2006.
- [83] Robert König, Ben W. Reichardt, and Guifré Vidal. Exact entanglement renormalization for string-net models. *Phys. Rev. B*, 79:195123, May 2009.
- [84] Christina V. Kraus, Norbert Schuch, Frank Verstraete, and J. Ignacio Cirac. Fermionic projected entangled pair states. *Phys. Rev. A*, 81:052338, May 2010.
- [85] R. B. Laughlin. Anomalous quantum hall effect: An incompressible quantum fluid with fractionally charged excitations. *Phys. Rev. Lett.*, 50:1395–1398, May 1983.
- [86] Michael Levin and Zheng-Cheng Gu. Braiding statistics approach to symmetry-protected topological phases. *Physical Review B*, 86:115109, Sep 2012. 16 pages, 12 figuresb.
- [87] Michael Levin and Zheng-Cheng Gu. Braiding statistics approach to symmetry-protected topological phases. *Phys. Rev. B*, 86:115109, Sep 2012.
- [88] Michael A. Levin and Xiao-Gang Wen. String-net condensation: a physical mechanism for topological phases. *Phys. Rev. B*, 71:045110, Jan 2005.
- [89] Elliott Lieb, Theodore Schultz, and Daniel Mattis. Two soluble models of an antiferromagnetic chain. *Annals of Physics*, 16(3):407–466, 1961.
- [90] Elliott Lieb, Theodore Schultz, and Daniel Mattis. Two soluble models of an antiferromagnetic chain. *Annals of Physics*, 16(3):407 – 466, 1961.
- [91] Chien-Hung Lin and Michael Levin. Generalizations and limitations of string-net models. *Phys. Rev. B*, 89:195130, May 2014.
- [92] Yuan-Ming Lu, Gil Young Cho, and Ashvin Vishwanath. Unification of bosonic and fermionic theories of spin liquids on the kagome lattice. *arXiv preprint arXiv:1403.0575*, 2014.
- [93] Yuan-Ming Lu, Ying Ran, and Patrick A. Lee. F_2 spin liquids in the $s = \frac{1}{2}$ heisenberg model on the kagome lattice: A projective symmetry-group study of schwinger fermion mean-field states. *Phys. Rev. B*, 83:224413, Jun 2011.

- [94] Yuan-Ming Lu and Ashvin Vishwanath. Theory and classification of interacting integer topological phases in two dimensions: A chern-simons approach. *Phys. Rev. B*, 86:125119, Sep 2012.
- [95] Yuan-Ming Lu and Ashvin Vishwanath. Classification and properties of symmetry-enriched topological phases: Chern-simons approach with applications to Z_2 spin liquids. *Phys. Rev. B*, 93:155121, Apr 2016.
- [96] Zhu-Xi Luo, Ethan Lake, and Yong-Shi Wu. The structure of fixed-point tensor network states characterizes pattern of long-range entanglement. *arXiv preprint arXiv:1611.01140*, 2016.
- [97] Andrej Mesaros and Ying Ran. Classification of symmetry enriched topological phases with exactly solvable models. *Physical Review B*, 87:155115, 2013.
- [98] Andrej Mesaros and Ying Ran. Classification of symmetry enriched topological phases with exactly solvable models. *Phys. Rev. B*, 87:155115, Apr 2013.
- [99] R. Moessner and S. L. Sondhi. Resonating valence bond phase in the triangular lattice quantum dimer model. *Phys. Rev. Lett.*, 86:1881–1884, Feb 2001.
- [100] J. E. Moore and L. Balents. Topological invariants of time-reversal-invariant band structures. *Phys. Rev. B*, 75:121306, Mar 2007.
- [101] Heidar Moradi and Xiao-Gang Wen. Universal wave function overlap and universal topological data from generic gapped ground states. *arXiv*, cond-mat.str-el, Jan 2014.
- [102] Antti Niemi. Exotic statistics of leapfrogging vortex rings. *Physical Review Letters*, 94(12):124502, Apr 2005.
- [103] Masaki Oshikawa. Commensurability, excitation gap, and topology in quantum many-particle systems on a periodic lattice. *Phys. Rev. Lett.*, 84:1535–1538, Feb 2000.
- [104] David Pérez-García, Mikel Sanz, CE Gonzalez-Guillen, Michael Marc Wolf, and J Ignacio Cirac. Characterizing symmetries in a projected entangled pair state. *New Journal of Physics*, 12(2):025010, 2010.
- [105] David Perez-Garcia, Frank Verstraete, Michael M Wolf, and J Ignacio Cirac. Matrix product state representations. *arXiv preprint quant-ph/0608197*, 2006.
- [106] Iztok Pizorn and Frank Verstraete. Fermionic implementation of projected entangled pair states algorithm. *Phys. Rev. B*, 81:245110, Jun 2010.
- [107] Didier Poilblanc, Norbert Schuch, David Pérez-García, and J. Ignacio Cirac. Topological and entanglement properties of resonating valence bond wave functions. *Phys. Rev. B*, 86:014404, Jul 2012.

- [108] Frank Pollmann, Erez Berg, Ari M. Turner, and Masaki Oshikawa. Symmetry protection of topological phases in one-dimensional quantum spin systems. *Phys. Rev. B*, 85:075125, Feb 2012.
- [109] Frank Pollmann, Ari M. Turner, Erez Berg, and Masaki Oshikawa. Entanglement spectrum of a topological phase in one dimension. *Phys. Rev. B*, 81:064439, Feb 2010.
- [110] Xiao-Liang Qi and Shou-Cheng Zhang. Topological insulators and superconductors. *Rev. Mod. Phys.*, 83:1057–1110, Oct 2011.
- [111] Y. Qi, Z.-C. Gu, and H. Yao. Double-Semion Topological Order from Exactly Solvable Quantum Dimer Models. *ArXiv e-prints*, June 2014.
- [112] Yang Qi and Meng Cheng. Classification of symmetry fractionalization in gapped z_2 spin liquids. *arXiv preprint arXiv:1606.04544*, 2016.
- [113] N. Read and Subir Sachdev. Valence-bond and spin-peierls ground states of low-dimensional quantum antiferromagnets. *Phys. Rev. Lett.*, 62:1694–1697, Apr 1989.
- [114] Rahul Roy. Topological phases and the quantum spin hall effect in three dimensions. *Phys. Rev. B*, 79:195322, May 2009.
- [115] Subir Sachdev. Kagome- and triangular-lattice heisenberg antiferromagnets: Ordering from quantum fluctuations and quantum-disordered ground states with unconfined bosonic spinons. *Phys. Rev. B*, 45:12377–12396, Jun 1992.
- [116] Anders W. Sandvik. Evidence for deconfined quantum criticality in a two-dimensional heisenberg model with four-spin interactions. *Phys. Rev. Lett.*, 98:227202, Jun 2007.
- [117] Norbert Schuch, Ignacio Cirac, and David Pérez-García. Peps as ground states: Degeneracy and topology. *Annals of Physics*, 325(10):2153–2192, 2010.
- [118] Norbert Schuch, David Pérez-García, and Ignacio Cirac. Classifying quantum phases using matrix product states and projected entangled pair states. *Phys. Rev. B*, 84:165139, Oct 2011.
- [119] Norbert Schuch, Didier Poilblanc, J Ignacio Cirac, and David Perez-Garcia. Resonating valence bond states in the peps formalism. *Physical Review B*, 86(11):115108, 2012.
- [120] T. Senthil and Michael Levin. Integer quantum hall effect for bosons. *Phys. Rev. Lett.*, 110:046801, Jan 2013.
- [121] T. Senthil, Ashvin Vishwanath, Leon Balents, Subir Sachdev, and Matthew P. A. Fisher. Deconfined quantum critical points. *Science*, 303(5663):1490–1494, 2004.

- [122] Sujeet K Shukla, M Burak Şahinoğlu, Frank Pollmann, and Xie Chen. Boson condensation and instability in the tensor network representation of string-net states. *arXiv preprint arXiv:1610.00608*, 2016.
- [123] Sukhwinder Singh, Robert N. C. Pfeifer, and Guifré Vidal. Tensor network decompositions in the presence of a global symmetry. *Phys. Rev. A*, 82:050301, Nov 2010.
- [124] Sukhwinder Singh, Robert NC Pfeifer, and Guifre Vidal. Tensor network states and algorithms in the presence of a global u (1) symmetry. *Physical Review B*, 83(11):115125, 2011.
- [125] Sukhwinder Singh and Guifre Vidal. Tensor network states and algorithms in the presence of a global su (2) symmetry. *Physical Review B*, 86(19):195114, 2012.
- [126] Hao Song, Sheng-Jie Huang, Liang Fu, and Michael Hermele. Topological phases protected by point group symmetry. *arXiv preprint arXiv:1604.08151*, 2016.
- [127] Brian Swingle and Xiao-Gang Wen. Topological properties of tensor network states from their local gauge and local symmetry structures. *arXiv preprint arXiv:1001.4517*, 2010.
- [128] Nicolas Tarantino, Netanel H Lindner, and Lukasz Fidkowski. Symmetry fractionalization and twist defects. *New Journal of Physics*, 18(3):035006, 2016.
- [129] Tiamhock Tay and Olexei I. Motrunich. Variational study of J_1 - J_2 heisenberg model on kagome lattice using projected schwinger-boson wave functions. *Phys. Rev. B*, 84:020404, Jul 2011.
- [130] Jeffrey C Y Teo. Globally symmetric topological phase: from anyonic symmetry to twist defect. *Journal of Physics: Condensed Matter*, 28(14):143001, 2016.
- [131] Sebastian Thomas. The third cohomology group classifies crossed module extensions. *arXiv preprint arXiv:0911.2861*, 2009.
- [132] Stanton M Trott. A pair of generators for the unimodular group. *Canad. Math. Bull.*, 5:245–252, 1962.
- [133] D. C. Tsui, H. L. Stormer, and A. C. Gossard. Two-dimensional magneto-transport in the extreme quantum limit. *Phys. Rev. Lett.*, 48:1559–1562, May 1982.
- [134] Ari M. Turner, Yi Zhang, Roger S. K. Mong, and Ashvin Vishwanath. Quantized response and topology of magnetic insulators with inversion symmetry. *Phys. Rev. B*, 85:165120, Apr 2012.
- [135] Laurens Vanderstraeten, Jutho Haegeman, Philippe Corboz, and Frank Verstraete. Gradient methods for variational optimization of projected entangled-pair states. *Phys. Rev. B*, 94:155123, Oct 2016.

- [136] Laurens Vanderstraeten, Michaël Mariën, Frank Verstraete, and Jutho Haegeman. Excitations and the tangent space of projected entangled-pair states. *Phys. Rev. B*, 92:201111, Nov 2015.
- [137] Frank Verstraete and J Ignacio Cirac. Renormalization algorithms for quantum-many body systems in two and higher dimensions. *arXiv preprint cond-mat/0407066*, 2004.
- [138] Frank Verstraete, Valentin Murg, and J Ignacio Cirac. Matrix product states, projected entangled pair states, and variational renormalization group methods for quantum spin systems. *Advances in Physics*, 57(2):143–224, 2008.
- [139] G. Vidal. Entanglement renormalization. *Phys. Rev. Lett.*, 99:220405, Nov 2007.
- [140] Guifré Vidal. Efficient classical simulation of slightly entangled quantum computations. *Physical Review Letters*, 91(14):147902, 2003.
- [141] Ashvin Vishwanath and T. Senthil. Physics of three-dimensional bosonic topological insulators: Surface-deconfined criticality and quantized magnetoelectric effect. *Phys. Rev. X*, 3:011016, Feb 2013.
- [142] TB Wahl, H-H Tu, N Schuch, and JI Cirac. Projected entangled-pair states can describe chiral topological states. *Physical review letters*, 111(23):236805, 2013.
- [143] Thorsten B. Wahl, Stefan T. Haßler, Hong-Hao Tu, J. Ignacio Cirac, and Norbert Schuch. Symmetries and boundary theories for chiral projected entangled pair states. *Phys. Rev. B*, 90:115133, Sep 2014.
- [144] Yidun Wan, Juven C. Wang, and Huan He. Twisted gauge theory model of topological phases in three dimensions. *Phys. Rev. B*, 92:045101, Jul 2015.
- [145] Chenjie Wang and Michael Levin. Braiding statistics of loop excitations in three dimensions. *arXiv*, cond-mat.str-el, Mar 2014.
- [146] Chong Wang and T. Senthil. Boson topological insulators: A window into highly entangled quantum phases. *Phys. Rev. B*, 87:235122, Jun 2013.
- [147] Fa Wang and Ashvin Vishwanath. Spin-liquid states on the triangular and kagomé lattices: A projective-symmetry-group analysis of schwinger boson states. *Phys. Rev. B*, 74:174423, Nov 2006.
- [148] Juven C. Wang and Xiao-Gang Wen. Non-abelian string and particle braiding in topological order: Modular $SL(3, \mathbb{Z})$ representation and $(3 + 1)$ -dimensional twisted gauge theory. *Phys. Rev. B*, 91:035134, Jan 2015.
- [149] Andreas Weichselbaum. Non-abelian symmetries in tensor networks: A quantum symmetry space approach. *Annals of Physics*, 327(12):2972–3047, 2012.

- [150] X. G. Wen. Topological orders in rigid states. *Int J Mod Phys B*, 4:239, Jan 1990.
- [151] X. G. Wen and A. Zee. Classification of abelian quantum hall states and matrix formulation of topological fluids. *Phys. Rev. B*, 46:2290–2301, Jul 1992.
- [152] Xiao-Gang Wen. Topological orders and edge excitations in fractional quantum hall states. *Advances in Physics*, 44:405, Sep 1995.
- [153] Xiao-Gang Wen. Quantum orders and symmetric spin liquids. *Phys. Rev. B*, 65:165113, Apr 2002.
- [154] Xiao-Gang Wen and Q Niu. Ground-state degeneracy of the fractional quantum hall states in the presence of a random potential and on high-genus riemann surfaces. *Physical Review B (Condensed Matter)*, 41:9377, May 1990.
- [155] Xiao-Gang Wen and A Zee. Classification of abelian quantum hall states and matrix formulation of topological fluids. *Physical Review B (Condensed Matter)*, 46:2290, Jul 1992.
- [156] Steven R. White. Density matrix formulation for quantum renormalization groups. *Phys. Rev. Lett.*, 69:2863–2866, Nov 1992.
- [157] C Wille, O Buerschaper, and J Eisert. Fermionic topological quantum states as tensor networks. *arXiv preprint arXiv:1609.02574*, 2016.
- [158] D. J. Williamson, N. Bultinck, M. Mariën, M. B. Sahinoglu, J. Haegeman, and F. Verstraete. Matrix product operators for symmetry-protected topological phases. *ArXiv e-prints*, December 2014.
- [159] Dominic J Williamson, Nick Bultinck, Jutho Haegeman, and Frank Verstraete. Fermionic matrix product operators and topological phases of matter. *arXiv preprint arXiv:1609.02897*, 2016.
- [160] Michael M. Wolf, Frank Verstraete, Matthew B. Hastings, and J. Ignacio Cirac. Area laws in quantum systems: Mutual information and correlations. *Phys. Rev. Lett.*, 100:070502, Feb 2008.
- [161] Cenke Xu. Three-dimensional z_2 topological phases enriched by time-reversal symmetry. *Physical Review B*, 88:205137, Nov 2013.
- [162] Simeng Yan, David A. Huse, and Steven R. White. Spin-liquid ground state of the $s = 1/2$ kagome heisenberg antiferromagnet. *Science*, 332(6034):1173–1176, 2011.
- [163] Fan Yang and Hong Yao. Frustrated resonating valence bond states in two dimensions: Classification and short-range correlations. *Phys. Rev. Lett.*, 109:147209, Oct 2012.

- [164] Shuo Yang, Thorsten B Wahl, Hong-Hao Tu, Norbert Schuch, and J Ignacio Cirac. Chiral projected entangled-pair state with topological order. *Physical review letters*, 114(10):106803, 2015.
- [165] Hong Yao and Steven A. Kivelson. Fragile mott insulators. *Phys. Rev. Lett.*, 105:166402, Oct 2010.
- [166] Peng Ye and Juven Wang. Symmetry-protected topological phases with charge and spin symmetries: Response theory and dynamical gauge theory in two and three dimensions. *Physical Review B*, 88:235109, Dec 2013.
- [167] Tsuneya Yoshida, Takahiro Morimoto, and Akira Furusaki. Bosonic symmetry-protected topological phases with reflection symmetry. *Phys. Rev. B*, 92:245122, Dec 2015.
- [168] Yi-Zhuang You, Zhen Bi, Alex Rasmussen, Meng Cheng, and Cenke Xu. Bridging fermionic and bosonic short range entangled states. *New Journal of Physics*, 17(7):075010, 2015.
- [169] Michael P Zaletel. Detecting two dimensional symmetry protected topological order in a ground state wave function. *arXiv*, cond-mat.str-el, Sep 2013.
- [170] Yi Zhang, Tarun Grover, Ari Turner, Masaki Oshikawa, and Ashvin Vishwanath. Quasiparticle statistics and braiding from ground-state entanglement. *Physical Review B*, 85:235151, Jun 2012.
- [171] HH Zhao, ZY Xie, QN Chen, ZC Wei, JW Cai, and T Xiang. Renormalization of tensor-network states. *Physical Review B*, 81(17):174411, 2010.